Phytochemical and anti-mycobacterial studies on selected medicinal plants

Cynthia Amaning Danquah

A thesis submitted for the degree of

Doctor of Philosophy

School of Pharmacy

University College London

2016

Declaration

The work presented in this thesis is my own, except where I have either given a bibliographic reference or acknowledged contributions.

Signed…… Date……..

PhD Student: Cynthia Amaning Danquah

Research Department of Pharmaceutical and Biological Chemistry

School of Pharmacy

University College London

Signed…… Date……..

Supervisor: Prof. Simon Gibbons

Research Department of Pharmaceutical and Biological Chemistry

School of Pharmacy

University College London

Signed…… Date……..

Supervisor: Dr Sanjib Bhakta

Microbiology, Department of Biological Sciences

Institute of Structural and Molecular Biology

Birkbeck, University of London

Abstract

Tuberculosis (TB) is an infectious disease caused by the pathogen *Mycobacterium tuberculosis*. Tuberculosis was first declared as a global health emergency in 1993 but is still a health crisis worldwide because of the emergence of extensively drug-resistant strains of *M. tuberculosis* coupled with the increased risk of infection in immune-compromised people and also by the fact that at least one third of the human population are latently infected with the TB causing bacilli. New, safer and more effective antimycobacterial compounds with novel mechanisms of action are urgently needed for treating resistant forms of tuberculosis. This has led to a renewed research interest in natural products, which offer an outstanding source of diverse bioactive chemical scaffolds with the hope of discovering novel anti-mycobacterial leads.

This thesis describes phytochemical studies on the genera *Allium and Andrographis.* The antibacterial activity of the crude extracts, various fractions and isolated compounds were evaluated. Antibacterial studies were carried out using a panel of Gram-positive, Gram-negative and acid fast group of bacterial species including *M. aurum*, *M. bovis* BCG, *M. tuberculosis* H_{37}Rv and multidrug-resistant clinical isolates of *M. tuberculosis.*

Furthermore, analogues of naturally isolated disulfides from the genus *Allium* were synthesized and evaluated for antibacterial activity. Eukaryotic cytotoxicity was estimated in order to determine the therapeutic selectivity index of the selected compounds. In addition, inhibition of both drug efflux and biofilm formation was observed at the whole-cell phenotypic level. These analogues have demonstrated anti-TB activity with the lowest MIC being 4 mg/L. They also exhibited whole cell multidrug efflux and biofilm inhibitory effect. These findings would serve as useful contribution to the development of novel anti-TB drugs.

Acknowledgements

First of all, I thank God almighty for his grace, guidance and protection and for bringing me this far in my studies.

I am most grateful to my supervisor Professor Simon Gibbons for giving me the opportunity to work in his group. I thank him for his useful suggestions and words of encouragement. Thank you for your patience and for believing in me.

My sincere thanks goes to my second supervisor Dr Sanjib Bhakta for his enthusiasm and the depth of exposure he gave me in learning experimental techniques and also training in other aspects of research such as presentations and attending scientific meetings.

I would also like to acknowledge all the group members at the School of Pharmacy, Dr Proma Khondkhar, Warunya, Blessing, Awo, Gugu, Tariq, Pedro, Sarah, Jeanne, Takahiro and to Mr Cory Beckwith for his technical support. Thanks to Dr Jane Faull and the microbiology laboratory manager Marie Maugueret-Minerve and to all members at the Mycobacteria Research laboratory Parisa, Jim, Camy and Arundhati.

Last but not the least thanks goes to my family especially my husband Daniel Amaning Danquah for holding the fort in my absence and to my sons David, Michael and Martin for being so understanding. To my parents Martin and Sarah Boamah, my siblings Felicia, Frank and Josephine, my in-laws and to the rest of the extended family I say thank you.

I acknowledge Ghana Education Trust Fund for funding my PhD studies.

Publications

Original research article

1. HT-SPOTi: a rapid, drug susceptibility test (DST), to evaluate antibiotic resistance profiles and novel chemicals for anti-infective drug discovery, (2016). **Cynthia Amaning Danquah**, Arundhati Maitra, Simon Gibbons, Jane Faull and Sanjib Bhakta. Current Protocols in Microbiology. 40:17.8.1-17.8.12. ISSN 1934-8533.

2. Development of a rapid, reliable and quantitative method - "SPOTi" for testing antifungal efficacy, (2015). Khalida Rizi, Sudaxshina Murdan, **Cynthia Amaning Danquah**, Jane Faull and Sanjib Bhakta. Journal of Microbiological Methods. 117, 36–40. ISSN 0167-7012.

Meeting report

3. Tackling tuberculosis: insights from an international TB Summit in London (2015). Arundhati Maitra, **Cynthia Amaning Danquah**, Francesca Scotti, Tracey Howard, Kamil Tengku and Sanjib Bhakta. Virulence. ISSN 2150-5594.

Manuscript under Review

4. Analogues of natural product disulfides from *Allium stipitatum* demonstrate potent anti-tubercular activities through drug efflux pump and biofilm inhibition (2016). **Cynthia Amaning Danquah**, Proma Khondkar, Elephtheria Kakagianni, Arundhati Maitra, Dimitrios Evangelopoulos, Timothy McHugh, Paul Stapleton, Mukhlesur Rahman, Sanjib Bhakta and Simon Gibbons. Angewandte Chemie International.

Conference Proceedings

Oral presentations/Talks

1. UCL School of Pharmacy Research Day, April 2016 in London.
   Synthetic analogues of natural product disulfides from *Allium stipitatum* demonstrate potent anti-tubercular activities through drug efflux pump and biofilm inhibition. **Cynthia Amaning Danquah**, Proma Khondkar, Arundhati Maitra, Dimitrios Evangelopoulos, Timothy McHugh, Sanjib Bhakta and Simon Gibbons.

2. British Society of Antimicrobial Chemotherapy Antibiotic resistance mechanisms (BSAC-ARM) workshop, November, 2015 in Birmingham. Synthetic analogues of natural product disulfides from *Allium stipitatum*

demonstrate potent anti-tubercular activities through drug efflux pump and biofilm inhibition. **Cynthia Amaning Danquah**, Proma Khondkar, Arundhati Maitra, Dimitrios Evangelopoulos, Timothy McHugh, Sanjib Bhakta and Simon Gibbons.

3. Won the Bill and Melinda Gates Travel Award to present research at the Interscience Conference on Antimicrobial Agents and Chemotherapy in San Diego California, USA. Synthetic analogues of natural product disulfides from *Allium stipitatum* demonstrate potent anti-tubercular activities through drug efflux pump and biofilm inhibition. **Cynthia Amaning Danquah**, Proma Khondkar, Arundhati Maitra, Dimitrios Evangelopoulos, Timothy McHugh, Sanjib Bhakta and Simon Gibbons.

4. Institute of Structural and Molecular Biology (UCL/ Birkbeck) Friday wrap January 2015 at UCL main Campus, London. Synthetic analogues of natural product disulfides from *Allium stipitatum* demonstrate potent anti-tubercular activities. **Cynthia Amaning Danquah**, Proma Khondkar, Arundhati Maitra, Dimitrios Evangelopoulos, Timothy McHugh, Sanjib Bhakta and Simon Gibbons.

5. Interscience Conference on Antimicrobial Agents and Chemotherapy (ICAAC), September, 2014 in Washington DC, USA. Antimycobacterial activity of synthetic analogues of the bioactive natural product disulfides. **Cynthia Amaning Danquah**, Proma Khondkar, Sanjib Bhakta and Simon Gibbons.

Poster presentations

1. Poster presented at the European Congress of Clinical Microbiology and Infectious Diseases (ECCMID), April, 2015 at Copenhagen, Denmark. Synthetic analogues of Pyridine-*N*-oxide disulfides from *Allium stipitatum* demonstrate potent anti-tubercular activities and inhibit mycobacterial drug efflux pumps. **Cynthia Amaning Danquah**, Proma Khondkar, Arundhati Maitra, Dimitrios Evangelopoulos, Timothy McHugh, Sanjib Bhakta and Simon Gibbons.

2. Poster for the ULLA Summer School, July 2015 in Paris, France. Synthetic analogues of pyridine-*N*-oxide disulfides from *Allium stipitatum* demonstrate potent anti-tubercular specific activities and inhibit drug efflux pumps. **Cynthia Amaning Danquah**, Arundhati Maitra, Proma Khondkar, Dimitrios Evangelopoulos, Timothy McHugh, Sanjib Bhakta and Simon Gibbons.

3. British Society of Antimicrobial Chemotherapy Antibiotic resistance mechanisms (BSAC-ARM) workshop, 2014 in Birmingham. Synthetic analogues of pyridine-*N*-oxide disulfides from *Allium stipitatum* demonstrate potent anti-tubercular activities and inhibit mycobacterial drug efflux pumps. **Cynthia Amaning Danquah**, Arundhati Maitra, Proma Khondkar, Dimitrios Evangelopoulos, Timothy McHugh, Sanjib Bhakta and Simon Gibbons.

4. Poster for the Interscience Conference on Antimicrobial Agents and Chemotherapy 2014, Washington DC. Synthetic analogues of pyridine-*N*-oxide disulfides from *Allium stipitatum* as efflux pump inhibitors of *Mycobacterium aurum*. **Cynthia Amaning Danquah**, Elephtheria Kakagianni, Proma Khondkar, Arundhati Maitra, Sanjib Bhakta and Simon Gibbons.

5. Poster for the TB Summit 2014, North Greenwich, London. Evaluation of antimycobacterial properties of phytochemicals from the plant family Alliaceae. **Cynthia Amaning Danquah**, Elephtheria Kakagianni, Proma Khondkar, Arundhati Maitra, Sanjib Bhakta and Simon Gibbons.

6. Phytochemicals from Alliaceae and evaluation of their anti-tubercular properties, poster for the UCL School of Pharmacy Research day, September 2013. **Cynthia Amaning Danquah**, Sanjib Bhakta and Simon Gibbons.

E-poster presentation

1. The World Congress on Infectious Diseases. August, 2015, West Drayton, London, UK. OMICs infectious Diseases Conference, 2015. Synthetic analogues of natural product disulfides from *Allium stipitatum* demonstrate potent anti-tubercular activities and inhibit mycobacterial drug efflux pumps. **Cynthia Amaning Danquah**, Proma Khondkar, Arundhati Maitra, Dimitrios Evangelopoulos, Timothy McHugh, Sanjib Bhakta and Simon Gibbons.

Table of contents

Declaration **2**
Abstract **3**
Acknowledgements **4**
List of Abbreviations **11**
List of Figures **13**
List of Tables **16**
Chapter 1: Introduction **17**
1.1 General introduction **17**
1.2 Understanding the molecular mechanism of antibiotic resistance **19**
1.2.1 Prevention of access to target **20**
1.2.2 Changes in antibiotic targets by mutation **21**
1.2.3 Direct modification of antibiotics **22**
1.3 Tuberculosis **23**
1.3.1 The genus: *Mycobacterium* **25**
1.3.2 History of tuberculosis **26**
1.3.3 Epidemiology **26**
1.3.4 Current control of tuberculosis **28**
1.3.5 Tuberculosis: Prevention **29**
1.3.6 Tuberculosis: Detection **30**
1.3.7. Tuberculosis: Treatment **31**
1.3.8 Limitations of current treatment **40**
1.3.9 Drug resistance in tuberculosis **41**
1.4. Multidrug efflux pumps **44**
1.5. Efflux pump inhibitors **46**
1.6 Biofilms **47**
1.7 Aims and Objectives **49**
Chapter 2: Materials and Methods **50**
2.1 Chemicals and reagents **50**
2.2 Apparatus **51**
2.3 Microorganisms and cells **53**
2.4 Phytochemical extraction **54**
2.5 Chromatographic techniques **56**
2.5.1 Vacuum liquid chromatography **57**
2.5.2 Solid phase extraction **58**

2.5.3 Column chromatography **59**
2.5.4 Thin layer chromatography **59**
2.5.5 Preparative thin layer chromatography **61**
2.5.6 High performance liquid chromatography **62**
2.6 Spectroscopic techniques **64**
2.6.1 Nuclear magnetic resonance spectroscopy **64**
2.6.2 Mass spectrometry **68**
2.6.3 Ultraviolet-visible spectroscopy **69**
2.6.4 Infrared spectroscopy **71**
2.7 Growth and maintenance of microorganisms **73**
2.8 Cryopreservation **74**
2.9 Optical density **74**
2.10 Acid-fast staining of mycobacteria **74**
2.1 1 Construction of a growth curve **76**
2.12 Determination of colony forming units **76**
2.13 Preparation of bacterial strains **79**
2.14 Preparation of required samples **79**
2.15 Screening for antibacterial activity (drug susceptibility assay) **79**
2.15.1 Spot culture growth inhibition assay (SPOTi) **79**
2.15.2 Microtitre broth dilution assay **80**
2.15.3 Disc diffusion assay **81**
2.16 Antifungal assay **83**
2.17 Cytotoxicity assay **86**
2.18 Efflux pump inhibition assay **88**
2.19 Biofilm assay **89**
Chapter 3: Bioguided isolation and characterisation of compounds from the genus *Allium* **90**
3.1 Introduction **90**
3.2 The genus *Allium* **90**
3.3 History of *Allium* use as food and medicine **92**
3.4 Chemical constituents in *Allium* species **93**
3.5 Antimicrobial activity of *Allium* species **97**
3.6 Antimycobacterial activity of the extracts **101**
3.7 Antibacterial activity using the Disc Diffusion Assay **101**
3.8 Characterisation of a compound from *Allium* "Ambassador" **104**

Chapter 4: Synthesis and biological evaluation of analogues of natural product disulfides from the genus *Allium* **110**

4.1 Introduction **110**

4.2 Procedure for synthesis **111**

4.3 Results **114**

4.3.1 Characterization of the methyldisulfides **114**

4.3.2 Biological evaluation **120**

4.6 Discussion **129**

Chapter 5: Bioguided isolation and characterisation of compounds from *Andrographis paniculata* **132**

5. 1 Introduction **132**

5.2 Characterization of the isolated natural products. **140**

5.2.1 Characterisation of CD-1 as 14-deoxy-11,12-didehydroandrographolide **140**

5.2.2 Characterisation of CD-2 as andrographolide **145**

5.2.3 Characterisation of CD-3 as andropanoside **150**

5.2.4 Characterisation of CD-4 as neoandrographolide **155**

5.2.5 Characterisation of CD-5 as andrographolide **158**

5.2.6 Characterisation of CD-6 as stigmasterol **161**

5.3 Antibiotic susceptibility testing **165**

5.4 Discussion **165**

Chapter 6: Overall discussion and future direction **167**

References **171**

Appendix **181**

List of Abbreviations

ADC Albumin, dextrose, catalase

BCG Bacillus calmette-guérin

CFU Colony forming units

COSY Correlation spectroscopy

DEPT Distortionless enhancement by polarisation transfer

DMSO Dimethyl sulfoxide

DOT Directly observed therapy

EtOAc Ethyl acetate

EMB Ethambutol

EPI Efflux pump inhibition

EtBr Ethidium bromide

ETH Ethambutol

GIC Growth inhibitory concentration

HAART Highly active anti-retroviral therapy

HIV Human immunodeficiency virus

HMBC Heteronuclear multiple bond correlation

HMQC Heteronuclear multiple quantum coherence

HT-SPOTi High-throughput spot culture growth inhibition assay

INH Isonicotinic acid hydrazide (Isoniazid)

NMR Nuclear magnetic resonance

NOESY Nuclear overhauser effect spectroscopy

MIC Minimum inhibitory concentration

MDR-TB Multidrug-resistant tuberculosis

MRSA Methicillin-resistant *Staphylococcus aureus*

MS Mass spectroscopy

MTT 3-(3,4-dimethylthiazole-2-yl)-2,5-diphenyltetrazolium bromide

NAD^+ Nicotinamide adenine dinucleotide

NADH Nicotinamide adenine dinucleotide

$NADP^+$ Nicotinamide adenine dinucleotide phosphate

NADPH Reduced nicotinamide adenine dinucleotide phosphate

NMR Nuclear magnetic resonance

NOESY Nuclear overhauser effect spectroscopy

OD Optical density

OADC Oleic acid, albumin, dextrose, catalase

PAS *P*-aminosalicylic acid

PG Peptidoglycan

PPM parts per million

PYR Pyrazinamide

RIF Rifampicin

SPE Solid phase extraction

STR Streptomycin

TLC Thin layer chromatography

UV Ultraviolet

UCL University College London

VLC Vacuum liquid chromatography

VOT Virtually observed treatment

WHO World health organisation

XDR-TB Extensively drug-resistant tuberculosis

List of Figures

Figure 1. 1 Representation of intrinsic mechanisms of resistance……... 23
Figure 1. 2 The global prevalence of extensively drug-resistant tuberculosis (XDR-TB)…….... 26
Figure 1. 3 Global TB Vaccine development pipeline……30
Figure 1. 4 The cell wall structure of Mycobacteria ……43

Figure 2.1 Extraction techniques used to obtain plant extracts (a-e: soxhlet extraction, acid-base extraction, ultrasonication, freeze drying, filtration, and rotary evaporation respectively)..... 56
Figure 2.2 Chromatographic techniques ((a) VLC, (b & c) column chromatography (d) SPE, (e-g) TLC tank, TLC visualizer and TLC plate respectively) 62
Figure 2. 3 High performance liquid chromatography..... 63
Figure 2. 4 NMR Bruker AVANCE 400 (left) and 500 (right) instruments 68
Figure 2. 5 Micromass Q-TOF premier Tandem Mass Spectrometer..... 69
Figure 2. 6 (a) Infrared and (b) ultraviolet-visible spectrophometer..... 71
Figure 2. 7 Light microscopic image showing acid-fast stained *M. aurum* cells..... 75
Figure 2. 8 Schematic representation of the process of colony forming unit (CFU) counting, growth curve determination and optical density (OD) measurement of *M. aurum* in the absence (control) and presence of different concentrations of compound **2** and at different time points..... 78
Figure 2. 9 A representative 96-well microtitre plate showing antibacterial activity 81
Figure 2. 10 Schematic representation of fungal SPOTi..... 84
Figure 2. 11 Growing dermatophytes: (1a, 1b) *Trichophyton equinum,* (2a, 2b) *T. rubrum,* (3a, 3b) *T. tonsurans,* (4a, 4b) *T. mentagrophytes*..... 85
Figure 2. 12 A representative 96-well microtitre plate resazurin treated and showing a change in colour from blue to pink indicating viable cells after incubation..... 87
Figure 2. 13 Light microscopic image showing growing RAW 264.7 murine macrophage cells. 87
Figure 2. 14 Schematic representation of the efflux pump assay..... 88

Figure 3. 1The flower of *Allium stipitatum*.....91
Figure 3. 2 Sulphoxides in *Allium* species. 94
Figure 3. 3 Conversion of Alliin to Allicin. 94
Figure 3. 4 Diallyldisulphide, diallyltrisulphide and diallyltetrasulphide in *Allium* species.....95
Figure 3. 5 Production of propanethial-*S*-oxide. 95
Figure 3. 6 Chemical structures of Quercetin and Kaempferol.....96
Figure 3. 7 Alliogenin. 96
Figure 3. 8 Flower of *Allium* "Ambassador". 98
Figure 3. 9 Flower of *Allium karataviense*. 99
Figure 3. 10 Flower of *Allium* "Gladiator". 100
Figure 3. 11 Growth inhibition of SPE fractions of *Allium* "Ambassador" chloroform extract by disc diffusion assay using *Staphylococcus aureus* strain SA 1199B on nutrient agar. 102

Figure 3. 12 Structure of Compound **A-1**. 104
Figure 3. 13 ^{1}H NMR spectrum of **A-1** in $CDCl_3$ (500 MHz). 106
Figure 3. 14 ^{13}C NMR spectrum of **A-1** in $CDCl_3$ (125 MHz). 106
Figure 3. 15 DEPT 135 NMR spectrum of **A-1** in $CDCl_3$ (125 MHz) 107
Figure 3. 16 ^{1}H-^{1}H COSY NMR spectrum of **A-1** in $CDCl_3$ (500 MHz). 107
Figure 3. 17 HMQC spectrum of **A-1** in $CDCl_3$ (500 MHz) 108
Figure 3. 18 HMBC spectrum of **A-1** in $CDCl_3$ (500 MHz). 108
Figure 3. 19 ESI-MS spectrum of **A-1**. 109

Figure 4. 1 Aromatic thiols used as starting materials. 112
Figure 4. 2 Reaction scheme leading to methyldisulfides 113
Figure 4. 3 (a) Process of synthesizing methyldisulfide using a magnetic stirrer and (b) Separation of the dichloromethane layer using a separating funnel. 113
Figure 4. 4 Synthesized methyldisulfides. 114
Figure 4. 5 Structure of compound **1**. 117
Figure 4. 6 ^{1}H NMR spectrum of compound **1** in CD_3OD (500 MHz). 119
Figure 4. 7 ^{13}C NMR spectrum of compound **1** in CD_3OD (125 MHz) 119
Figure 4. 8 HMBC spectrum of compound **1** in CD_3OD (500 MHz). 120
Figure 4. 9 Representative SPOTi plate showing minimum inhibitory concentration of methyldisulfides using (a) *M. aurum and* (b) *Trichophyton equinum respectively*. 122
Figure 4. 10 Cell toxicity assay using murine macrophage RAW 264.7 cell line. The number of viable cells was quantified using the Trypan blue exclusion assay with the use of an haemocytometer and inverted microscope. The 50 % growth inhibitory concentration was determined based on the resazurin fluorescence assay and the SI calculated as SI = GIC_{50}/MIC. 124
Figure 4. 11 Efflux pump inhibition effect of disulfide compounds. Ethidium bromide (EtBr) is an efflux pump substrate (used at a final concentration of 0.5 mg/L). Verapamil (VP) is a known efflux pump inhibitor and was used as the reference standard. 125
Figure 4. 12 Growth curve of *Mycobacterium aurum* (cells were grown at 180 rpm). 125
Figure 4. 13 Growth analysis of *M. aurum* in the presence of different concentrations (MIC, 2x MIC, 4x MIC, 8x MIC) of disulfide compound **2** at different time points. (Insert) Bar diagram of the number of Colony forming units (CFU) recorded at one time-point of liquid cultures of *M. aurum* treated with different concentrations of compound **2** MIC (15.17), 2x MIC (31.13), 4x MIC (62.5 mg/L). The aliquots were taken and plated on agar after 8 h. 127
Figure 4. 14 Dose-dependent inhibition of biofilm formation by compound **2** in (a) polypropylene tubes (b) 96-well plates (g) quantification of formed biofilm using the crystal violet technique, (c & d) SEM images and (e & f) light microscope images of *M. smegmatis* cells (planktonic form) and (biofilm form) at early stationary phase (OD 3.5) respectively by compound **2**. (h) SEM image of *M. smegmatis* cells (planktonic form) only at early stationary phase (OD_{600} 3.5) (i-n) dose-dependent SEM images of *M. smegmatis* (biofilm form) at early stationary phase (OD 3.5). 128

Figure 5. 1 Labdane diterpenoids and flavonoids from *Andrographis paniculata* 134
Figure 5. 2 Flow chart for the isolation of **CD-1**, **CD-2**, and **CD-3** from *Andrographis paniculata*....135
Figure 5. 3 Flow chart for the isolation of **CD-4** and **CD-5** from *Andrographis paniculata.*.....136
Figure 5. 4 Flow chart for the isolation of **CD-6** from *Andrographis paniculata.* 137
Figure 5. 5 The TLC profile of VLC fractions, solvent system Hexane: EtOAc 50:50.....138
Figure 5. 6 The TLC profile of column chromatography fractions, solvent system Hexane: EtOAc 50:50 139
Figure 5. 7 Structure of **CD-1** (14-deoxy-11,12-didehydroandrographolide).....140
Figure 5. 8 ^{1}H NMR spectrum of **CD-1** in CD_3OD (500 MHz) 141
Figure 5. 9 ^{13}C NMR spectrum of **CD-1** in CD_3OD (125 MHz).....141
Figure 5. 10 HMQC spectrum for **CD-1** in CD_3OD (500 MHz) 142
Figure 5. 11 HMQC spectrum for **CD-1** in CD_3OD (500 MHz) 142
Figure 5. 12 ESI-MS spectrum of **CD-1**.....143
Figure 5. 13 Structure of **CD-2** (Andrographolide) 145
Figure 5. 14 ^{1}H spectrum of **CD-2** in $(CD_3)_2SO$ (500 MHz) 146
Figure 5. 15 ^{13}C spectrum for **CD-2** in $(CD_3)_2SO$ (125 MHz).....146
Figure 5. 16 HMQC spectrum of **CD-2** in $(CD_3)_2SO$ (500 MHz) 147
Figure 5. 17 HMBC spectrum of **CD-2** in $(CD_3)_2SO$ (500 MHz).....147
Figure 5. 18 ESI-MS spectrum of **CD-2**.....148
Figure 5. 19 Structure of **CD-3** as Andropanoside 150
Figure 5. 20 ^{1}H spectrum for **CD-3** in CD_3OD (500 MHz).....151
Figure 5. 21 ^{13}C NMR spectrum for **CD-3** in CD_3OD (125 MHz).....151
Figure 5. 22 HMQC NMR spectrum for **CD-3** in CD_3OD (500 MHz) 152
Figure 5. 23 HMBC NMR spectrum for **CD-3** in CD_3OD (500 MHz).....152
Figure 5. 24 Structure of **CD-4** as neoandrographolide.....155
Figure 5. 25 ^{1}H NMR spectrum of **CD-4** in C_5D_5N (500 MHz).....156
Figure 5. 26 ^{13}C NMR spectrum of **CD-4** in C_5D_5N (125 MHz).....156
Figure 5. 27 Structure of **CD-5** as Andrographolide 158
Figure 5. 28 ^{1}H NMR spectrum for **CD-5** in CD_3OD (500 MHz).....159
Figure 5. 29 ^{13}C NMR spectrum for **CD-5** in CD_3OD (125 MHz).....159
Figure 5. 30 Structure of **CD-6** as Stigmasterol.....161
Figure 5. 31 ^{1}H spectrum for **CD-6** in $CDCl_3$ (500 MHz) 162
Figure 5. 32 ^{13}C spectrum for **CD-6** in $CDCl_3$ (125 MHz) 162

List of Tables

Table 1. 1 Mechanism of action and resistance of first-and selected second-line anti-tubercular drugs. 34

Table 2. 1 Chemical shift of deuterated solvents used 65
Table 2. 2 Preparation of microbiological media 72

Table 3. 1. Antibacterial activity of SPE fractions of *Allium* "Ambassador" chloroform extract by disc diffusion assay 103
Table 3. 2 ^{1}H NMR (500 MHz) and ^{13}C (125 MHz) data of compound **A-1** in $CDCl_3$ 105

Table 4. 1 ^{1}H (500 MHz) and ^{13}C (125 MHz) spectral data and ^{1}H -^{13}C long-range correlations of Compound **1** in CD_3OD 118
Table 4. 2 Minimum inhibitory concentration (MIC) mg/L of synthesized disulfides using different strains of bacteria 121
Table 4. 3 Minimum Inhibitory Concentrations (MIC) mg/L of synthesized disulfides against fungi (dermatophytes) 123
Table 4. 4 Cytotoxicity profile of the compounds 124
Table 4. 5 Optical density readings of *M. aurum* in the presence of different concentrations (MIC, 2x MIC, 4x MIC, 8x MIC) of disulfide compound **2** at different time points 126

Table 5. 1 ^{1}H NMR (500 MHz) and ^{13}C NMR (125 MHz) data of **CD-1** in CD_3OD 144
Table 5. 2 ^{1}H NMR (500 MHz) and ^{13}C NMR (125 MHz) data for **CD-2** in $(CD_3)_2SO$ 149
Table 5. 3 ^{1}H NMR (500 MHz) and ^{13}C NMR (125 MHz) data for **CD-3** in CD_3OD 153
Table 5. 4 ^{1}H NMR (500 Hz) and ^{13}C NMR (125 MHz) data for **CD-4** in C_5D_5N 157
Table 5. 5 ^{1}H NMR (500 MHz) and ^{13}C NMR (125 MHz) data for **CD-5** in CD_3OD 160
Table 5. 6 ^{1}H NMR (500 MHz) and ^{13}C (125 MHz) NMR data for **CD-6** in $CDCl_3$ 163

Chapter 1: Introduction

1.1 General introduction

Antibiotic resistance is one of the major threats to global health and well-being, having been described by the World Health Organisation (WHO) as the single greatest challenge in infectious diseases today, threatening rich and poor countries alike, and yet it has not had sufficient attention in terms of medical research (Bragginton and Piddock, 2014, Piddock, 2013, Laxminarayan *et al*., 2013, Carlet *et al*., 2014).

According to the World Economic Forum Global Risks report, it is estimated that in Europe 25,000 people die each year as a result of multidrug-resistant bacterial infections and that this costs the European Union economy €1.5 billion annually; whilst in the United States more than 2 million people are infected with antibiotic-resistant bacteria annually, with 23,000 deaths as a direct result (Blair *et al*., 2015, Hampton, 2013, WHO, 2014, Davies *et al*., 2013, Global risks, 2014).

The past decade has seen an alarming rise in the evolution and spread of drug-resistant strains of pathogenic microbes. The unabated spread of multidrug-resistant tuberculosis (MDR-TB) coupled with the emergence of extensively drug-resistant (XDR) strains of *Mycobacterium tuberculosis,* antimicrobial resistance among the ESKAPE pathogens (***E****nterococcus faecium,* ***S****taphylococcus aureus,* ***K****lebsiella pneumoniae,* ***A****cinetobacter baumanii,* ***P****seudomonas aeruginosa*, and ***E****nterobacter* species) as well as fungal pathogens (such as certain species of *Candida*, *Aspergillus*, *Cryptococcus,* and *Trichophyton*) poses a significant 21st century scientific challenge (Shah *et al*., 2007, Lawn and Zumla, 2011, Zumla *et al*., 2015b). The death toll of MDR- and XDR-TB is estimated to be more than a million people each year (Zumla

et al., 2014). The scenario remains similar with other bacterial pathogens such as methicillin-resistant *Staphylococcus aureus* (MRSA) and Gram-negative organisms where transposon- or plasmid-mediated resistance is spreading faster than modern medicine can keep pace.

Despite increased resistance to existing agents, ironically, the pace at which novel antibiotics are being discovered had slowed drastically in the last few decades and there are extremely limited new antibiotics in development. Much of the basic arsenal of drugs for treating TB was developed in the 1940s and 1960s (Zumla *et al*., 2014, Zumla *et al*., 2015a) and since then only a few promising candidates have been introduced (Matteelli *et al*., 2014, Belard *et al*., 2015).

There is no doubt a pressing need to speed up the discovery of new molecules to augment the lean pipeline for novel therapeutics to treat drug-resistant infections exist, especially when the numerous target-based approaches originating from the boom of postgenomic research have unfortunately failed to deliver bioactive molecules for future development (Guzman *et al*., 2013). The discovery of novel chemical entities is urgent, as this serves as an assurance for the development of new chemotherapeutic regimens in the near future. These novel compounds must be potent enough to reduce the length of treatment and possibly prevent the emergence of resistance, but at the same time be safe. New drugs with pleiotropic modes or mechanisms of action against these resistant strains will potentially help address this serious global health and economic challenge.

Natural products continue to provide leads for the development of novel drugs to treat infectious diseases because they are a source of secondary metabolites, which display extensive functional group chemistry and chirality indicating that they are a rewarding resource for drug discovery (Ling *et al*., 2015, Gibbons, 2004, Janin, 2007, Walsh and

Goodman, 1999, Stapleton, 2003). Plants remain a relatively untapped source of antibacterial compounds and for the few which have been studied, there is a lack of depth in terms of their biological evaluation, mammalian cell cytotoxicity or determination of potential modes or mechanism(s) of action (Guzman *et al*., 2012). Interestingly, they are an outstanding source of novel bioactive chemical scaffolds, which can be extensively exploited with the potential of developing novel therapeutics for a wide array of diseases. This choice is logical given the ecological rationale that plants produce natural products as a chemical defence against microbes in their environment and also produce mammalian cytotoxic compounds par excellence (Gibbons, 2004, Gibbons *et al*., 2005, Shiu *et al*., 2013). This is justified by the successes of taxol, and the vinca alkaloids as clinically used anticancer drugs (Walsh and Goodman, 1999). Several interesting antimycobacterials have been isolated with the renewed interest in natural sources for finding novel antimycobacterials (O'Donnell *et al*., 2009, Osman *et al*., 2012, Guzman *et al*., 2010, Wube *et al*., 2012, O'Donnell *et al*., 2006)

This research continued the search for novel chemical compounds from plants with antimicrobial/antimycobacterial properties using the bioassay-guided isolation and characterization of compounds approach.

1.2 Understanding the molecular mechanism of antibiotic resistance

Antibiotic resistance is a natural ecological phenomenon, and bacteria have been evolving to resist the action of natural antibacterial products for many years (D'Costa *et al*., 2011, Wellington *et al*., 2013). However, as a result of the widespread use of antibiotics in human medicine, as well as in animal treatment, horticulture, beekeeping, anti-fouling paints (used in the marine and oil industries) and laboratories

carrying out genetic manipulation, the evolutionary pressure for the emergence of antibiotic resistance is great. Even though the discovery of antibiotics was a huge success story in modern medicine as they have been able to kill or stop the growth of many microorganisms, unfortunately bacteria have proven to be much more innovative and adaptive than was ever imagined and have developed resistance to antibiotics at an increasing pace (D'Costa *et al*., 2011).

Bacteria can be intrinsically resistant to certain antibiotics (Figure 1.1) but can also acquire resistance or develop resistance to antibiotics via mutations in chromosomal genes and by horizontal gene transfer.

The mechanisms of antibiotic resistances can be grouped mainly into five: 1) those that minimize the intracellular concentrations of the antibiotic as a result of poor penetration into the bacterium in combination with 2) antibiotic efflux; 3) those that modify the antibiotic target by genetic mutation or post-translational modification of the target; 4) those that use alternative pathway or metabolic shunt and 5) those that inactivate the antibiotic by hydrolysis or modification (Fernández and Hancock, 2012, Blair *et al*., 2015, Wright, 2011, Nikaido, 2009).

1.2.1 Prevention of access to target

Reduced permeability: Gram-negative bacteria are intrinsically less permeable to many antibiotics as their outer membrane forms a permeability barrier as compared with Gram-positive bacteria. Hydrophilic antibiotics cross the outer membrane by diffusing through outer-membrane porin proteins (Kojima and Nikaido, 2013). In *Mycobacterium* (an acid-fast bacterium) intrinsic resistance is attributed to the unusual structure of its covalently linked mycolyl-arabinogalactan-peptidoglycan

(mAgp) complex that gives the bacteria a low permeability to antibiotics (Almeida Da Silva and Palomino, 2011).

Increased efflux: Another major contributor to intrinsic resistance is bacterial efflux pumps, which actively transport many antibiotics out of the cell thus rendering therapeutically effective agents inactive. When overexpressed, efflux pumps can also confer high levels of resistance to previously clinically useful antibiotics. Some efflux pumps have narrow substrate specificity (for example, the Tet pumps), but many transport a wide range of structurally dissimilar substrates and are known as multidrug resistance (MDR) efflux pumps (Nikaido and Takatsuka, 2009, Blair *et al*., 2014).

1.2.2 Changes in antibiotic targets by mutation

Most antibiotics specifically bind to their targets with high affinity, thus preventing the normal activity of the target. Changes to the target structure that prevent efficient antibiotic binding, but that still enable the target to carry out its normal function, can confer resistance. Apart from this, a single point mutation in the gene encoding an antibiotic target can confer resistance to the antibiotic; strains with this mutation can then proliferate. For example linezolid targets the 23S rRNA ribosomal subunit of Gram-positive bacteria, which is encoded by multiple, identical copies of its gene. Clinical use of linezolid has selected for resistance in *S. pneumoniae* and *S. aureus* by mutation in one of these copies, followed by recombination at high frequency between homologous alleles, which rapidly produces a population weighted in favour of carriage of the mutant allele (Blair *et al*., 2015).

Modification (and protection) of targets

The protection of targets has been found to be a clinically relevant mechanism of resistance for several important antibiotics. Protection by modification of the target

can also be an effective means of antibiotic resistance that does not require a mutational change in the genes encoding the target molecules.

1.2.3 Direct modification of antibiotics

Bacteria are able to destroy or modify antibiotics and therefore resist the action of the antibiotics. This is achieved by enzymatic inactivation or by transfer of chemical groups that modify the antibiotic.

Inactivation of antibiotics by hydrolysis

The enzyme-catalysed modification of antibiotics is a major mechanism of antibiotic resistance. Enzymes have been identified that can degrade and modify antibiotics of different classes, including β-lactams, aminoglycosides and macrolides (Haas *et al*., 1976).

Inactivation of antibiotic by transfer of a chemical group

Antibiotic resistance can result from the addition of chemical groups to vulnerable sites on the antibiotic molecule by bacterial enzymes. This prevents the antibiotic from binding to its target protein as a result of steric hindrance. Various different chemical groups can be transferred, including acyl, phosphate, nucleotidyl and ribitoyl groups, and the enzymes that are responsible form a large and diverse family of antibiotic-resistance enzymes including acetyltransferases, phosphotransferases and nucleotidyltransferases (Wright, 2011).

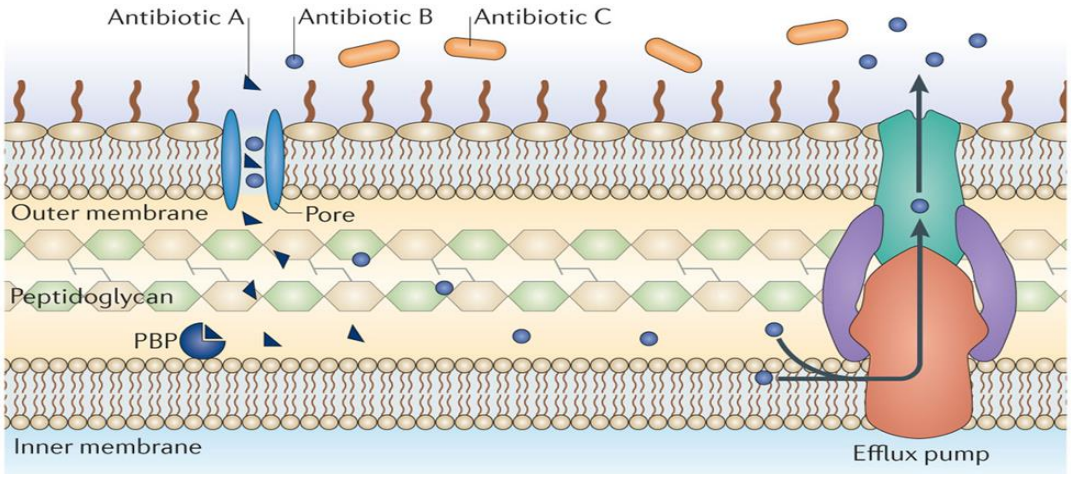

Figure 1. 1 Representation of intrinsic mechanisms of resistance

(The example shown is of β-lactam antibiotics targeting a penicillin-binding protein (PBP). Antibiotic A can enter the cell via a membrane-spanning porin protein, reach its target and inhibit peptidoglycan synthesis. Antibiotic B can also enter the cell via a porin, but unlike Antibiotic A, it is efficiently removed by efflux. Antibiotic C cannot cross the outer membrane and so is unable to access the target PBP. Adopted from Nature Reviews, Microbiology).

1.3 Tuberculosis

Tuberculosis or the Tubercle Bacillus (TB) remains one of the leading public health problems worldwide. Declared as a global health emergency in 1993 by the WHO, its control is hampered by the emergence of multidrug-resistance (MDR), defined as resistance to at least rifampicin and isoniazid, two key drugs in the treatment of the disease. More recently, severe forms of drug resistance such as extensively drug-resistant (XDR) TB (strains, that are resistant to isoniazid and rifampicin, in addition to any fluoroquinolone and to at least one of the three second line injectable drugs amikacin, capreomycin or kanamycin) have been described. After the discovery of several drugs with anti-TB activity, multidrug therapy became fundamental for control of the disease (Rock, 1997, Grange and Zumla, 1999). Tuberculosis is a contagious disease caused by *Mycobacterium tuberculosis*, which most commonly affects the lungs (Sepkowitz, 1996). It is transmitted from person to person via

droplets from the throat and lungs of people with the active respiratory disease. Chest pains, prolonged cough sometimes with blood-tinged sputum are some of the clinical symptoms of TB. Systemic symptoms of pulmonary TB include high fever, chills, night sweats, body weakness and a tendency to fatigue easily, reduced appetite and unusual weight loss. People who have the clinical symptoms are contagious as they propel the Tubercle Bacilli (TB germs) into the air by sneezing, talking, singing, laughing, spitting etc. (Caminero, 2007).

The immune system of humans is able to "wall off" the Tubercle Bacilli and therefore it can remain dormant for several years. When the lungs are infected, the alveoli macrophages engulf the bacterium but are unable to digest it as their cell wall prevents the fusion of the phagosome with a lysosome but does not prevent fusion of nutrient filled vesicles, hence the bacteria continues to multiply within the macrophages and also evade macrophage killing by neutralising reactive nitrogen intermediates (Hernandez-Pando et al., 2000, Sundaramurthy and Pieters, 2007). Thus, a person is said to have latent tuberculosis. People with latent tuberculosis test positive to the tuberculin skin test and X-ray on diagnosis but do not develop the disease or spread the infection even though one out of ten may develop active disease when the immune system is compromised. This can have serious consequences in the advanced stage because the bacteria multiply and attack not only various parts of the lungs but also different parts of the body, through blood circulation and the bacteria develop numerous foci throughout the body while the human host also develops the clinical symptoms described. This type of widespread infection is referred to as miliary TB (Wang *et al*., 2007). Tuberculosis can be cured when detected early and treated with the appropriate drugs. Anti-TB drugs can be used to treat TB infections of the oropharynx, larynx, trachea and bronchi however, infections of the urinary tract and

gastrointestinal tract do not respond to treatment. Tuberculosis still remains a major cause of death and disability in the world particularly among those with HIV (Janin, 2007).

1.3.1 The genus: *Mycobacterium*

Mycobacterium tuberculosis is a slow-growing bacterium evolved from soil bacteria. *M. tuberculosis* belongs to the genus *Mycobacterium*, which is highly diverse with over 139 species (Cook *et al*., 2009). Mycobacteria are pseudo-Gram-positive, acid fast, non-sporing, non-motile, rod-shaped, aerobes belonging to the order Actinomycetales and the family Mycobacteriaceae (Gordon and Smith, 1955). Some cause diseases only in humans like *M. tuberculosis* and to some extent *M. bovis* and *M. africanum*, whilst others cause disease only in animals and a few are omnipresent in nature. *Mycobacterium leprae* is another species in the genus that is very close to *M. tuberculosis* in shape and size and causes leprosy (Hanson's disease) in humans. The cell-wall structure of *Mycobacterium* deserves special attention, as it is a major determinant of virulence for the bacterium. Chemically the cell-wall is composed of three covalently linked macromolecules: peptidoglycan, arabinogalactan and mycolic acids (Crick *et al*., 2001). More than 60 % of the mycobacterial cell-wall is lipid making it least permeable to stains, dyes, resistant to many antibiotics, resistant to killing by alkaline and acidic compounds, resistant to osmotic lysis via complement deposition, resistant to lethal oxidations and allowing survival inside of macrophages (Brennan, 2003). Cell-wall biosynthesis is therefore a good target for killing *Mycobacterium* as enzymes involved in the biosynthesis is pathogen-specific and they do not have homologues in the mammalian system (Lee *et al*., 2012). Thus the cell-wall represents a potential target for antibacterial drug discovery.

1.3.2 History of tuberculosis

Tuberculosis has been present in humans since antiquity. As far back as 1000-1300 AD, DNA fragments of the pathogenic bacilli have been reported in Peruvian mummies (Salo *et al*., 1994). *Mycobacterium tuberculosis* complex DNA and typical mycobacterial lipids have also been found in the bones of an extinct long-horn bison in Wyoming, North America, dating back to 17000 years BC (Lee *et al*., 2012). *Mycobacterium tuberculosis* has inhabited *Homo sapiens* lungs for a very long time, and it was initially hypothesized that human-infecting bacilli derived from bovine species of acid fast bacteria, later disseminated to humans during the domestication of animals (Chalke, 1962). Reference to bone deformities and Pott's disease (tuberculosis spondylitis or spinal inflammation), two anatomical characteristics of tuberculosis appears in numerous reports describing mummies from Africa and Eurasia dating back as early as 3000 years ago (Herzog, 1998).

1.3.3 Epidemiology

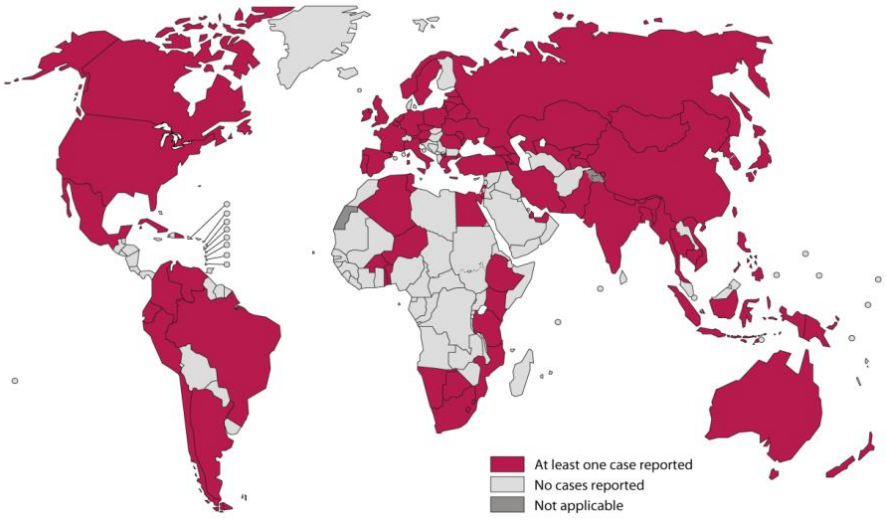

Source: Global tuberculosis Report 2016

Figure 1. 2 The global prevalence of extensively drug-resistant tuberculosis (XDR-TB).

The global burden of TB remains enormous even though *M. tuberculosis* was discovered back in 1882 and has been declared a global health emergency since 1993 (Grange and Zumla, 2002). In 2014, there was an estimated 9.6 million new cases of TB (12 % co-infected with the human immunodeficiency virus (HIV) and 1.5 million people died from TB, including almost 1.1 million deaths among HIV-negative individuals and 0.4 million among people who were HIV-positive (World Health Organisation, 2015).

Tuberculosis remains a challenging problem worldwide due to the rapid spread of tuberculosis strains resistant to the major antituberculosis drugs on the market. The reason why drugs are available but more people are dying needs to be addressed.

The recent emergence of XDR tuberculosis (Figure 1.2) has greatly contributed to the control of TB becoming harder because there is virtually no effective drug available for its treatment. New drugs with novel mechanisms of action are urgently required to tackle the spread of drug-resistant TB strains. Enormous effort by all concerned to combat the disease is utterly necessary and this explains why this research is timely.

1.3.4 Current control of tuberculosis

Tuberculosis control can currently be summarized by the flow chart below

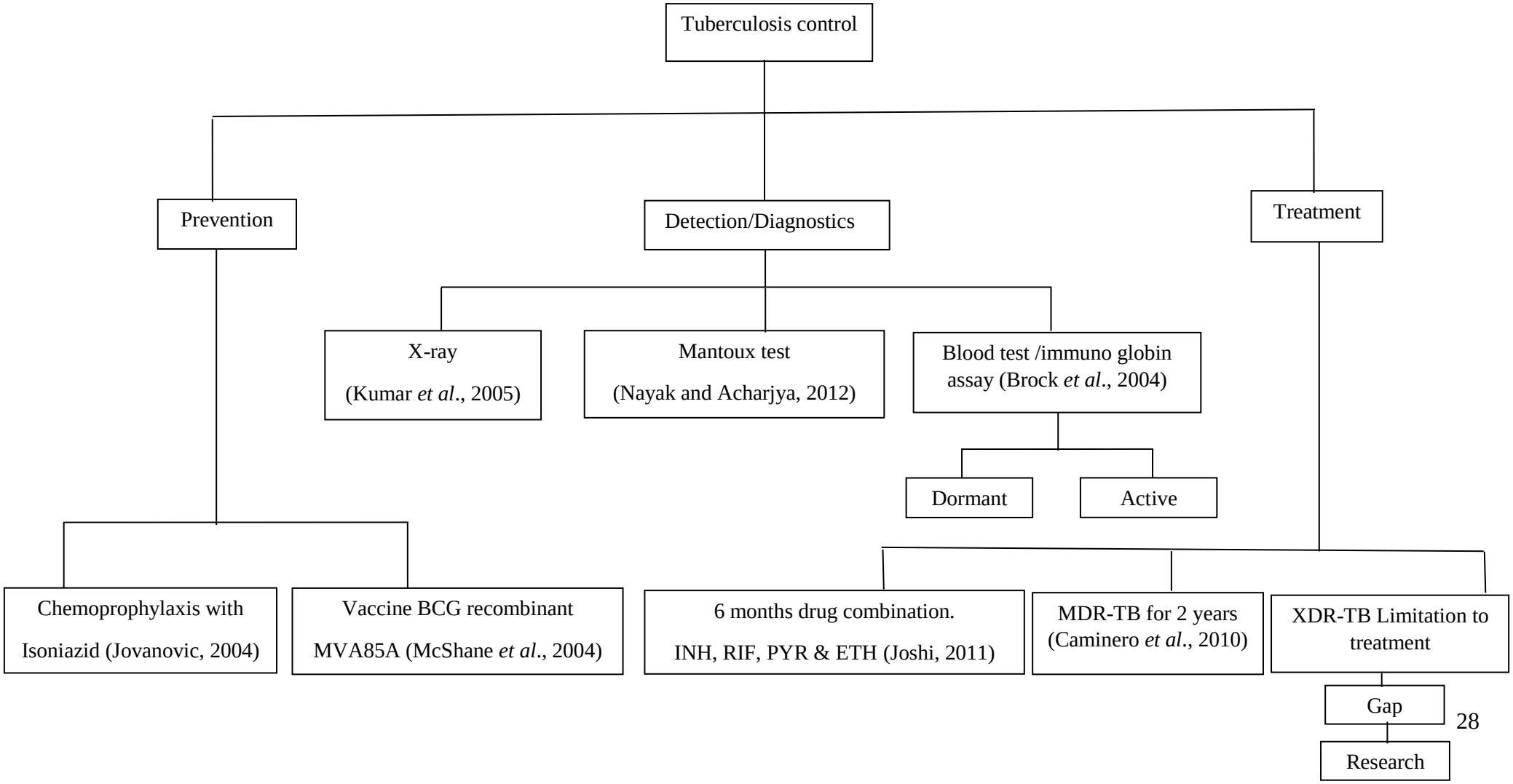

1.3.5 Tuberculosis: Prevention

Prevention of tuberculosis can be by chemoprophylaxis (vaccination) or by boosting immunity. *Mycobacterium bovis* BCG (Bacillus Calmette-Guérin) has been the vaccine most predominantly used all over the world since its discovery in 1921 (Fine, 1995). It is estimated that more than one billion people have received the BCG vaccine. BCG is the only vaccine currently licensed for the prevention of TB (von Reyn and Vuola, 2002). The global TB Vaccine development pipeline is shown in figure 1.3.

Mycobacterium bovis BCG has a proven efficacy for protecting new-borns against the most serious forms of the disease such as tubercular meningitis and miliary TB with a high protective ratio of 86 % (Rodrigues *et al.*, 1993). BCG vaccination reduces the risk of any form of TB disease by half and the protection continues for more than 10 years post vaccination. A further advantage of this vaccine is its low cost, as being live attenuated bacteria; the mass scale production is readily performed by simply culturing the organism. BCG vaccination is absolutely contraindicated for HIV-positive individuals and other immunocompromised individuals due to the risk of developing disseminated *M. bovis* BCG tuberculosis (Tamaris, 2013).

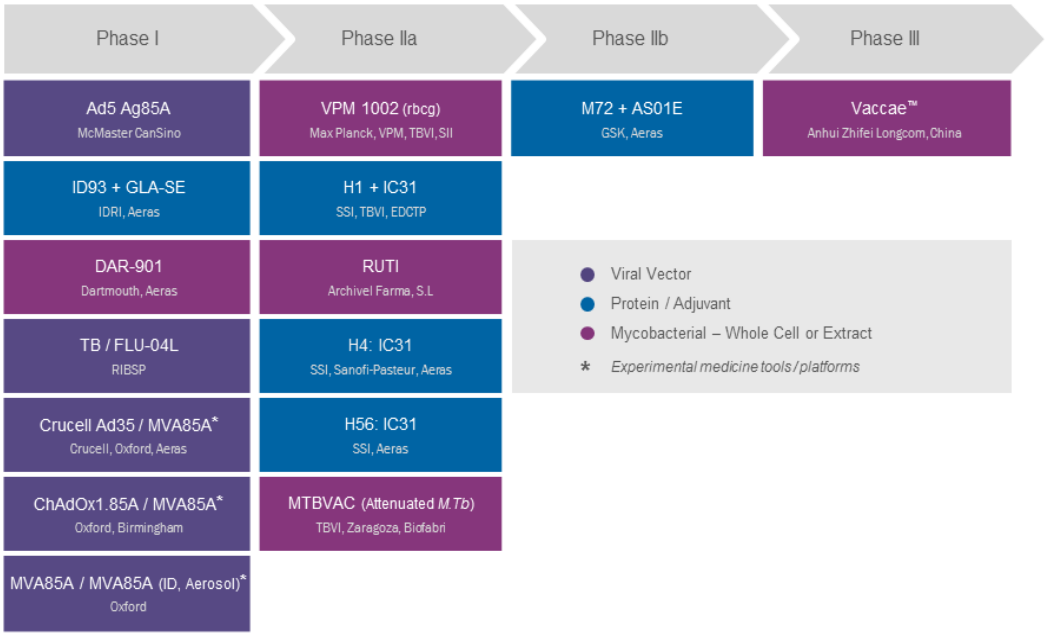

Sources: Aeras, 2015 - www.aeras.org; working group on new TB vaccines, 2015- www.newtbvaccines.org

Figure 1. 3 Global TB Vaccine development pipeline.

1.3.6 Tuberculosis: Detection

Tuberculosis diagnosis relies on acid fast staining of specimens (sputum, tissue or body fluids) after a process of decontamination using sodium hydroxide or oxalic acid (Eisenstadt and Hall, 1995). The staining is performed by using carbol-fuchsin stain (Zielh-Neelsen) with microscopy for the detection of pink bacilli. Carbol fuschin slides must be examined under oil immersion (x1000). Apart from microscopy, culture is considered the most sensitive method for TB diagnosis and it is carried out typically on Löwenstein-Jenson (LJ) slants containing malachite green dye, which prevents growth of other bacteria and fungi (Mitchison, 2005). The main drawback of culture is the long time required for cultivation as it is necessary to incubate for eight weeks before reporting a negative culture. Other growth detection systems have been introduced such as the Bactec system using a mycobacterial growth indicator tube

(MGIT), which contains a ruthenium-based dye for the detection of oxygen reduction in growing bacteria in Middlebrook 7H9 media (Tortoli *et al*., 1999).

GeneXpert MTB/RIF is a major advancement for TB diagnostics, especially for MDR-TB and HIV-associated TB. The Xpert MTB/Rif test is a cartridge-based fully automated nucleic acid amplification test for TB case detection and rifampicin resistance testing, suitable for use in disease endemic countries. It purifies concentrates, amplifies (by rapid, real time polymerised chain reaction) and identifies targeted nucleic acid sequences in the TB genome, and provides results from unprocessed sputum samples in less than 2 hours, with minimal hands-on technical time.

1.3.7. Tuberculosis: Treatment

Mycobacterium is extremely tolerant to chemical agents due to its impermeable cell wall which consist of a covalently linked mycolyl-arabinogalactan-peptidoglycan (mAGP) complex. The cell wall peptidoglycan, which is unique to bacteria, provides a rigid support that gives the cell its shape and maintains its turgidity. Peptidoglycan biosynthesis is the target of several clinically useful antibiotics such as the antimycobacterial drugs isoniazid, which inhibits mycolic acid synthesis and ethambutol, which inhibits the polymerization step of arabinan biosynthesis of arabinogalactan (Anishetty *et al*., 2005). However, the emergence of multidrug resistant varieties of *M. tuberculosis* has warranted a search for novel targets. The currently recommended short course chemotherapy for TB stemmed from 40 years of trials performed by the British Medical Research Councils' Tuberculosis Research centre in India (Santha *et al*., 1989). Drugs used for the management of tuberculosis can currently be grouped into first-line and second-line drugs.

First line-drugs include isoniazid (INH), rifampicin (RIF), pyrazinamide (PYR), ethambutol (EMB) and streptomycin (STR). Second-line drugs include kanamycin, amikacin, capreomycin, cycloserine, para-amino salicylic acid and fluoroquinolones. The most advantageous combination was found to be a two phase regimen based on four first line drugs INH, RIF, EMB and PYR for the first two months and INH and RIF for the next four months. Replacing EMB with STR gives an alternate drug regimen (Joshi, 2011).

Isoniazid and rifampicin are the most important anti-TB drugs used today, primarily because isoniazid is able to kill the bulk of the dividing bacteria, and rifampicin eliminates persisting bacterial cells, enabling the length of treatment to be considerably shortened (Mitchison, 2012). The appearance of drug resistance is prevented by adding pyrazinamide and ethambutol to the isoniazid and rifampicin regimen thus increasing the sterilizing power of the first two months regimen, and the full course of treatment can be reduced to six months.

Directly Observed Therapy (DOT) consist of an intermittent regimen of 8 weeks of thrice weekly isoniazid, rifampicin, pyrazinamide and streptomycin or ethambutol followed by a continuation phase of 18 weeks of thrice weekly isoniazid and rifampicin (Mitchison, 1998).

The virtual/video observed treatment (VOT) method is a new and alternative method to directly observed treatment (DOT). It requires people to send a short video of them taking their medication, to their healthcare provider using a mobile phone. After an initial visit to the clinic, this can be completed remotely, with any issues being followed up when required.

The recommended daily dose of the first-line drugs are INH 5 mg/kg (maximum 300 mg/day) RIF 10 mg/kg (maximum 600 mg/day) EMB 15 mg/kg (maximum 1 g/day), PYR 25 mg/kg (maximum 2 g/day) and STR 15 mg/kg (maximum 1 g/day) (Joshi, 2011).

The mechanism of action and resistance of these drugs is summarised in Table 1.1

Table 1. 1 Mechanism of action and resistance of first-and selected second-line anti-tubercular drugs.

Antibiotic	Structure	Modes/mechanism of action	Genes involved in resistance
First-line anti-TB drugs			
Isoniazid (1952)	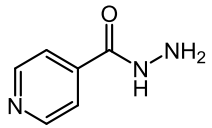	Bactericidal Inhibits mycolic acid synthesis, primary target is InhA.	*KatG, InhA*
Ethambutol (1961)	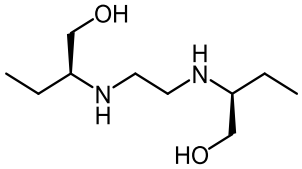	Bacteriostatic Inhibits arabinogalactan synthesis, possible EmbB.	*embB*
Pyrazinamide (1952)	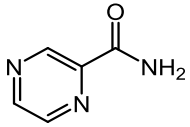	Bactericidal Primarily inhibits FAS-I or alters membrane energy.	*PncA*

Antibiotic	Structure	Mode of Action	Resistance mutations
Rifampicin (1966)	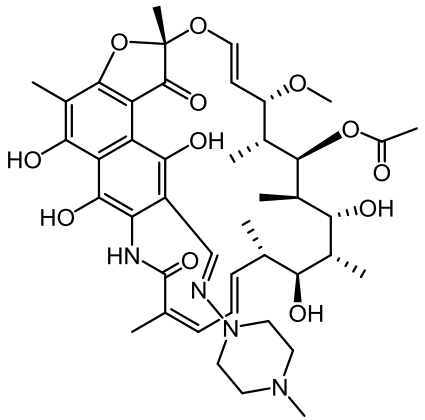	Bactericidal Inhibits transcription, RNA polymerase beta subunit.	*rpoB*
Streptomycin (1943)	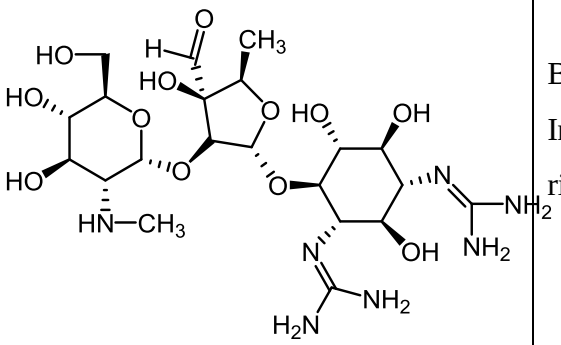	Bacteriostatic Inhibits protein synthesis, 30S ribosomal subunit.	*rpsL* , *rrs*

Antibiotic	Structure	Mode of Action	Resistance mutations
Second-line anti-TB drugs			
Fluoroquinolones (1976) e.g. ciprofloxacin	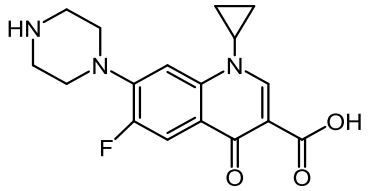	Bactericidal Inhibits DNA gyrase.	*gyrB*
Ethionamide (1956)	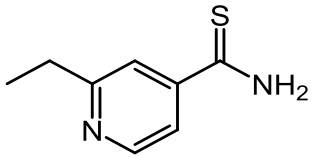	Bactericidal Inhibits mycolic acid synthesis.	*ethA, InhA*
Cycloserine (1952)	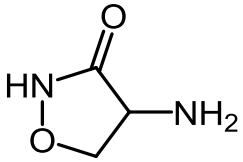	Bacteriostatic Inhibits peptidoglycan synthesis by blocking the synthesis and use of D-alanine, Ala racemase and D-Ala-D-Ala ligase.	*alrA, Ddl*

Antibiotic	Structure	Mode of Action	Resistance mutations
Amikacin (1976)	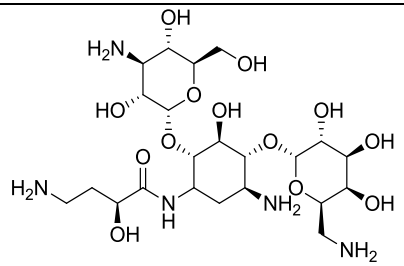	Bactericidal Inhibits protein synthesis	*rrs*
Capreomycin (1960)	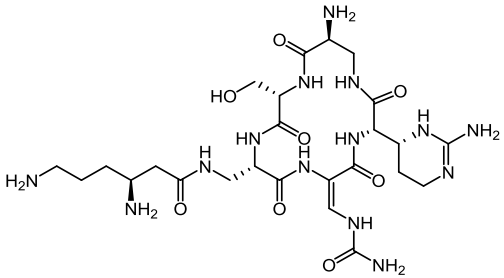	Bactericidal Inhibits protein synthesis, methylated nucleotides in ribosomal subunits	*tlyA* , *rrs*
Kanamycin (1957)	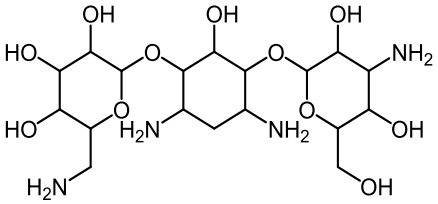	Bactericidal Inhibits protein synthesis	*rrs*

Mechanism of action and resistance of first and selected second line antitubercular drugs (Sacchettini *et al.*, 2008)

Isoniazid

Isoniazid also known as isonicotinic acid hydrazide (INH) is bactericidal to growing tubercle bacilli but has no activity against non-replicating bacilli. Its mechanism of action is inhibition of the synthesis of mycolic acid required for the cell wall. Isoniazid is a prodrug that is activated by the catalase-peroxidase Kat G protein to form an isoniazid adduct with NAD^+, which then inhibits one of the crucial enzymes of the fatty acid synthase-II (FAS-II), the enoyl-acyl carrier protein reductase InhA, required in the two carbon atom chain extension cycle for the biosynthesis of the long chain essential cell wall components known as mycolic acids (Rawat *et al*., 2003). Isoniazid resistances are attributed to mutations both on the activating KatG and on the InhA target genes.

Rifampicin

Rifampicin is bactericidal and inhibits RNA synthesis by targeting RNA polymerase *β*-sub units. The MIC of rifampicin is 0.1-0.4 mg/L for *M. tuberculosis* H_{37}Rv however; rifampicin-resistant strains have an MIC higher than 2 mg/L.

Ethambutol

Ethambutol produces bacteriostatic activity against proliferating cells and acts by inhibition of cell wall arabinogalactan synthesis by inhibiting the enzyme arabinosyl transferase. Arabinogalactan is one of the constitutive layers of the mycobacterial cell wall. The second line anti-TB drugs are used mainly in the treatment of drug-resistant TB strains. Second line drugs are more expensive, less effective, more toxic and with side effects.

Fluoroquinolones

The fluoroquinolones target principally type-II DNA topoisomerase known as DNA gyrase and type-IV topoisomerase, both of which are essential for altering the local

DNA topology in order for bimolecular processes such as transcription, recombination and replication to take place (Higgins *et al*., 2003).

Cycloserine

Cycloserine inhibits two enzymes of the peptidoglycan biosynthesis pathway, alanine racemase (Alr) and D-alanine ligase. Even though cyloserine is an effective agent, its use is limited by its toxicity (Simeon *et al*., 1970).

***Para*-aminosalicylic acid**

Para-aminosalicylic acid (PAS) targets the enzyme thymidalylate synthase, which is an enzyme catalysing the reductive methylation of deoxyuridine 5-monophosphate to deoxythymidine 5-monophosphate which is required for DNA synthesis.

Aminoglycosides

Amikacin and kanamycin both inhibit protein synthesis, specifically the 16S rRNA of the 30S ribosomal subunit. Kanamycin-resistant strains have an MIC greater than 200 mg/L and the resistance can be caused by enzymatic amino glycoside modification, specific methylation of rRNA or mutation in the 16S rRNA (rrs) (Suzuki *et al*., 1998). All amikacin-resistant strains are resistant to kanamycin but not all kanamycin-resistant strains are resistant to amikacin implying a more difficult step for the bacteria to become resistant to amikacin (Jugheli *et al*., 2009). The clinical adverse effect of the aminoglycosides is nephrotoxicity and/or ototoxicity caused by a perturbation of the membrane function of the cells, leading to damage of the renal tubule and/or vestibule (Begg and Barclay, 1995).

Capreomycin

Capreomycin is another important second-line anti-TB drug due to its ability to inhibit multi-drug resistant strains and non-replicative forms. The exact mechanism of action

is unknown but capreomycin interacts with the ribosome by inhibiting translation and therefore protein synthesis. This antibiotic has the same toxicity as the aminoglycosides causing ototoxicity and nephrotoxicity, but can also cause tubulopathy characterised by alkalosis (Di Perri and Bonora, 2004).

Thionamides

The thionamides, ethionamide and propionamide are similar in structure to isoniazid and they inhibit the same target, namely the enoyl-acyl carrier protein-reductase InhA, by a similar mechanism requiring activation to form adducts. The activation protein is thought to be EthA and not KatG as for isoniazid (DeBarber *et al*., 2000). However, isoniazid and the thionamides interact with the same pocket of the InhA enzyme and therefore some InhA mutations also confer resistance to the thionamides (Larsen *et al*., 2002).

1.3.8 Limitations of current treatment

Even though TB can be cured within 6-months, the main limitation to the current treatment of TB is non-adherence to the treatment regimen. Many patients fail to complete treatment for various reasons, which include drugs having unpleasant side effects, the complicated nature of treatment, patients not being aware of the consequences of the discontinuation of medication, and patients feeling better after several weeks of treatment. Poor compliance leads to patients remaining infected for longer periods and mostly suffer a relapse and die.

1.3.9 Drug resistance in tuberculosis

The problem of drug-resistant TB and the need to shorten the lengthy TB chemotherapy makes TB drug development challenging. Drug-resistance was reported since the introduction of the first anti-TB drug, streptomycin which was used as a monotherapy and this led to the introduction of combination therapy. These regimens were effective in preventing the emergence of resistance because combination chemotherapy makes it highly unlikely that there will be a spontaneous mutant resistant to all of the components of chemotherapy (Gillespie, 2002). However, a better understanding of the molecular mechanisms of drug resistance in TB assists in the exploration of new targets for drug activity and drug development. Resistance in Mycobacteria is either intrinsic or acquired (Piddock, 2014, Viveiros *et al*., 2003).

Intrinsic resistance: The intrinsic drug resistance of *M. tuberculosis* has traditionally been attributed to the unusual structure of its mycolic acid-containing cell wall (Figure 1.4) that gives the bacteria a low permeability for many compounds such as antibiotics and other chemotherapeutic agents (Dmitriev *et al*., 2000, Niederweis *et al*., 2010). The peptidoglycan and arabinogalactan layers limit the entry of hydrophobic molecules, whereas the mycolic acid layer limits the access of both hydrophobic and hydrophilic molecules (Jarlier and Nikaido, 1994). Relatively hydrophobic antibiotics, such as rifampicin and fluoroquinolones, may enter the cell by diffusion through the hydrophobic bilayer, whereas hydrophilic antibiotics and nutrients use porin-like channels (Nguyen and Thompson, 2006).

Working synergistically with mycobacterial cell wall impermeability are efflux pumps which have been recognized as an important factor in the natural resistance of mycobacteria against antibiotics such as tetracycline, fluoroquinolones and aminoglycosides (Viveiros *et al*., 2012, Machado *et al*., 2012).

Acquired resistance: Acquired drug resistance in *Mycobacterium* is caused mainly by spontaneous mutations in chromosomal genes, producing the selection of resistant strains during sub-optimal drug therapy. This is different in other bacteria where acquired drug resistance is generally mediated through horizontal transfer by mobile genetic elements, such as plasmids, transposons or integrons (Kochi *et al*., 1993). The selection of naturally occurring drug-resistant mutants happens when the therapeutic regimen is not correctly followed. This is intimately associated with the long generation time of *M. tuberculosis*, its low metabolic activity and its ability to enter dormancy (Ramaswamy and Musser, 1998).

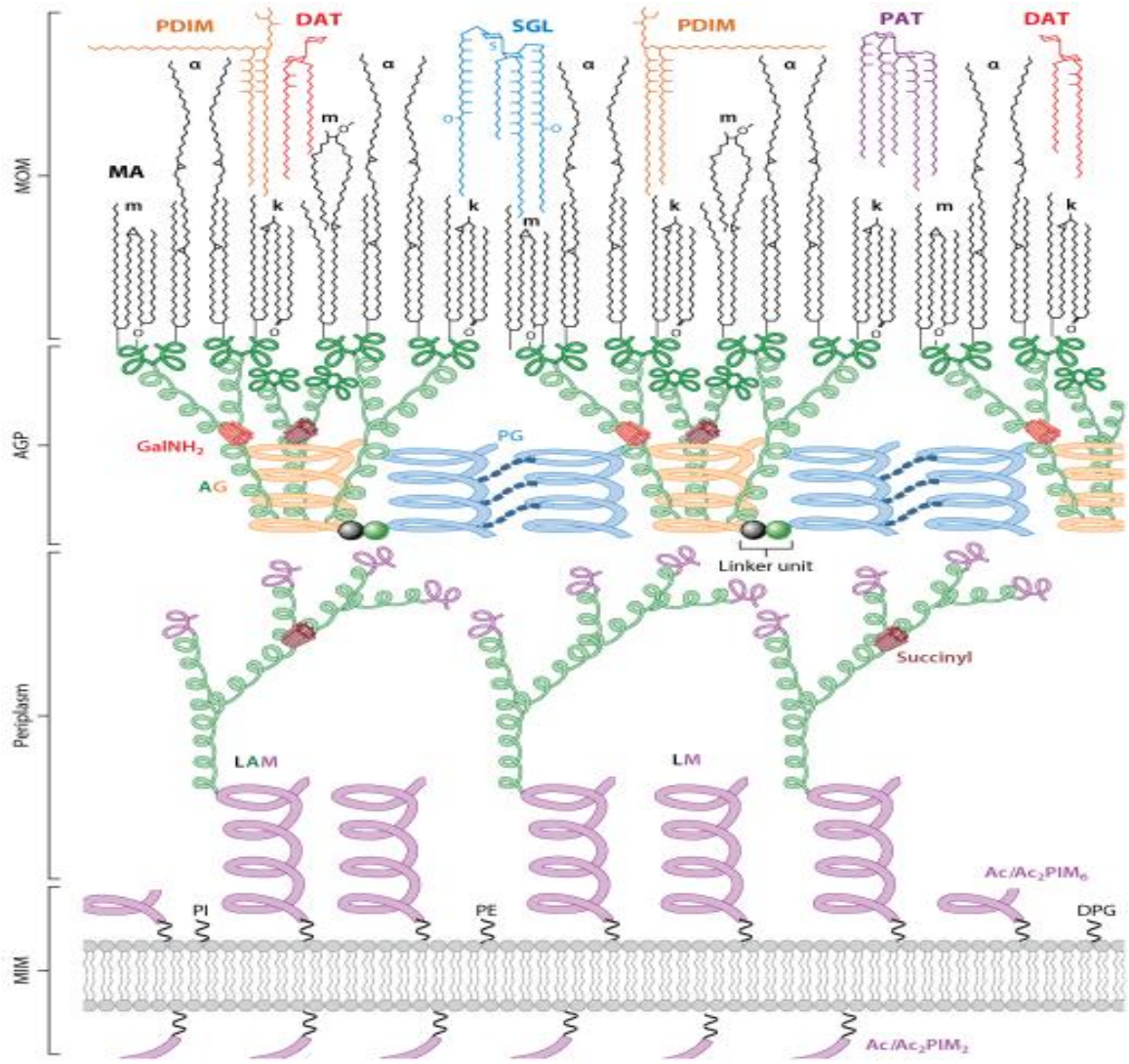

Figure 1. 4 The cell wall structure of mycobacteria comprising of the arabinogalactan peptidoglycan and mycolic acid layers.

(Adopted from Jankute M. *et al*., Annual Reviews in Microbiology, 2015: 69:405-423).

(AG, arabinogalactan; AGP, arabinogalactan-peptidoglycan complex; DAT, diacyltrehalose; DPG, diphosphatidylglycerol; $GalNH_2$, galactosamine residue; k, keto; LAM, lipoarabinomannan; LM, lipomannan; m, methoxy; MA, mycolic acids; MIM, mycobacterial inner membrane; MOM, mycobacterial outer membrane; PAT, polyacyltrehalose; PDIM, phthiocerol dimycocerosate; PE, phosphatidylethanolamine; PG, peptidoglycan; PI, phosphatidyl-*myo*-inositol; SGL, sulfoglycolipid).

1.4. Multidrug efflux pumps

Efflux pumps are membrane-spanning proteins involved in the outward transport of a wide variety of substrates to the exterior of the cell in an energy-dependent manner (Viveiros *et al*., 2003, Stavri *et al*., 2007, da Silva *et al*., 2011, Piddock, 2014). Bacterial efflux transporters can be organized into several families according to their energy source, the type of substrate that the pump exports and phylogenetic relationship. The five main families primarily based on amino acid sequence homology are the major facilitator (MF) superfamily, the resistance-nodulation-division (RND) family, the small MDR (SMR) family, the ATP binding cassette (ABC) family and the multiple antibiotic and toxin extrusion (MATE) family (Figure 1.5).

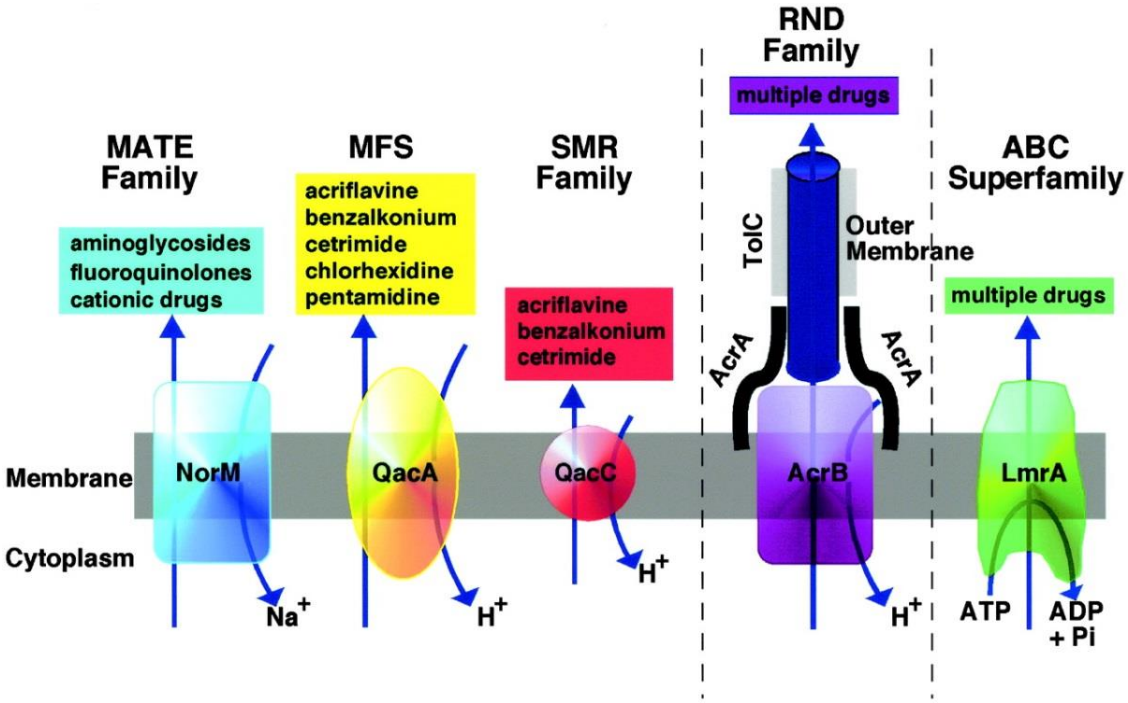

Figure 1. 5 Diagrammatic comparison of the five families of efflux pumps.
(Adopted from Laura J. V. Piddock *Clinical Microbiology Rev*iews 2006; 19:382-402).

The first three families achieve the energy required to extrude a drug out of the cell via the proton motive force in a proton-drug antiport system, whilst the MATE family is driven by the exchange of either proton or sodium ions. In contrast, the ABC family couples drug extrusion with the hydrolysis of ATP (Piddock, 2006, Blair *et al*., 2015, Almeida Da Silva and Palomino, 2011). Every class of the five existing families of efflux pumps is present in *M. tuberculosis* (Lechner *et al*., 2008, De Rossi *et al*., 2006).

The expression of efflux pumps has been implicated in multidrug resistance. Efflux pumps can be specific for one substrate or can transport a range of structurally dissimilar compounds (including antibiotics of different chemical classes). Those pumps that transport several compounds can be associated with multidrug resistance (MDR). In mycobacteria, it has been proven that efflux emerges prior to acquisition of mutations in the drug target genes and that overexpression of efflux pump genes results in an increase in antibiotic resistance and in particular following isoniazid and ethambutol exposure, conferring a low-level resistance phenotype (Lomovskaya and Bostian, 2006, Morris *et al*., 2005, Srivastava *et al*., 2010). Most likely, this prolonged exposure to sub-inhibitory antibiotic concentrations may increase the probability of acquiring mutations in genes encoding the target protein. This will result in the emergence of a new subpopulation of mycobacteria presenting a high-level resistance phenotype, as already seen in other groups of bacteria (Quinn *et al*., 2006, Piddock, 2006, Nikaido and Pagès, 2012).

1.5. Efflux pump inhibitors

Multidrug resistance due to the expression of efflux pumps is a major clinical challenge which renders many antibiotics redundant. In order to suppress the rise of MDR bacteria novel antibiotics with new modes of action are urgently required. Alternatively, identification of molecules that can circumvent or interfere with the process of efflux is a potential way forward given the contribution of efflux systems to the development of drug resistance (Viveiros *et al*., 2012, Piddock, 2014). Mycobacterial efflux pump inhibitors include verapamil, a calcium channel blocker used for the treatment of various disorders, such as angina, hypertension and cardiac arrhythmia and it is also an inhibitor of P-glycoprotein (Andersen *et al*., 2006); the phenothiazines (chlorpromazine, thioridazine and fluphenazine) which are antipsychotic drugs, and natural plant metabolites like the alkaloid extracted from the root of the climbing shrub *Rauwolfia*, reserpine, which has been used for decades as an antihypertensive agent but now no longer used (Lemieux *et al*., 1956). Several studies have demonstrated that verapamil, chlorpromazine, thioridazine and reserpine possess the capacity to inhibit efflux of ethidium bromide by *Mycobacterium* (Gibbons and Udo, 2000, Lechner *et al*., 2008, Stavri *et al*., 2007, Rodrigues *et al*., 2011, Viveiros *et al*., 2012, Rodrigues *et al*., 2008).

The rationale for our interest in this area of research is based on the fact that, the inhibition of efflux activity with a non-antibiotic inhibitor may restore activity of an antibiotic subject to efflux and thus provide a way to enhance the activity of current anti-TB drugs. Therefore, the use of bacterial resistance modifiers such as EPIs could facilitate the re-introduction of therapeutically ineffective antibiotics back into clinical use (such as ciprofloxacin and streptomycin) and might even suppress the emergence of MDR strains.

The ethidium bromide efflux inhibition assay is a detailed study of the potentiation activity of a test compound. Ethidium bromide is a substrate for a number of MDR efflux pumps. The activity of putative inhibitors can be measured fluorimetrically due to the retention of fluorescence over time if efflux is reduced (Lechner *et al*., 2008, Rodrigues *et al*., 2008, Rodrigues *et al*., 2011).

1.6 Biofilms

Biofilms are structured multicellular aggregates of bacterial cells that are embedded in self-produced extracellular polymeric substances (EPS) (Flemming and Wingender, 2010, O'Toole *et al*., 2000, Junutula *et al*., 2010). The biofilm matrix offers protection to the microbial community from various host-derived, environmental and xenobiotic stresses. The formation of a biofilm is generally established through several steps: Initially, planktonic cells attach to the surface in a process known as surface attachment; once attached to the surface, biofilm-associated bacteria initiate the synthesis of an extracellular matrix, which generally signifies their commitment to a sedentary existence. It is at this maturation stage that they form a structured architecture. After maturation, the cell leaves the biofilm in the dispersal stage. Each stage is affected by several environmental factors and is a highly regulated process (Branda *et al*., 2005). The ability to adopt a strategy which enables bacteria to adhere to different medical devices, forming biofilms makes it possible to evade antibiotics and host-immune responses, thereby making the threat they pose to human health a very serious concern. Targeting biofilm formation is therefore a key mechanism for the development of new therapeutic interventions (Lewis, 2007, Baugh *et al*., 2012).

Biofilms are clinically significant and there are many examples of human infections caused by biofilms, including *Pseudomonas aeruginosa* in the lungs of cystic fibrosis

patients, *Legionella pneumophilia* causing legionellosis, many bacterial species involved in periodontal diseases and various device-associated infections of temporary and permanent medical devices (Benoit *et al*., 2010, De Kievit *et al*., 2001).

Biofilms are difficult to eradicate due to their inherent drug resistance; the concentration of many antibiotics needed to kill bacteria when residing in a biofilm can be up to 1000 times greater than that required to kill cells from corresponding planktonic cultures (Watnick and Kolter, 2000).

Multidrug efflux pumps have been recognised as playing a central role in the biology of bacteria and have roles in drug resistance, cell division, pathogenicity and, as recently described, the formation of biofilms (Kvist *et al*., 2008, Baugh *et al*., 2014). The demonstration that EPIs can prevent biofilm formation whilst also potentiating antibiotics and possibly reducing the pathogenic potential of virulent bacteria suggests that there may be value in the discovery and development of compounds as EPIs which can also serve as anti-biofilm agents (Jonas *et al*., 2007, Baugh *et al*., 2014).

1.7 Aims and Objectives

The aim of this project was to discover novel phytochemicals and to evaluate their antimicrobial potential as well as possible modes or mechanism of action

The specific objectives were:

1. Bioassay-guided isolation and characterisation of compounds from the genera *Allium* and *Andrographis.*
    a. To screen extracts from different species for their inhibitory activity against *Mycobacterium aurum, M. bovis* BCG, *M. tuberculosis* H_{37}Rv and multi-drug-resistant variants of *Staphylococcus aureus* as well as other selected Gram-positive and Gram-negative bacteria.
    b. To fractionate, isolate and purify compounds from selected species and to test for their possible antibacterial activity.
    c. To characterise the compounds using various spectroscopic techniques **(Chapter 3 - *Allium*)** and **(Chapter 5 - *Andrographis*)**.

2. To synthesize analogues of isolated natural products.
    a. To evaluate their inhibitory activity against different species of *Mycobacterium*, Gram-positive and Gram-negative bacteria as well as fungi.
    b. To study the modes and mechanisms of action of the bioactive compounds such as their possible inhibition of multidrug efflux pumps and inhibition of biofilms and to carry out selective eukaryotic cell toxicity assays in order to determine the therapeutic indices **(Chapter 4)**.

Chapter 2: Materials and Methods

2.1 Chemicals and reagents

Solvents: acetonitrile, methanol and water (HPLC grade) were obtained from Fisher Scientific UK, Ltd. Chloroform, hexane, petroleum ether, ethyl acetate and butanol were purchased from Sigma-Aldrich, UK. Deuterated solvents: methanol-D_4 (CD_3OD) 99.8%, chloroform-D ($CDCl_3$), dimethyl sulfoxide-D6 ($(CD_3)_2S=O$), deuterium oxide (D_2O) were from Cambridge Isotope Laboratories, Inc. (CIL). Thin layer chromatography visualisation reagents used included vanillin, p-anisaldehyde and dragendorff. Composition and preparation of the spray reagents is described. Vanillin - 0.5 g of vanillin was dissolved in 80 ml sulphuric acid and 20 ml ethanol. P-anisaldehyde - 0.5 mL p-anisaldehyde was mixed with 10 mL glacial acetic acid, followed by 85 mL methanol and 5 mL concentrated sulphuric acid, in that order.

Dragendorff Reagent Preparation - Solution A: 1.7 g basic bismuth nitrate in 100 mL water/acetic acid (4:1). Solution B: 40 g potassium iodide in 100 ml of water. The reagents were mixed together as follows: 5 mL A + 5 mL B + 20 mL acetic acid + 70 mL water. Middlebrook 7H9, Middlebrook 7H10, albumin-dextrose-catalase (ADC, Difco™) and oleic acid-albumin-dextrose-catalase (OADC, Difco™) were purchased from BD Diagnostics, UK. Nutrient agar, Muller Hinton broth and Muller Hinton agar were purchased from Oxoid Limited, UK. Luria Bertani broth, Sabouraud's dextrose broth, Sabouraud's dextrose agar, RPMI-1640 medium, 3-(4,5-dimethylthiazole-2-yl)-2,5-diphenyltetrazolium bromide (MTT), dimethyl sulfoxide, antibiotics (isoniazid, rifampicin, norfloxacin, oxacillin, erythromycin, and tetracycline) and other reagents namely trypan blue, lidocaine, glycerol (50 % v/v), tween-80 (0.05%) and L-glutamine were obtained from Sigma-Aldrich, UK. Sodium chloride and

ethylenediaminetetraacetic acid (EDTA) were procured from Fisher Scientific UK Ltd.

2.2 Apparatus

For analytical thin layer chromatography, aluminium plates coated with silica gel 60 F_{254} (Merck KGaA) were used. Silica gel 60 F_{254} (Merck KGaA) was used for column chromatography. For visualizing TLC plates, CAMAG UV Cabinet dual wavelength, 254/366 nm, 2 x 8 watt in combination with CAMAG Viewing Box 3 was used. Ultrasonic water bath (Grant instruments), BUCHI Rotavapor (R-200), freeze dryer (Thermo savant modulyoD-115), Solid phase extraction (SPE) was performed using Si-1 silica normal phase and C18 reverse phase (55 µm, 70 Å), 10 g / 60 mL, Giga tubes Strata® columns from Phenomenex. Mettler Toledo AB 135-S/Fact analytical balance was used for taking weights. Nuclear magnetic resonance (NMR) tubes were from Sigma-Aldrich. The NMR spectra were recorded on a Bruker AVANCE 400 MHz and 500 MHz spectrometers. The NMR spectra were processed using Topspin Version 1.3 NMR software. The infrared (IR) spectra were recorded on PerkinElmer Spectrum 100 FT-IR spectrometer and data was analysed using PerkinElmer Spectrum Express version 1.02.00 software. The UV spectra were recorded on a Helios alpha version 7.09 spectrophotometer and the VISIONpro software was used for data collection. The Mass spectra were recorded on a Thermo LCQ Duo Mass Spectrometer coupled with an LC system for nominal mass determination, and on a Micromass Q-TOF premier Tandem Mass Spectrometer for accurate mass determination. The software used for nominal mass measurement on the LCQ-duo instrument was Xcalibur™ version 1.2 SP1 and for accurate mass measurement on the Q-Tof was MassLynx™ Version 4.1.

The culturing and handling of *Mycobacterium* was performed in a Class-II TopSafe 1.2 BioAir Euroclone laminar biosafety cabinet with the exception of *M. tuberculosis*, which was handled in a Class-III biosafety cabinet in a containment laboratory under negative pressure and all air filtered through Hepa filters. Bacteria other than mycobacteria were handled in a Class-II ultrasafe laminar biosafety cabinet.

The Sartorius Certomat® 15 shaking incubator and Wheaton® roll-in standard incubator were used for incubation of *Mycobacterium* cultures. Ultracentrifugation was carried out in a Beckman Coulter J-26XP Avanti centrifuge with temperature control. Water bath (Grant Instruments), Gilson pipettes (single and multichannel) dispensing volumes 2-200 µL. Fridges (14 ºC) and freezers (-80 ºC and -4 ºC) were employed. A WPA Biowave DNA spectrophotometer was used in taking optical density readings. A Multidrop® combi dispenser (Thermo Scientific) was used for dispensing agar.

Microscopic digital images of bacterial and mammalian cells were captured using a light microscope and inverted microscope respectively with adapted Canon Powershot G10 camera. The FEI Quanta 200F Scanning Electron Microscope was used to capture Scanning Electron Microscopic images with the assistance of Mr David McCarthy, UCL School of Pharmacy, UK.

Microbiological consumables included antimicrobial susceptibility testing discs and blank sterilized discs which were purchased from Oxoid Limited, UK. Petri dishes (9 cm), 96-well microtitre plates, pipette tips, universal containers, polypropylene tubes were obtained from Greiner Bio-one Ltd, UK.

2.3 Microorganisms and cells

Mycobacterial strains: Fast-growing *Mycobacterium smegmatis* mc^2 155 (ATCC 700084) and *Mycobacterium aurum* (ATCC 23366); slow-growing *Mycobacterium bovis* BCG Pasteur (ATCC 35734) and *Mycobacterium tuberculosis* $H_{37}Rv$ (ATCC 27294) were used in this study. Multidrug-resistant clinical isolates (MDR 1 and MDR 2) were obtained from Professor Timothy D. McHugh at the Centre for Clinical Microbiology, University College London, Royal Free Hospital, UK.

Other bacterial strains: Gram-positive *Staphylococcus aureus* strains such as methicillin-resistant *Staphylococcus aureus* (MRSA 12981), methicillin-susceptible *Staphylococcus aureus* (MSSA 13373), SA-1199B a fluoroquinolone-resistant *Staphylococcus aureus* which overexpresses the NorA multidrug-resistant efflux pump (Kaatz *et al*., 1993), a tetracycline-resistant MRSA, XU212, which possesses the *tet*(K) gene which encodes for the Tet(K) efflux protein (Gibbons and Udo, 2000), RN4220 contains the Msr(A) macrolide efflux protein (Ross *et al*., 1989), epidemic methicillin-resistant *Staphylococcus aureus* (EMRSA-15) found in the United Kingdom (Richardson and Reith, 1993) and *Enterococcus faecalis* NCTC (12697) were used in this study. Gram-negative strains used included *Escherichia coli* (NCTC 10418), *Klebsiella pneumoniae* (17), *Proteus mirabilis* (10830) obtained from Dr Paul Stapleton at the School of Pharmacy, University College of London.

Mammalian cells: Murine macrophages RAW 264.7 (ATCC TIB71) provided by Professor Siamon Gordon, University of Oxford, UK were used for the assessment of cytotoxicity.

Fungal strains: Dermatophytic strains used included *Trichophyton rubrum* (CBS 118892), *Trichophyton tonsurans* (CBS 112818), *Trichophyton equinum* (CBS

127.97) and *Trichophyton mentagrophytes* (MUCL 9823) from Dr Jane Faull, Department of Biological Sciences, Birkbeck, University of London.

2.4 Phytochemical extraction

In the isolation of compounds, the first step was to generate extracts from the plant material followed by chromatographic and spectroscopic analysis. The plant material was chopped up, dried and powdered to increase the surface area of contact with the solvent which ultimately increased the yield. Solvent extraction was the technique used to obtain the extracts. This was referred to as solid-liquid extraction and was carried out by either ultrasonication (without heat) or Soxhlet extraction which involved the application of heat. Cold extraction, a soft extraction method had the advantage that the extract was not heated and there was little potential degradation of natural products.

In this research, all the thermolabile samples were extracted using cold extraction by **ultrasonication**. Ultrasound-assisted extraction employs mechanical stirring and sound energy to agitate particles in a sample to increase both the diffusion rate and the surface of solvent-plant material contact. The phenomenon of cavitation involved in ultrasonication promotes a better penetration of solvent into the plant cells releasing the contents with a resultant benefit of increased extraction yield. Organic solvents were evaporated off using a rotavap and water extracts were freeze dried.

Soxhlet extraction was used for non-thermolabile plant samples. It involved a continuous recycling of the same batch of solvent by condensing vapours of the solvent with a water cooling system to obtain a concentrated extract. Solvents of

increasing polarity were used sequentially, starting with a non-polar solvent hexane, medium-polar chloroform and finally a polar solvent such as methanol.

Acid-base extraction was used for the extraction of alkaloids. The dried plant material (or methanol extract obtained from Soxhlet extraction) was made alkaline with aqueous ammonia. This left the alkaloids as free bases that were no longer ionic salts and were more soluble in organic solvents such as ethyl acetate (EtOAc) or dichloromethane (DCM). The free bases were then partitioned into EtOAc and separated from the aqueous ammonia layer in a separating funnel as the solvents formed immiscible layers. The EtOAc layer containing the free bases were then extracted with aqueous acid by extracting three times with hydrochloric acid (HCL) and the alkaloids were transferred from the organic phase to the aqueous phase as hydrochloride salts (the remaining EtOAc layer was tested with Dragendorff's reagent to ensure that all of the alkaloids had been transferred to the acidic aqueous layer). This acidic layer was basified resulting in the precipitation of the alkaloids (no longer soluble in aqueous media), which were then extracted back into an organic solvent such as ethyl acetate or dichloromethane. Figure 2.1 shows the various extraction techniques used to obtain the plant extracts.

Figure 2.2 Extraction techniques used to obtain plant extracts (a-e: soxhlet extraction, acid-base extraction, ultrasonication, freeze drying, filtration, and rotary evaporation respectively).

2.5 Chromatographic techniques

Chromatography is a physical method of separation in which the components to be separated are distributed between two phases, the stationary and the mobile phase. Chromatographic techniques are therefore effective for the separation, identification, and determination of closely related components of complex mixtures and are useful analytical techniques for the isolation of natural products. The method largely depends on the adsorption and/or partition effects of the stationary phase to achieve the separation of components. A wide range of stationary phase adsorbents are available, which can be used depending on the chemistry of the sample to be separated. However, standard sorbents normally used were silica gel for the separation of non-polar extracts and C18 for more polar extracts.

Normal phase chromatography utilises a polar stationary phase and non-polar solvents to achieve an effective separation. Silica gel is a popular adsorbent for natural product separation as it can be used with a wide range of organic solvents, acids and bases. The surface of the silica gel matrix is composed of exposed silanol groups that give rise to the interaction between the compounds and the stationary phase. Natural products with polar functional groups interact with the hydroxyl groups by hydrogen-bonding and are only displaced by increasing the solvent polarity.

For reversed phase chromatography, the stationary phase is composed of a non-polar matrix and polar solvents are used to elute the sample constituents. Reverse phase silica is created by the chemical modification of silica gel with chloro alkoxysilanes (most frequently C8 and C18). Unlike silica gel, reverse phase silica can withstand the use of polar solvents such as water and therefore the separation of highly polar natural products is possible. Chromatographic separation is highly dependent on the choice of mobile phase. (Douglas and Skoog, 2007). Chromatographic techniques used during this study are described below.

2.5.1 Vacuum liquid chromatography

Vacuum Liquid chromatography (VLC**)** is a useful technique for the initial fractionation of crude extracts. In this method, vacuum was applied to the bottom of the column filled with silica gel 60 (0.040-0.063 mm; 230-400 mesh, Merck KGaA) which increased the velocity of elution. The advantage of VLC is that a large quantity of the crude extract, which is usually formulated into a free flowing powder adsorbed on to silica, can be loaded. Solvent elution was commenced with the solvent of lowest polarity to the solvent of highest polarity by a 10 % step by step increment. Solvents

used were *n*-hexane, ethyl acetate and methanol. After collecting the fractions the solvent was evaporated off to obtain the fractions, which were further analysed by other phytochemical and spectroscopic techniques.

2.5.2 Solid phase extraction

Solid Phase Extraction (SPE) is generally used for the fractionation, purification and separation of compounds for analysis. In this separation technique, compounds dissolved or suspended in a liquid are separated according to their affinity for a solid through which the sample is passed depending on its physical properties. This technique has the advantage of using pre-packed cartridges and relatively small amounts of solvent to achieve effective separation and additionally, it is rapid and easy to perform. The SPE tube was attached to a vacuum manifold and primed with 200 mL of the same solvent as the starting conditions used for fractionation. The sample (50-300 mg) was then dissolved in the same solvent and applied evenly to the top of the column with a Pasteur pipette. Fractions were collected in 100 mL round bottom flasks. The flow rate was controlled by altering the amount of vacuum applied. Creating a slow flow allowed more interaction between the sample and adsorbent and therefore a better separation. Starting conditions for SPE were determined by analytical TLC where the highest Rf value was not more than 0.3. A gradient solvent system was used. The SPE columns are of different sizes, for example Strata SI-silica 10 g/60 mL Giga tubes (Phenomenex) were used for normal phase separation with non-polar solvents and C18 for reverse phase.

2.5.3 Column chromatography

Column chromatography can be used for further fractionation of extracts after using VLC or SPE and it is also widely used as a purification technique. The quantity of the analyte determines the size of the column and the quantity of stationary phase, which is usually silica gel. The first step was to pack the column by making a slurry of the stationary phase using the eluting solvent of lowest polarity. This was slowly poured down the column whilst tapping the column gently to ensure that the packing was homogeneous. The sample was then loaded onto the wet silica gel either dissolved in a minute quantity of solvent or loaded as a dry powder by mixing with silica. The column was prevented from drying out by adding eluting solvent frequently.

2.5.4 Thin layer chromatography

Thin layer chromatography (TLC) is generally used to analyse and separate plant extracts, to identify compounds present in them and to determine the purity of a substance. The method is based on the different migration properties of a compound in different solvents depending on their solubility and polarity. It utilises a thin layer of sorbent which is applied to a rigid inert backing (glass or aluminium) for the separation of compounds. This technique has a number of advantages over other chromatographic methods in that the materials used for making the plates are relatively cheap; only small amounts of analyte are needed, the process is quick and easy for the purification of a small number of components or the analysis of complex mixtures (Poole, 2003).

For analytical TLC the samples were dissolved in a volatile solvent and applied as small spots approximately 1 cm from the bottom of the plate. The plate was placed in

a developing tank containing the appropriate solvent system and allowed to develop until the solvent front was approximately 1 cm from the top of the plate.

Preparative TLC was performed similarly however, the sample was applied as a narrow band across the plate (1.5 cm from the bottom) but was developed in the same way and once the desired bands had been detected, the sorbent was scraped from the backing and transferred into a beaker where the sample was washed from the silica. The solvent mixture migrated to the top of the plate by capillary action. The strength of the solvent mixture and the affinity of compounds for the sorbent determined which compounds will travel to the top of the plate. For polar compounds, the solvent mixture needs to have polar properties and vice versa. The fluorescent coating on the plates allowed visualization of UV active compounds once viewed under long- and short-wave UV light, while non-UV active compounds were visualized by application of staining reagents.

To quantify the migration of the compounds on a particular plate and the solvent system, the Retention Factor (Rf) value was used and defined as:

$$Rf = \frac{\text{Compound distance from the origin}}{\text{Solvent front distance from the origin}}$$

In this research, a small quantity of the plant extracts was dissolved in 50 μL of the appropriate solvent. The sample was applied 1 cm from the bottom of a silica gel 60-F254 pre-coated TLC plate which was then placed in a tank saturated with an appropriate mobile phase. After the separation was completed, the plate was air dried and viewed under UV (254 and 366) nm to determine the absorbance and fluorescence properties of the separated compounds. Substances that absorbed UV light appeared dark in short wavelength UV-254 nm and those that fluoresce in long

wave ultraviolet light UV-366 nm appeared bright as either blue or yellow bands. The plates were sprayed at the edge with different detection reagents to visualize the characteristic compounds. The spray reagents used were anisaldehyde and 4 % vanillin both in concentrated sulphuric acid.

2.5.5 Preparative thin layer chromatography

Preparative thin layer chromatography (PTLC) is a technique for the purification of compounds. The process involved extracting the compounds adsorbed on a silica plate after separation was achieved by the eluting power of a mobile phase. The sample was uniformly applied as a band to the bottom of the TLC plate with a capillary tube. When the components were separated based on their Rf, the bands were observed by UV or by using a visualisation spray reagent applied to the edge of the plate. The bands containing pure compounds were scraped off the plate into a beaker and sonicated for a few minutes with solvent to help extract the compound which was filtered from the silica. The solvent was dried off and the compound was further analysed using spectroscopic techniques. The PTLC technique was very useful provided the right solvent system was selected such that compounds were well separated on the TLC plate. Several PTLC plates were used when the quantity of analyte was large. The TLC plates were run many times using the same mobile phase in some cases as this also contributed to a good separation since the compounds separated further every time leading to an overall better separation.

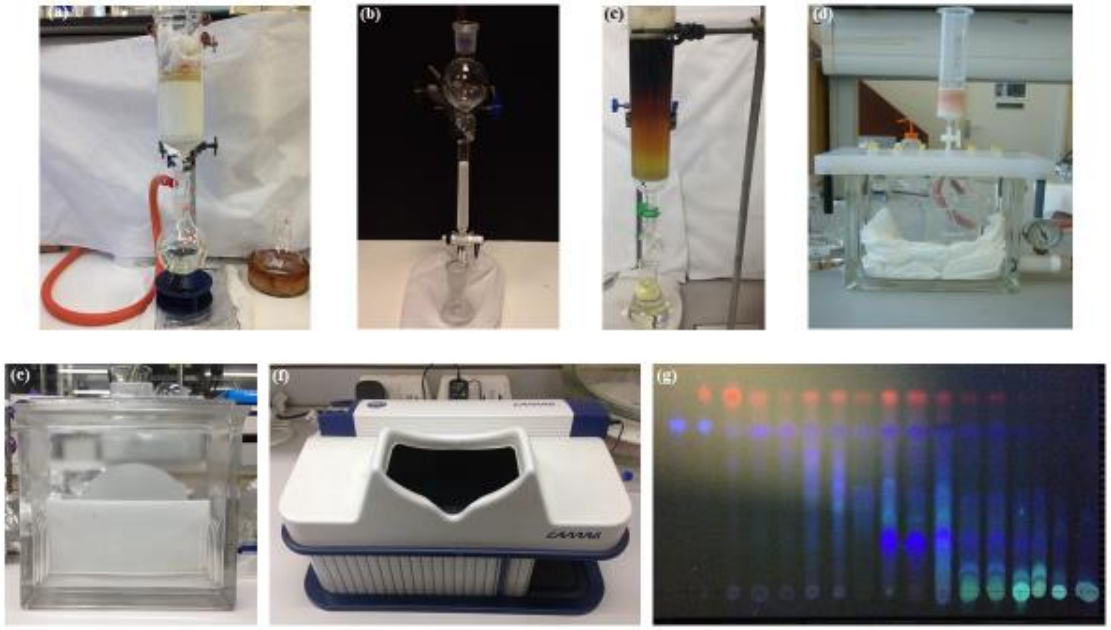

Figure 2.3 Chromatographic techniques ((a) VLC, (b & c) column chromatography (d) SPE, (e-g) TLC tank, TLC visualizer and TLC plate respectively).

2.5.6 High performance liquid chromatography

High performance liquid chromatography (HPLC) is an efficient, fast and versatile technique. Elution can be carried out using the same solvent composition (isocratic) or by using a changing solvent composition during the time of the run (gradient). To obtain high purity, the isocratic method is preferred to the gradient system, which is good for fast analysis (Ivanov *et al*., 2000, Koza *et al*., 2012). Reverse phase columns (C18) are largely used even though normal phase columns could be used. Two types of HPLC were largely used in this research. The analytical-HPLC, which helped in the identification or quantification of the compounds present in a sample and Preparative-HPLC, which helped in the purification of the compounds present in the sample. Isocratic elution was used for preparative-HPLC with the injection of 500-1000 µL of a sample while the selection of an appropriate mobile phase was done using analytical-HPLC with the injection of very small quantities of the sample, 2-10

µL. The HPLC systems had a fraction collector that enabled the consistent collection of a chromatographic peak into the same vial. In this research, samples were prepared by dissolving 5-50 mg in methanol (500-1000 µL). The mixture was vortexed for 1 minute and filtered through a 0.45 µm membrane into an HPLC vial, which was then placed in the HPLC chamber prior to injection. The HPLC solvents were also sonicated for 30 minutes to degas them. The HPLC instrument used was an Agilent 1100 Series system consisting of a solvent reservoir, a degasser, dual HPLC pumps an automated injection port, a UV visible detector and a fraction collector. An Ascentis® C18 HPLC column (Supelco) 150 x 4.6 mm was used, with an injection volume of 10 µL, column temperature 25 ºC, DAD detector 254 nm, and a flow rate was 1 mL/minute. The collected samples were dried by nitrogen gas or freeze dried to obtain pure compounds, which were weighed and subjected to spectroscopic analysis.

Figure 2. 4 High performance liquid chromatography.

2.6 Spectroscopic techniques

Spectroscopic techniques are widely used to characterize or determine the structures of isolated compounds. In this research, Nuclear Magnetic Resonance (NMR) and Mass Spectrometry (MS) were mostly used for the structure elucidation of isolated and synthesised compounds, while Infrared (IR) and Ultraviolet (UV) spectroscopy helped by determining the presence of certain functional groups and conjugation in the molecules respectively.

2.6.1 Nuclear magnetic resonance spectroscopy

Nuclear Magnetic Resonance (NMR) spectroscopy is considered the most powerful tool in organic structure analysis. The development of high-field NMR spectrometers with increased sensitivity, resolution, and dynamic range, has made possible the rapid study of complex mixtures of compounds. The NMR spectroscopy utilizes the fact that the atomic nuclei of many elements have magnetic properties. These atomic nuclei have a nuclear spin (*I*), and the presence of spin makes them behave like bar magnets. Nuclear magnets can orient themselves in $2I+1$ ways when a magnetic field is applied to them. Both ^{1}H and ^{13}C have spins of $\frac{1}{2}$, providing two spin states that allow a spherical charge distribution (Williams and Flemming, 1995).

The NMR experiment required the selection of an appropriate deuterated solvent depending on the solubility or polarity of the compound being investigated. The samples were prepared by dissolving 5-10 mg of the compound in 800 µL of the deuterated solvent and transferring this into an NMR tube which was then submitted to the NMR instrument and the NMR spectrometer collected the data from the experiment and displayed them as an NMR spectrum. An NMR spectrum is a collection of one or more resonance peaks at different frequencies and the chemical

shift expresses the resonance frequency position observed for a specific nucleus in an individual structural environment. The signals appeared at different places in a spectrum, due to the influence of atoms and groups that either removed their electron density and appeared at higher energy level (deshielding) or increased their electron density and appeared at lower energy (shielding) (Crews *et al*., 1998, Williams and Flemming, 1995).

Table 2. 1 Chemical shift of deuterated solvents used

Deuterated solvent	Chemical formula	^{1}H-NMR Chemical shift (δ_H)	^{13}C-NMR Chemical shift (δ_C)
Chloroform	$CDCl_3$	7.26 (1)	77.2 (3)
Dimethyl sulfoxide	$(CD_3)_2S=O$	2.50 (5)	39.5 (7)
Methanol	CD_3OD	4.87 (1), 3.31 (5)	49.1 (7)
Deuterium oxide	D_2O	4.80 (1)	-

Proton (^{1}H) NMR spectroscopy

The ^{1}H NMR spectrum indicated the number of hydrogen atoms associated with a particular group (integration) and how shielded or deshielded the group was. Shielding and deshielding occurs due to the presence of groups that are either electron-withdrawing (deshielding) or electron-donating (shielding). The area under the absorption peak is proportional to the number of protons that give rise to each signal. In addition, the energy levels of a nucleus will be affected by the spin state of the nuclei nearby. Therefore, neighbouring magnetic nuclei can have a significant effect on a specific signal and will be responsible for the multiplicity of a peak, which can be interpreted by the multiplicity rule, where M = n+1 (where n is the number of protons on neighbouring carbons). This phenomenon is called spin-spin splitting and the coupling constant (*J*) is a measure of how strongly the nuclear spins influence

each other for one nucleus split by a neighbouring nucleus three bonds away (Williams and Flemming, 1995).

Carbon (^{13}C) NMR spectroscopy

The ^{13}C NMR spectrum gives further information regarding the environment of the different groups and the number of carbons present in a compound. The position at which a signal occurs is indicative of its chemical shift. As with proton spectra, the carbon signals occur over a large range (0-220 ppm), which is determined by whether the carbons are shielded or deshielded (Heinrich *et al*., 2012).

Distortionless Enhancement by Polarisation Transfer spectrum

Distortionless enhancement by polarisation transfer (DEPT 135) spectrum is useful in the identification of primary, secondary and tertiary carbon atoms (CH, CH_2 and CH_3). The DEPT 135 gives all methine (CH) and methyl (CH_3) groups in a phase opposite to methylene (CH_2). Quaternary carbons (carbons with no protons attached) and solvent peaks do not appear in the DEPT 135 spectrum.

Homonuclear Correlation Spectroscopy

The homonuclear correlation spectroscopy (COSY) spectrum revealed coupling between protons (through bond correlation). It is referred to as homonuclear because they are acquired by detecting only one type of nucleus, ^{1}H (i.e. they detect the presence of the same nuclei both of which are ^{1}H). It is described as a two-dimensional technique because the data was displayed in a matrix format with two one-dimensional experiments (^{1}H spectra) displayed on the x- and y-axes.

Nuclear Overhauser Effect Spectroscopy

The Nuclear Overhauser Effect Spectroscopy (NOESY) spectrum is useful as it showed through space correlation and through bond coupling between protons. This gave an insight into how close one proton was from another, which was very useful in assigning the relative stereochemistry of natural products.

Heteronuclear Multiple Quantum Coherence Spectroscopy

The Heteronuclear Multiple Quantum Coherence (HMQC) spectrum showed which protons are directly attached to which carbon and therefore is known as one bond ^{1}J correlation. This experiment was very useful in distinguishing functional groups.

Heteronuclear Multibond Coherence (HMBC) Spectroscopy

The heteronuclear multibond coherence (HMBC) spectrum shows correlations between carbons and hydrogens that are two or three bonds distant, and are often referred to as ^{2}J and ^{3}J correlations respectively. It is highly informative and assists partial structure fragments to be constructed which can enable the full structure elucidation of natural products (Heinrich *et al*., 2012).

Figure 2. 5 NMR Bruker AVANCE 400 (left) and 500 (right) instruments.

2.6.2 Mass spectrometry

Mass spectrometry (MS) is a useful analytical technique for the examination of a broad array of organic molecules, and provides information about the molecular weights and the fragments of compounds, which are useful for the structure elucidation of the compounds. Once the sample was introduced into an ion source, ions were produced from the resulting gas-phase molecules. The resultant ions were then separated according to their mass-to-charge ratio (*m/z*) and subsequently analysed, detected and recorded according to this ratio, enabling the determination of their molecular weights (Williams and Flemming, 1995).

In this research, samples were dissolved in methanol or chloroform, depending on their solubility properties, and ESIMS was performed on a Finnigan Navigator instrument. The mass spectrum was plotted as arrays of vertical lines (ion peaks) on relative abundance of the ions in % (y-axis) and mass to charge ratio (*m/z*) value (x-

axis). The highest peaks represented the most abundant ion which typically were the most stable ions generated from the ionization.

High Resolution Mass Spectrometry (HRMS) for accurate mass determination was done using Ion trap and Quadrupole/Time of flight (Q-ToF) analysers. The HRMS gave *m/z* values accurately up to four decimal places, which made it possible to distinguish between different formulas with the same nominal mass and therefore was very useful to confirm atomic composition and molecular formula of the compounds.

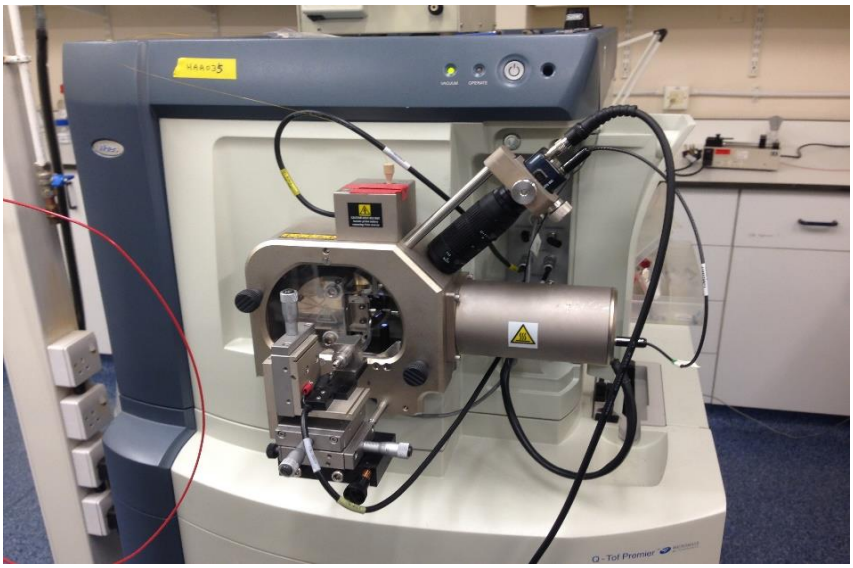

Figure 2. 6 Micromass Q-TOF premier Tandem Mass Spectrometer.

2.6.3 Ultraviolet-visible spectroscopy

Ultraviolet-visible (UV) spectroscopy is useful for the determination of structures of organic compounds as it provides information about the presence or absence of unsaturated functional groups. It is based on the theory that any organic molecule exposed to UV or visible light is capable of absorbing electromagnetic radiation because it contains valence electrons that can be excited to higher energy levels. The

electronic transition from a lower to a higher energy state is the phenomenon responsible for the UV peaks (Reusch, 2007).

Most applications of absorption spectroscopy are based on transitions from π electrons to the π* excited state. The transition occurs at wavelengths into the ultraviolet-visible region (approximately 200-700 nm). These transitions require the presence of an unsaturated functional group to provide the π orbitals. Chromophores are the functional groups present in molecules that are responsible for electron transitions from a basal electronic state to an excited state. The main structural feature responsible for ultraviolet-visible (UV-Vis) absorption of molecules is the conjugated π-bond system (Williams and Flemming, 1995).

In this research, the samples were dissolved in methanol forming solutions of 20 and 10 μg/mL that allowed an absorbance <1. The solution was then placed in 10 mm transparent cuvettes (Hellma Analytics) and the absorption bands were recorded on a Beckman Coulter spectrophotometer (Figure 2.6b) at wavelengths between 200-400 nm. The absorbance at the wavelength where the maximum absorption takes place (λ_{max}) was obtained and the Molar extinction coefficient or molar absorptivity (ε) calculated from Equation 1 (where *A* is the absorbance at the wavelength of interest, *c* is the concentration of the solution of compound under investigation and *l* is the path length which the UV beam passes through in centimetres) (Mabry *et al*., 1970, Pace *et al*., 1995).

$$\varepsilon = \frac{A}{c.l}$$

Equation 1. Beer- Lambert Law

2.6.4 Infrared spectroscopy

Infrared spectroscopy (IR) is a simple, fast and reliable method in the structure elucidation of organic compounds. It is used for the determination of the functional groups present in the molecule such as carboxylic acid, ketones, alcohol, ester, ether, aldehyde, nitro and nitrile. A compound placed in an IR beam, absorbs energy due to bond vibration changes. The energy of most molecular vibrations corresponds to that of the mid-IR region (approximately 500 to 4000 cm^{-1}) of the electromagnetic spectrum. Since each functional group has its own characteristic frequency, a compound can be easily assigned to its structural class. The infrared spectra for this research were obtained on a Perkin-Elmer Spectrum 100 FTIR spectrometer. A drop of the neat liquid of the compound, or sample dissolved in minute quantities of chloroform or a crystal of a solid compound was placed at the centre of the sample holder and pressure was applied by lowering down the pressure arm in order to give a thin layer of the sample. The whole spectrum was measured in a few seconds. Once an infrared beam passes through the sample, the signals were immediately recorded and Fourier transformed into a fine spectrum labelled as frequency of IR radiation (x-axis) against percentage (%) transmission (y-axis).

Figure 2. 7 (a) Infrared and (b) ultraviolet-visible spectrophometer.

Table 2. 2 Preparation of microbiological media

Microbiological media	**Method**	**autoclave**
Middlebrook 7H9 broth	Middlebrook 7H9 powder (4.7 g) + 900 mL of deionised water + 4 mL of glycerol (50 % v/v in deionised water) + 2.5 mL of Tween 80 (20 % v/v in deionised water) and mixed thoroughly to dissolve completely. Middlebrook ADC growth supplement was added when culturing mycobacteria.	The preparation was autoclaved at 121º C (15 psi) for 12 minutes.
Middlebrook 7H10 agar	Middlebrook 7H10 powder (19 g) was added to 900 mL of deionised water and mixed thoroughly to dissolve completely. Then 5 mL of glycerol (50 % v/v in deionised water). Middlebrook OADC growth supplement was added just before inoculum when culturing mycobacteria.	The preparation was autoclaved at 121 ºC (15 psi) for 12 minutes.
Mueller Hinton Broth	Mueller Hinton powder (5.25 g) + 250 mL deionised water. Mixed thoroughly to dissolve completely.	The preparation was autoclaved at 121 ºC (15 psi) for 15 minutes
Nutrient Agar	Nutrient agar (7 g) + 250 mL of deionised water, mixed thoroughly to dissolve completely.	The preparation was autoclaved at 121 ºC (15 psi) for 15 minutes.
Luria Bertani broth	Luria Bertani powder (6.25 g) was added to 250 mL of deionised water, mixed thoroughly to dissolve completely.	The preparation was autoclaved at 121 ºC (15 psi) for 15 minutes

2.7 Growth and maintenance of microorganisms

Growth and maintenance of *Mycobacterium* species: *Mycobacterium aurum*, *M. smegmatis* MC^2 155, *Mycobacterium bovis* BCG and *M. tuberculosis* $H_{37}Rv$ were all grown in Middlebrook 7H9 broth with 0.05 % Tween-80 and 0.2 % glycerol and supplemented with ADC 10 % v/v. A glycerol cryopreserved stock was taken and a 1:100 dilution in fresh media was done. To provide enough aeration for the mycobacteria, the Middlebrook 7H9 was one-fifth of the volume of the culturing container (for example, a 50 mL falcon tube was used for culturing the inoculum in 10 mL of broth). The stock of inoculum (100 µL) was added to 10 mL of Middlebrook 7H9 and incubated (*M. aurum* was incubated at 35 ºC with constant shaking at 150 rpm and *M. smegmatis* at 37 ºC with shaking at 150 rpm. For *M. bovis* BCG 90 mL of Middlebrook 7H9 was added to 10 mL ADC in rolling bottles kept at 2 rpm and incubated at 37 ºC, the colonies were observed after 14 days of incubation). For *M. tuberculosis* $H_{37}Rv$ and the clinical isolates, the culture was incubated for 21 days at 37 ºC as standing cultures. The growth was monitored by measuring the optical density at 600 nm using the spectrophotometer. At the mid-exponential phase (OD_{600} ~ 0.7-1.2), the culture was passaged into a fresh enriched media and incubated.

Growth and maintenance of other bacteria: All strains were cultured on nutrient agar slopes and incubated for 14 h at 37 ºC. An inoculum turbidity equivalent to No. 0.5 of the Mcfarland standard (1.5x 10^8 cfu/mL) was prepared in normal saline for each test organism prior to testing.

2.8 Cryopreservation

Bacteria at the mid-exponential phase were preserved by suspending 250 µL of culture into 250 µL of sterile aqueous glycerol (50 %v/v) solution. This mixture was dispensed into 2 mL cryovials, tightly closed, inverted five times to allow even mixing of the cells in the fluid and then transferred into the -80 ºC freezer for preservation. Murine macrophage RAW 264.7 cells were preserved using cryoprotectant BAMBANKER™ Cell Freezing Media.

2.9 Optical density

The optical density determined at a wavelength of 600 nm (OD_{600}) is an indirect measure of the cell concentration of a microbiological culture since the optical density is proportional to the cell concentration (Monod, 1949, Schaefer *et al*., 1949). The OD_{600} is the measure of light-scattering due to the cell density of a culture which is seen as turbidity. To measure the $OD_{600,}$ a 1:2 dilution of the culture and media was made in a plastic cuvette, sterile liquid media only (1 mL) served as a blank or reference to zero the spectrophotometer before the readings were taken.

2.10 Acid-fast staining of mycobacteria

Mycobacteria are said to be acid-fast because a wax-like coating (the lipid-rich cell wall) on these organisms prevents the release, on acid treatment, of the dye once it has been absorbed. The acid-fast staining or Ziehl-Neelsen staining (TB-color kit, BDH) technique was used to check the quality of the mycobacterial culture (quality control). At an OD_{600} of (0.8-1), 20 µL of the culture was spread on a glass slide and dried in an oven at 110 ºC for 20 minutes (fixation) and stained with Tb-color carbol fuchsin solution for 5 minutes. Double-distilled water was used to rinse the slide

until the dye was no longer released, then the slide was covered with Tb-color destaining decolourising solution (EtOH-HCL) and rinsed down immediately. The specimen was completely covered with malachite green solution and counter-stained for 1 minute. The slide was rinsed with tap water for approximately 10 sec and dried in air. The slide was observed under bright-field microscope with 100x oil emersion. The acid-fast mycobacteria were clearly distinguished by being red rod-shaped bacilli.

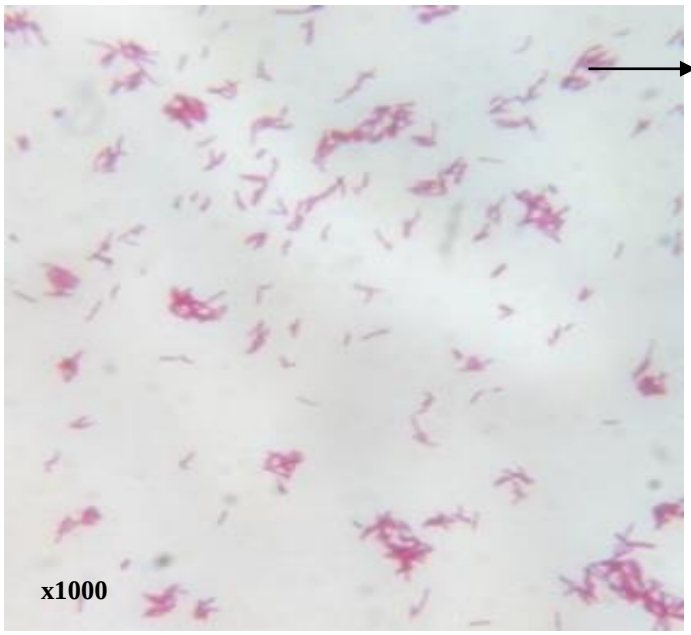

M. aurum cells growing in Middlebrook 7H9 stained with modified Ziel-Neelsen. Mycobacterial cell wall contains mycolic acid which retains carbol fuchsin despite washing with acid-ethanol.

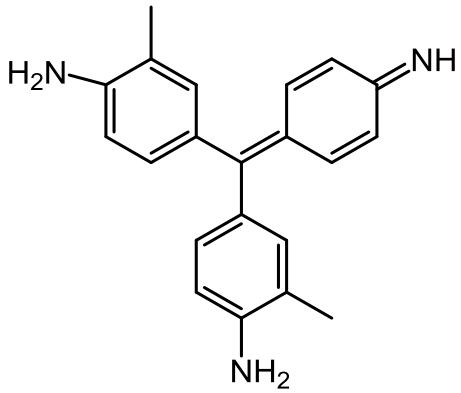

Carbol-fuchsin

Figure 2. 8 Light microscopic image showing acid-fast stained *M. aurum* cells

2.1 1 Construction of a growth curve

To construct the growth curve for *M. aurum,* the OD_{600} readings were taken every 12 h and plotted with time on the x-axis and optical density on the y-axis. The growth curve saves information about the doubling time (t_d) of the bacteria on the exponential phase.

2.12 Determination of colony forming units

The colony forming unit (CFU/mL) count helps us to quantify the number of viable cells in a culture by plating the culture on solid media and counting how many colonies can be formed.

Middlebrook 7H10 media supplemented with OADC (10 % v/v) and glycerol (0.25 % v/v) was pipetted into 9 cm petri-dishes and allowed to solidify. Middlebrook 7H9 supplemented with ADC (10 % v/v), glycerol (0.2 % v/v) and Tween-80 (0.05 % v/v) was pipetted into four centrifuge tubes. A stock of the compound (50 mg/mL) in DMSO was prepared and different volumes added to the media to obtain the required concentrations, using DMSO only as the control. A ten-fold serial dilution of the culture (at optimum growth OD_{600} 0.8-1.2) was made in Eppendorf tubes and 100 µL of the various dilutions were spread on the petri dish and incubated. The count of single colonies allowed the calculation of colony forming units using:

CFU mL^{-1} = (colonies on plate x final plate dilution)/ inoculum (in mL).

In this study, the growth curve and CFU counting can be found in Chapter 4 (Figures 4.13 - 4.14). The growth curve was determined by measuring the optical density at 600 nm (OD_{600}) of cultures of *M. aurum* every 12 h. The CFU were determined by spreading (in triplicate) 100 µL of different dilutions (10^{-4}, 10^{-5}, 10^{-6}, 10^{-7}, 10^{-8} and

10^{-9}) of the bacterial cultures in petri dishes containing 25 mL of supplemented Middlebrook 7H10. The petri dishes were incubated at 35 °C for 5 days and the number of colonies was counted. For the first experiment, the CFU of all samples were analysed when the OD_{600} of the control was 0.75 and for the second experiment, the CFU was determined for all samples 8 h after the addition of the inhibitors.

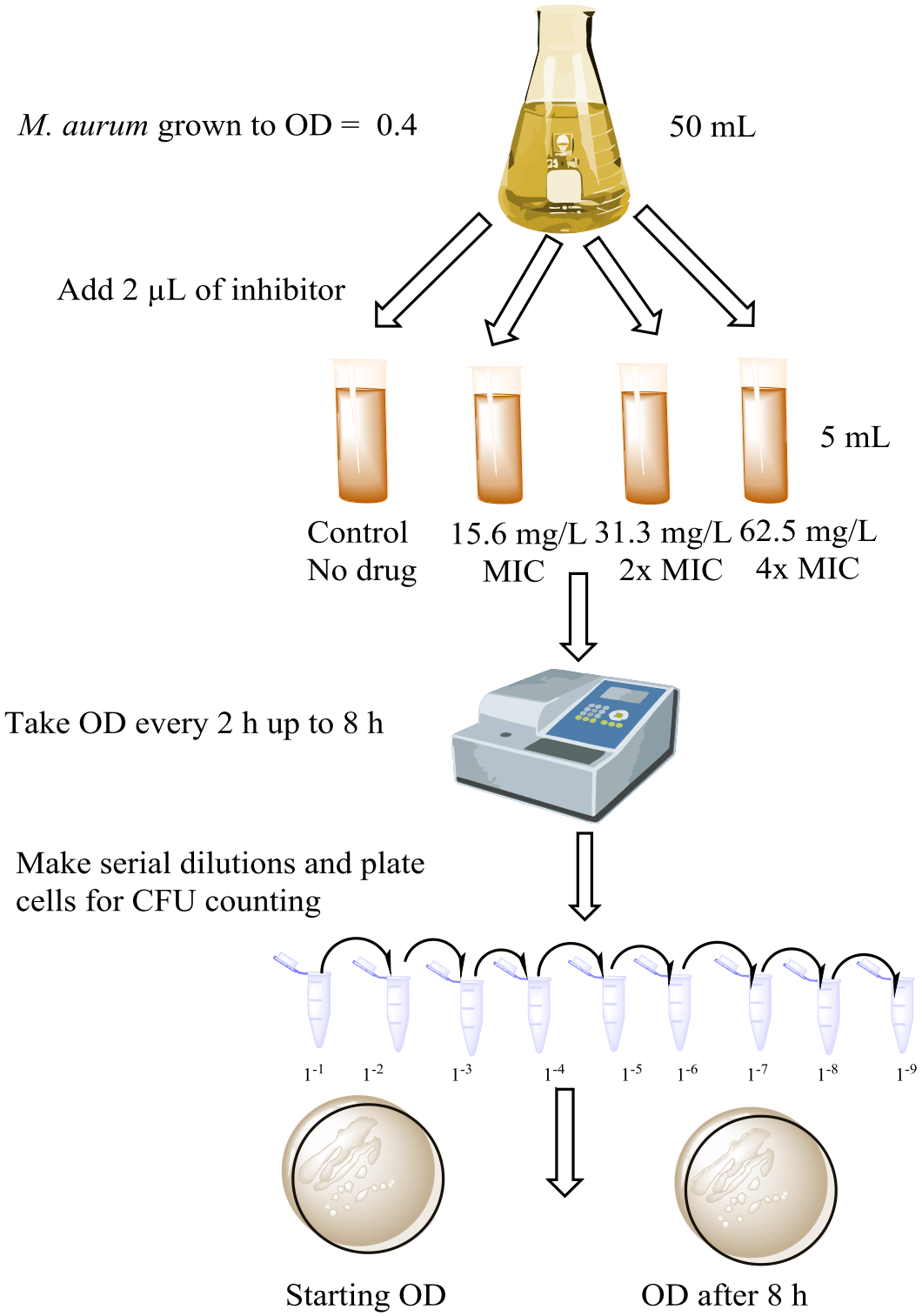

Figure 2. 9 Schematic representation of the process of colony forming unit (CFU) counting, growth curve determination and optical density (OD) measurement of *M. aurum* in the absence (control) and presence of different concentrations of compound **2** and at different time points.

2.13 Preparation of bacterial strains

Prior to the antibacterial assay for Gram-positive and Gram-negative strains, the selected bacterial strains were sub-cultured on nutrient agar slopes and incubated at 37 °C for 14 h.

2.14 Preparation of required samples

For Gram-positive and Gram-negative strains, MHB and 0.9 % NaCl solution were prepared and autoclaved as described. A pre-calculated amount of the compounds and reference drugs norfloxacin, oxacillin, tetracycline and erythromycin used as drug controls, were dissolved in DMSO and then diluted with MHB to give a starting concentration of 512 mg/L for the samples and 64 mg/L for norfloxacin, 32 mg/L for oxacillin, and 128 mg/L for tetracycline and erythromycin. On the day of the assay, the overnight cultures of each of the tested strains were made up in the 0.9 % NaCl solution to an inoculum density of 5x 10^5 cfu/mL.

2.15 Screening for antibacterial activity (drug susceptibility assay)

2.15.1 Spot culture growth inhibition assay (SPOTi)

The spot culture growth inhibition assay is a rapid, convenient and relatively inexpensive method for antimycobacterial screening of compounds. The aim of this assay was to test the biological activity of newly discovered natural products and novel chemical entities synthesized on the basis of basic structural studies. It is a solid agar-based method which helps determine the minimum inhibitory concentration of crude natural extracts, purified fractions, pure semi-synthetic or synthetic inhibitor molecules against species of *Mycobacterium*. The assay is principally based on the nature of the bacilli growth where growth is measured from

generated spots grown from approximately 1000 bacilli inoculated to the centre of the wells containing a range of different concentrations of the inhibitors. Since the compounds to be tested were mixed with the molten agar, they had optimum access to the bacilli and this reflected on their biological property through growth inhibition or killing. Results were obtained within 5 days for *M. aurum* and 14 days for the slow-growing species *M. bovis* BCG and *M. tuberculosis* H_{37}Rv. The SPOTi assay was performed as originally reported (Bhakta *et al*., 2004, Evangelopoulos and Bhakta, 2010) and developed further to a 24-well plate (Gupta and Bhakta, 2012) and now a high-throughput format in 96-well microtitre plates (Guzman *et al*., 2013). The compounds were dissolved in DMSO or water depending on their solubility to make a stock of 50 mg/mL. Isoniazid and rifampicin were used as positive controls.

2.15.2 Microtitre broth dilution assay

Mueller Hinton Broth (MHB) Oxoid^{TM} containing 20 mg/L of Ca^{2+} and 10 mg/L of Mg^{2+} (prepared from 3.68 mg/L $CaCl_2 \bullet 2H_2O$, 83.6 mg/L of $MgCl_2 \bullet 6H_2O$), normal saline 9 g/L and nutrient agar were prepared and autoclaved. The MHB (100 µL) was dispensed into wells 1-11 of the 96-well microtitre plate and 100 µL of the extracts/compounds and the antibiotics were dispensed into well 1 and serially diluted across the plate to well 10 and 12 leaving out well 11 as the growth control and ensuring that column 12 was the sterility control. Lastly, 100 µL of bacterial suspension was dispensed in to wells 1-11 and the plate was incubated at 37 °C for 14 h. All procedures were performed in duplicate. To facilitate observation, 20 µL of a 5 mg/mL methanolic solution of 3-(3,4-dimethylthiazole-2-yl)-2,5-diphenyltetrazolium bromide (MTT) was added to all of the wells and incubated for 30 minutes. A dark blue colour in wells indicated bacterial growth compared to the

yellow wells where there was no bacterial growth. The tetrazolium salt MTT 3-(4, 5-dimethylthiazole-2-yl)-2,5-diphenyltetrazolium bromide is a pale yellow substrate that produces a dark blue formazan product when incubated with live cells. The MTT is cleaved by all living metabolically active cells within the mitochondria and not by dead cells (Mosmann, 1983). The MIC was recorded as the lowest concentration at which no growth was observed.

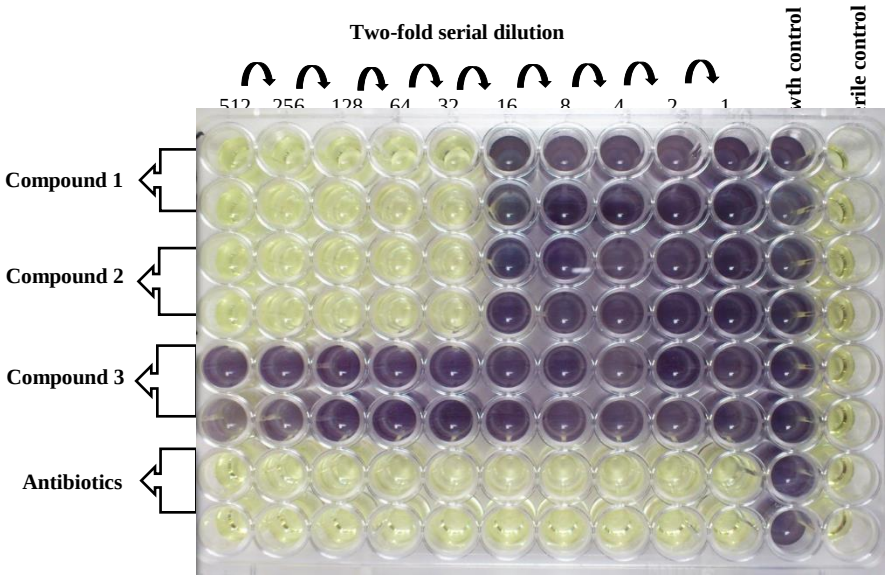

Figure 2. 10 A representative 96-well microtitre plate showing antibacterial activity.

2.15.3 Disc diffusion assay

The agar disc diffusion assay is a common method for drug susceptibility testing. It is a simple, reliable and inexpensive method which involves the application of the extract on to a sterile filter paper disc that is placed on to a solid agar medium seeded with the test organism (Singh *et al*., 2007).

This assay relies on the diffusion of compounds contained in extracts or fractions from a paper disc into agar that has been seeded with a particular microorganism. The compounds in the extract diffuse from the disc into the agar and their

concentration reduces with distance. If the compounds are antimicrobial and present at sufficient concentrations to prevent microbial growth, a clear zone appears around the disk after the plate has been incubated to allow the development of a microbial lawn of growth on the agar. As a result, zone size corresponds approximately to the total antimicrobial activity of the compound and the output data are considered to be semiquantitative.

To perform the disc diffusion assay, blank paper discs were prepared by perforating Whatman filter paper no.1 to obtain discs of diameter 5 mm. The discs were poured into a bottle and together with nutrient agar were autoclaved at 121 °C for 15 minutes. The molten agar (25 ml) was poured into 9 cm petri dishes to a depth of approximately 4 mm and allowed to solidify. The blank disc was loaded with the extract by pipetting (100 µL) to the centre of the disc. This was done for all the different extracts and fractions. The impregnated discs were allowed to dry out completely at room temperature. Standard antimicrobial susceptibility discs (Oxoid) of the antibiotics streptomycin and rifampicin packed in cartridges and of the same diameter were used as positive control. Blank discs with no extracts added served as negative control. A sterile cotton swab was used to evenly spread the bacteria inoculum in multiple strokes on the surface of the agar. The loaded paper discs and corresponding controls were placed with sterile forceps onto the agar surface and pressed down gently on each disc. The agar plates were incubated for 18-24 h to allow the development of a lawn of growth. The plates were read by placing the petri dishes on a dark paper to clearly see the zones of inhibition which were then measured using a ruler.

2.16 Antifungal assay

The anti-fungal assay was performed as described by (Rizi *et al*., 2015). Inoculum suspensions of the dematophytes were prepared from 14-day old cultures grown on Sabouraud's dextrose agar (SDA) slants at 25 °C. The fungal colonies were covered with 2 mL of Sabouraud's dextrose broth (SDB), and suspensions were obtained by gently probing the surface of the agar generating a mixture of conidial and hyphal fragments. The obtained suspensions were then filtered through four layers of sterile muslin, which retained hyphal fragments but permitted the passage of dermatophyte micro-conidia. The filtration process was used as this has been shown to provide a greater reproducibility and reliability of susceptibility testing. The number of conidia/mL of the inocula was determined by: 1) counting the number of conidia using a haemocytometer and 2) determining colony forming units per mL (CFU/mL) with plate dilution assays. The SPOTi assay was carried out as described previously (Guzman *et al*., 2013, Evangelopoulos and Bhakta, 2010, Gupta and Bhakta, 2012). Fungal species grown for the experiment are shown in Figure 2.11.

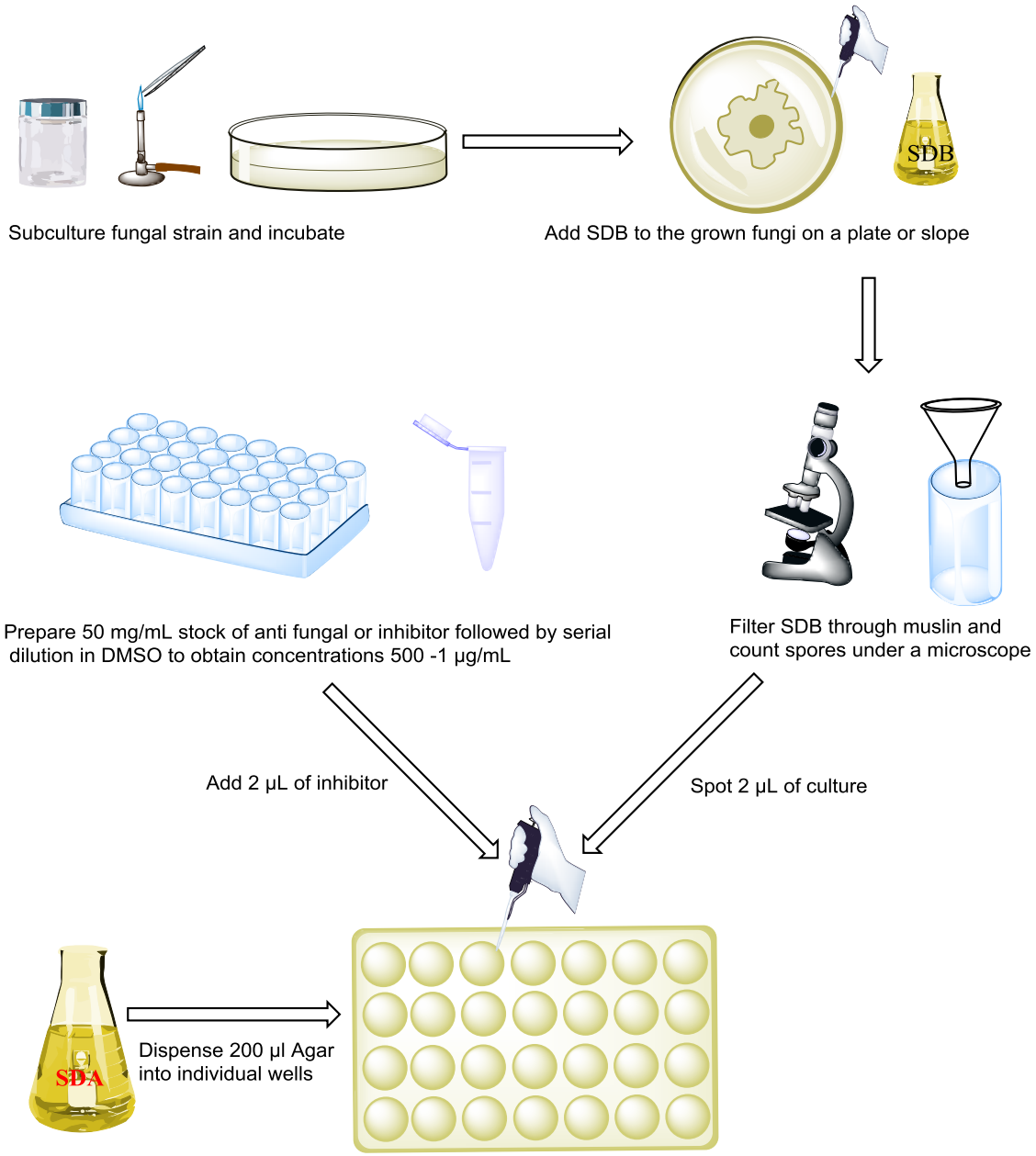

Figure 2. 11 Schematic representation of fungal SPOTi.

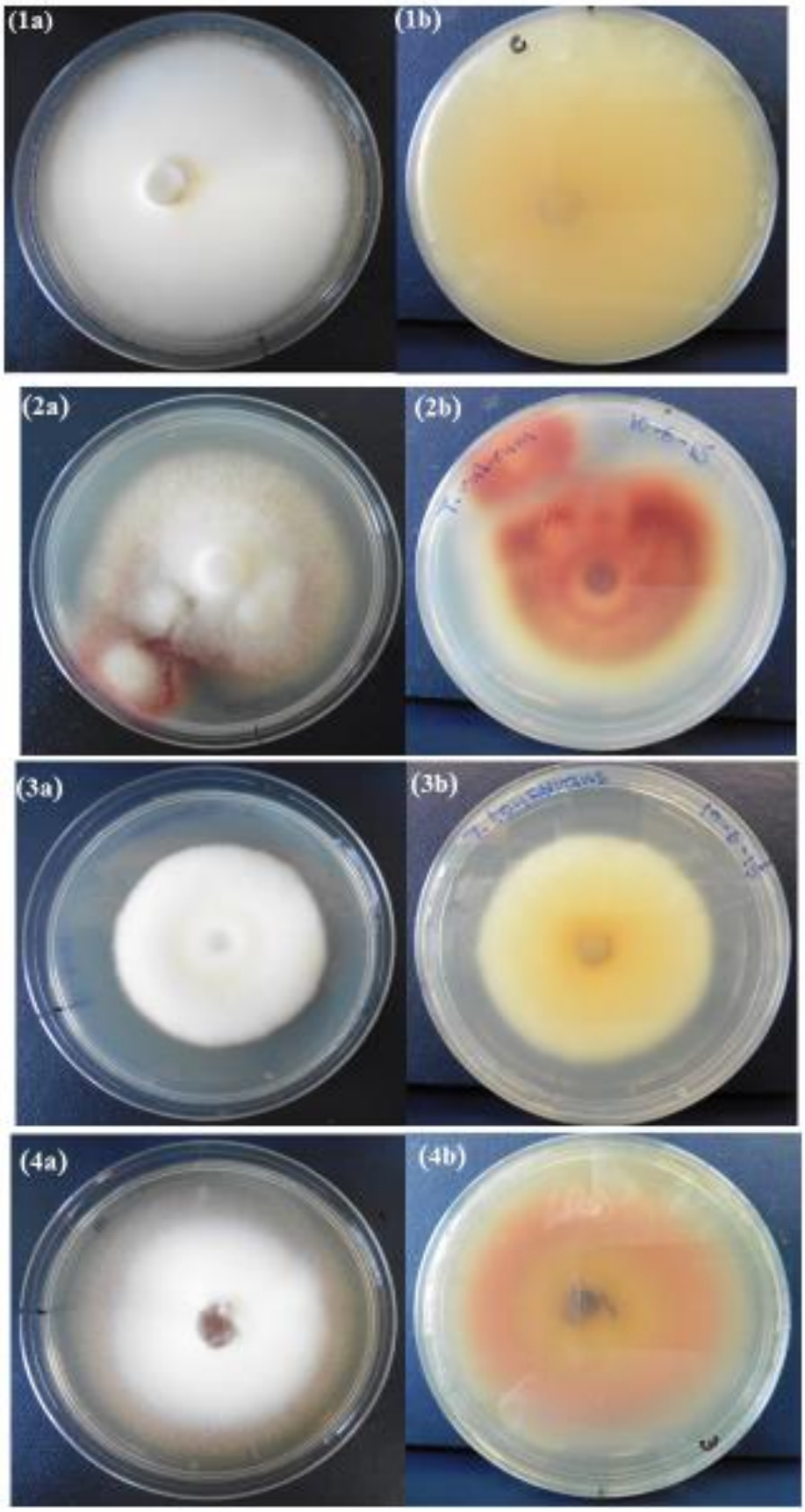

Figure 2. 12 Growing dermatophytes: (1a, 1b) *Trichophyton equinum,* (2a, 2b) *T. rubrum*, (3a, 3b) *T. tonsurans,* (4a, 4b) *T. mentagrophytes*.

2.17 Cytotoxicity assay

Assessment of eukaryotic cell toxicity was carried out using RAW 264.7 macrophage cells, grown in complete RPMI-1640 medium supplemented with 2 mM L-glutamine and 10 % heat inactivated fetal bovine serum and 1 % L-glutamine in a 25 cm^2 vented, screw-cap cell culture flask (Flowgen Bioscience Ltd., Hessle, UK) and incubated at 37 ºC with a supply of 5 % CO_2 until confluent growth was observed. For use in the cytotoxicity assay, cells were detached using 5 mL of lidocaine–ethylene diaminetetraacetic acid (EDTA) for 10 minutes at room temperature, followed by banging the side of the flask against the palm of the hand, and diluting with an equal volume of fresh media. Cells were then centrifuged at 1000 rpm for 5 minutes at room temperature, washed twice with phosphate-buffered saline and re-suspended in complete RPMI-1640 medium. Cell viability was determined using the trypan blue assay counted and diluted to adjust to 5×10^5 cells/mL. Cytotoxicity of the compounds towards the murine macrophages was determined using the resazurin assay (Gupta and Bhakta, 2012). Firstly, 2 µL of the stock solution of the compounds were added to 198 µL of complete RPMI-1640 medium in the first row of the 96-well plate and a two-fold serial dilution was done subsequently. Then, 100 µL of macrophage cells were seeded to each well of a 96-well plate containing final concentrations (250-3.9 mg/L) of inhibitors and controls that had been pre-plated by serial dilution. DMSO was used as a control, and the experiment was performed in triplicate. After 48 h of incubation, the cells were washed twice with PBS and fresh complete RPMI-1640 medium was added. Plates were then treated with 30 µL of a freshly prepared 0.01 % resazurin solution and incubated overnight at 37 ºC. The plate was observed after 16 h incubation at 37 ºC in 5 % CO_2, a change in color from blue to pink indicated the viability of cells. For

quantitative analysis, the fluorescence intensity was measured at $\lambda_{ex}560/\lambda_{em}590$ nm using a FLUOstar OPTIMA microtitre plate reader. The 50 % growth inhibitory concentration (GIC_{50}) was determined based on the resazurin fluorescence assay and the selectivity index (SI) was calculated as SI = GIC_{50}/MIC.

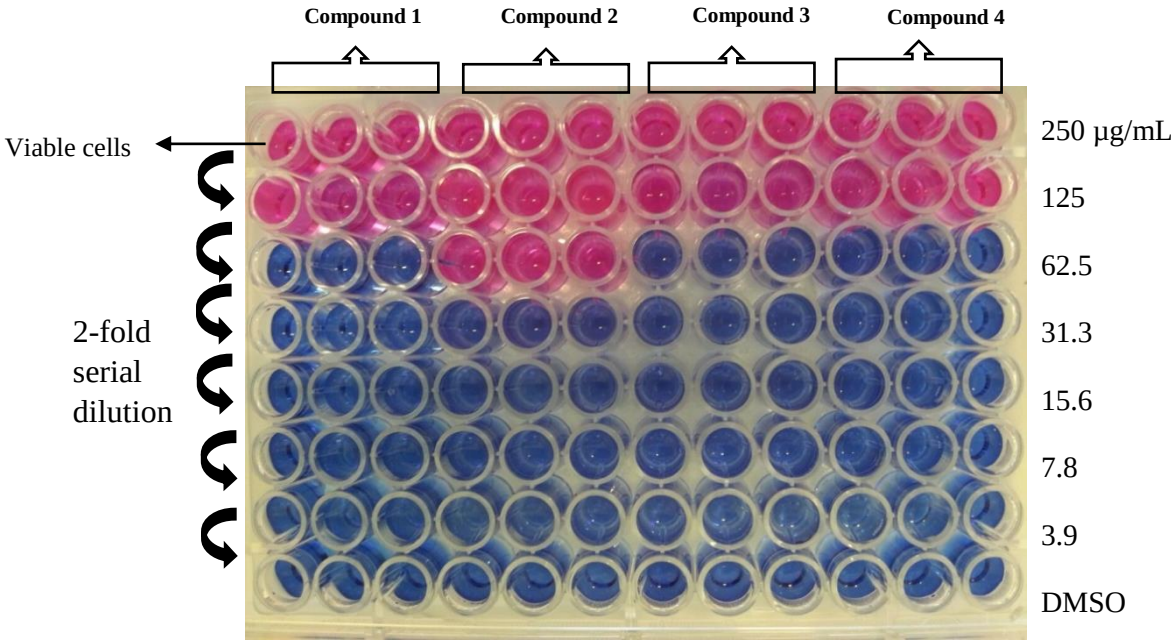

Figure 2. 13 A representative 96-well microtitre plate resazurin treated and showing a change in colour from blue to pink indicating viable cells after incubation**.**

Figure 2. 14 Light microscopic image showing growing RAW 264.7 murine macrophage cells.

2.18 Efflux pump inhibition assay

The whole-cell efflux pump inhibition assay was performed as described (Rodrigues *et al*., 2008, Rodrigues *et al*., 2011, Baugh *et al*., 2014) with some modification. All solutions were prepared on the day of the experiment. *Mycobacterium aurum* was grown at 35 ºC in Middlebrook 7H9 broth supplemented with 10 % ADC (shaking at 150 rpm) until an optical density (OD_{600}) of 0.8. The culture was centrifuged at 3000 rpm for 10 minutes, the supernatant discarded and the pellets washed in PBS. The OD_{600} was diluted to 0.4 with PBS and glucose was added at a final concentration of 0.4 %. Aliquots (100 µL) of a mixture of the compound, glucose and bacterial suspension were dispensed into 96-well plates, followed by EtBr at a concentration of 0.5 mg/L. The effect of chlorpromazine, verapamil and the synthesized compounds on the accumulation of EtBr was determined by measuring fluorescence using the fluorimeter (FLUOstar OPTIMA, BMG Labtech) and fluorescence data was acquired every 60 seconds for a total period of 60 minutes.

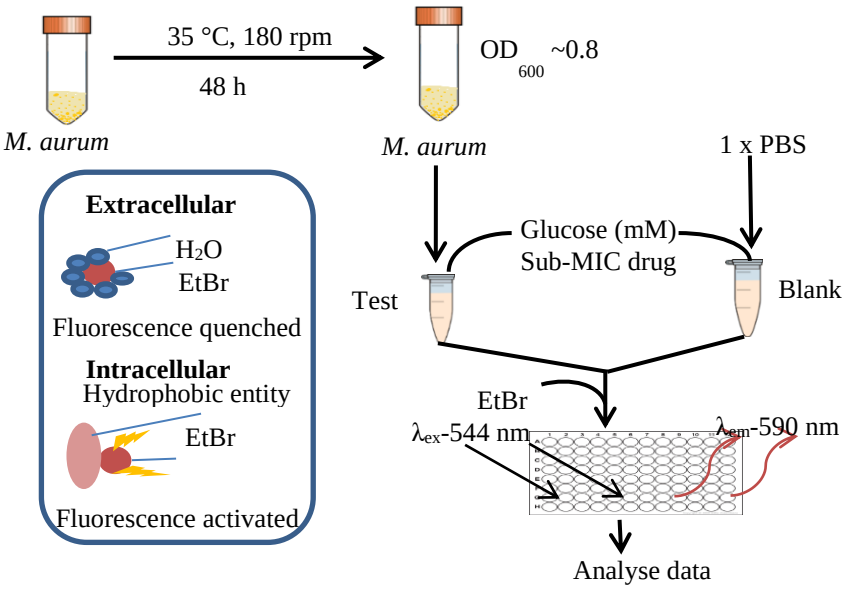

Figure 2. 15 Schematic representation of the efflux pump assay.

2.19 Biofilm assay

(a) Formation of biofilm: *Mycobacterium smegmatis* (100 µL) was inoculated into 10 mL of MB7H9 dispensed in to 50 mL polypropylene tubes and incubated at 37 ºC (150 rpm); this was grown to the late log phase (OD_{600} = 3.0). The late log phase culture was then inoculated into Sauton's media as 1:100 dilutions in triplicates. This preparation (2 mL) was transferred into polypropylene tubes and the cap was tightly screwed to avoid evaporation of media, another 200 µL was dispensed into a 96-well plate avoiding the periphery wells and the plate sealed with parafilm. Sauton's media without inoculum served as a control in each case and all the sets were kept at 37 °C in a non-rotating incubator for 5 days.

(b) Staining of biofilm: The biofilms formed in the 96-well plate were stained by pipetting out the media from each well leaving the biofilm settled at the bottom of the well which was then left to dry in the incubator for 20 minutes without the lid. After drying, each well was stained with 1 % crystal violet for 10 minutes. This was then pipetted out and each well washed 3 times with distilled water and placed in the incubator to dry for 20 minutes. After drying, 95 % ethanol was added to each well and left for 10 minutes before placing the plate in the plate-reader at 600 nm.

Chapter 3: Bioguided isolation and characterisation of compounds from the genus *Allium*

3.1 Introduction

Liliales particularly of the Alliaceae family produce bulbs as part of their reproductive system. These bulbs are in contact with soil bacteria such as members of the actinomycetes and the genus *Mycobacterium* and it is highly likely they would have evolved an antimicrobial defence against these bacteria. Such antimicrobial defence may be useful to find leads against these particular bacteria, hence the rationale for our interest in this plant family. Garlic has also been used clinically to treat TB in the early part of the 20th century and has been popularly known as 'Russian penicillin' (Bolton *et al*., 1982).

A combination of the ethnobotanical use of plants and chemotaxonomic knowledge of the presence of antimycobacterials in some *Allium* species and the likelihood that other related species may contain structurally similar compounds motivates screening of members of the genus *Allium* and other species belonging to the Alliaceae family for bioactivity.

3.2 The genus *Allium*

The genus *Allium* has been grown for many centuries for their culinary use due to their characteristic flavour but most importantly for their medicinal properties. Additionally they are used as ornamental plants because of their beautiful and colourful flowers. Well-known species belonging to the genus *Allium* include *Allium sativum* (garlic), *Allium cepa* (onions) and *Allium schoenoprasum* (chives).

There are over 750 species belonging to the genus *Allium* distributed all over the world especially in temperate, arid, semi-arid and tropical regions. The majority are natives of dry and mountainous areas of the Northern hemisphere but they have adapted to live in almost every plant habitat on the planet from ice cold tundra to burning, arid deserts. These are perennials and biennials, ranging in height from 10-150 cm or more. They are mostly herbaceous plants with varied underground storage structures such as rhizomes or bulbs and upright to spreading linear-shaped leaves. The tubular based flowers are bell, star or cup shaped which are borne in spherical umbels.

Figure 3. 1The flower of *Allium stipitatum*.

3.3 History of *Allium* use as food and medicine

Members of the genus *Allium* have been cultivated in the Middle and Far East for at least five thousand years and there is evidence to support the use of these plants as foodstuffs, items of religious significance and medicines (Fenwick and Hanley, 1985).

In ancient China, Egypt and India, *Allium* species (especially onions and garlic) have been highly prized as food stuffs. Onions and leeks were used for cooking four thousand years ago. In ancient Egypt the consumption of onions, leeks and garlic is shown on the decoration of tombs dating from the first and second dynasties (3200-2800 BC). The Greek historian Herodotus (450 BC) reported that radishes, onions and garlic formed the staple diet of labourers who built the Great Pyramid of Giza (Jones and Mann, 1963). The popularity of these species in Egypt is also recorded in the Old Testament (Numbers 11:5) where the Israelites during their exodus (1500 BC) unfavourably compared their diet of manna with that remembered from Egypt including fish, cucumbers, melons and leeks as well as the ubiquitous onions and garlic.

Tradition has it that shallot and other *Allium* species were introduced into Western Europe following the holy wars however, leeks were widely cultivated in Britain in Saxon times (6^{th} century AD). By 1340, however, the English writer Chaucer was able to refer to "Wel loved garleek, onyons, and leekes" (Hedrick, 1972).

The Codex Ebers, an Egyptian medical papyrus dating from 1500 BC described 22 garlic preparations that were active against a variety of complaints including headache, body weakness, and throat disorders. A major influence on successive generations of herbalists and doctors were the writings of the Greek Military

physician, Dioscorides (first century AD), Pliny the Elder (79 AD) and Hippocrates. These provided details of medicinal values of garlic and onions and other *Allium* species, which included their use for pneumonia, tuberculosis, asthma and bronchitis (Fenwick and Hanley, 1985).

Garlic in the form of inhalants, compresses and ointments has been used successfully against tuberculosis. The medicinal use of garlic-based products is especially common in Japan and Russia, in the latter garlic-based antibiotics were widely used and on one occasion large quantities of garlic were imported to combat the outbreak of tuberculosis (Fenwick and Hanley, 1985).

3.4 Chemical constituents in *Allium* species

Sulfenic acids and thiosulfinates are the first chemical compounds to be formed upon tissue damage when the intact *Allium* bulb is cut or crushed (Block, 1985). These compounds are intermediates in the formation of the majority of sulphur volatiles. The fresh flavours characteristic of *Allium* species are produced by enzymatic decomposition of *S*-alkyl cysteine-L-sulphoxides and *S*-alkenyl-L-cysteine sulphoxide from which the primary products are thiosulfinates containing alkyl and alkenyl-disulfide sulphoxides. Four sulphoxides are found to occur in *Allium* species namely, (+)-*S*-methyl-1-cysteine sulphoxide (methyl CSO), (+)-*S*-propyl-L-cysteine sulphoxide (propyl CSO), *trans*-(+)-*S*-(1-propenyl)-L-cysteine sulphoxide (propenyl CSO) and (+)-*S*-(2-propenyl)-L-cysteine sulphoxide (figure 3.2) (Rose *et al*., 2005).

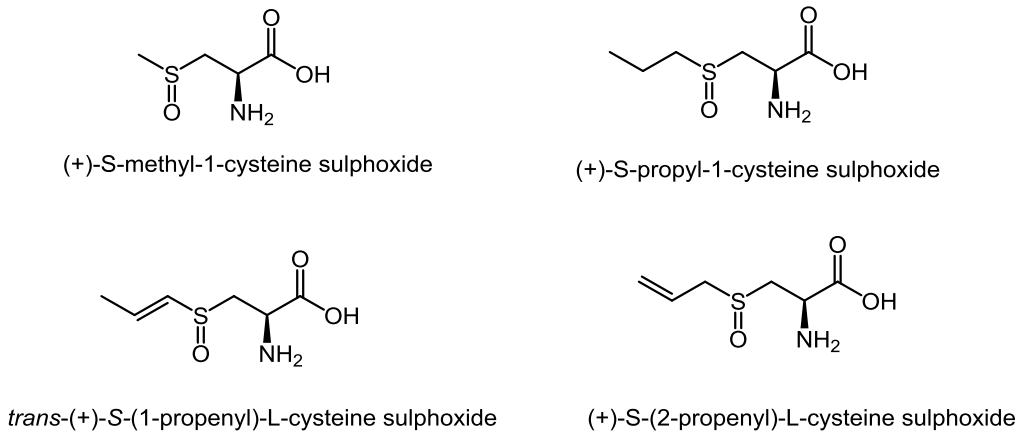

Figure 3. 2 Sulphoxides in *Allium* species.

The enzyme allinase found in plants of the genus *Allium* is responsible for catalysing the chemical reaction that produces the volatile chemicals that give these species their flavours, odours and tear producing properties. Allinase converts the chemical alliin to allicin when the intact bulb is cut. In garlic, the amino acid flavour precursors are (+) *S*-methyl-L-cysteine sulphoxide, (+) *S*-propyl-L-cysteine sulphoxide and (+) *S*-2-propenyl L-cysteine sulphoxide. The initial flavour of freshly chopped garlic is due mainly to the enzymic product 2-propenyl-2-propenethiosulfinate. On standing, these compounds are converted to disulfides, trisulfides and more complex sulphur containing compounds (Block, 1985).

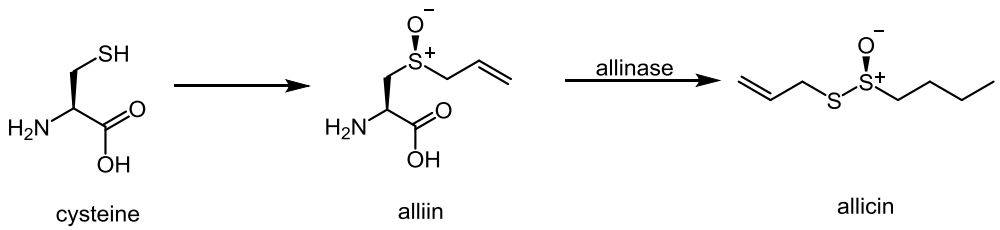

Figure 3. 3 Conversion of Alliin to Allicin.

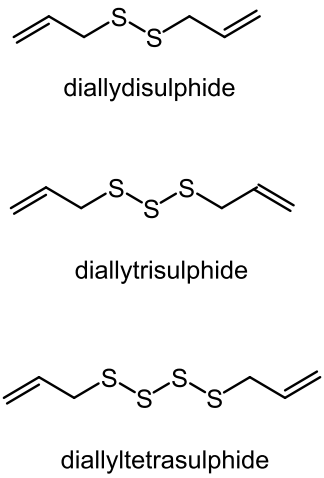

Figure 3. 4 Diallyldisulphide, diallyltrisulphide and diallyltetrasulphide in *Allium* species.

In onions, allinase cleaves isoalliin giving 1-propenesulfenic acid which is converted by lachrymatory synthase to the lachrymatory factor, propanethial-*S*-oxide. On standing or on heating, the thiosulphinates decompose to yield a mixture of disulfides and trisulfides containing methyl, propyl and 1-propenyl groups and small quantities of thiophene derivatives and other sulphur containing compounds.

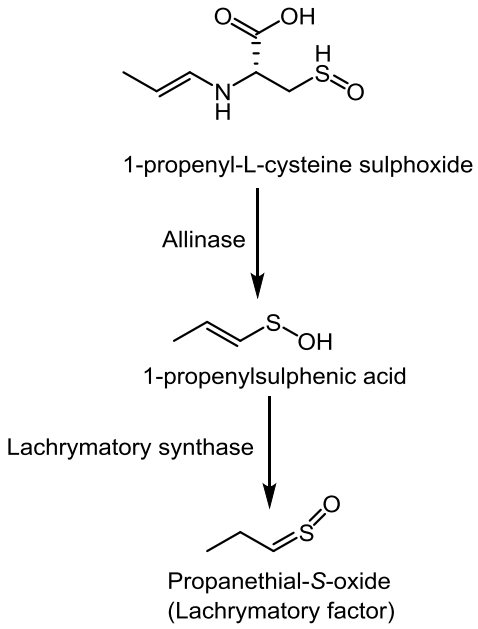

Figure 3. 5 Production of propanethial-*S*-oxide.

In addition to sulphur compounds, flavonoids such as quercetin and kaempferol (figure 3.6), fatty acids, phenolics and organoselenium compounds are present in *Allium* species. Flavonoids have many pharmaceutically useful properties such as antibacterial, antioxidant, anti-inflammatory, antifungal, antitumour and anti-thrombotic properties (Gibbons, 2004).

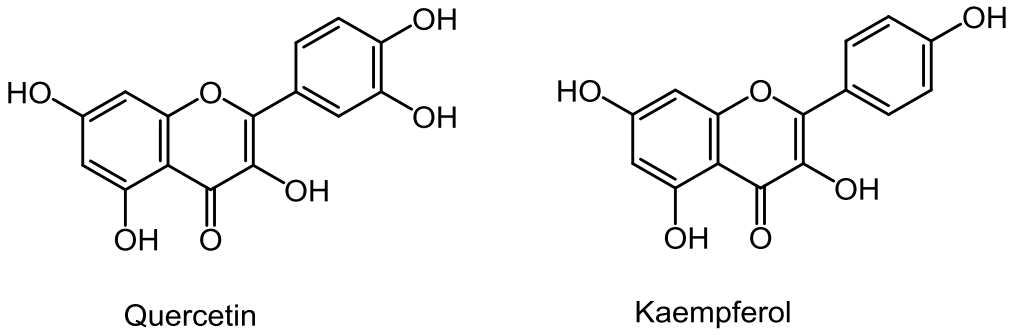

Figure 3. 6 Chemical structures of Quercetin and Kaempferol.

Triterpenes, specifically steroidal saponins such as spirostanes and furostanes are well documented constituents of the genus *Allium* and have been shown to possess haemolytic, antifungal, anticancer and anti-inflammatory activity (Lanzotti, 2006).

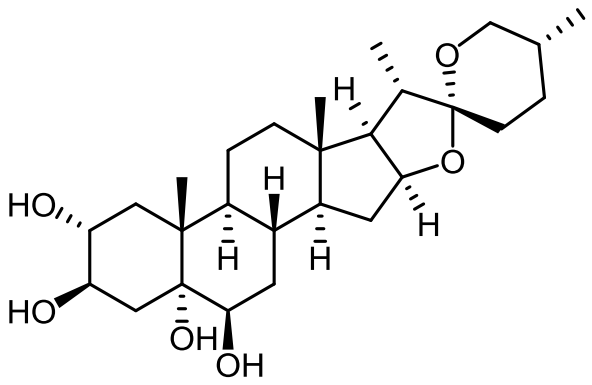

Figure 3. 7 Alliogenin.

3.5 Antimicrobial activity of *Allium* species

The importance of the genus *Allium* as medicinal plants dates back to ancient times. Their multiple medicinal properties are due to the presence of sulphur-containing substances (cysteine sulfoxides). Members of the genus *Allium,* such as *Allium sativum* (garlic) has been widely studied for its pharmaceutical properties with allicin being identified as the major antibacterial component in the 1940s (Cavallito and Bailey, 1944).

The first systematic study of antibiotic properties of garlic was that of Cavallito and co-workers who found that allicin, the principal fresh flavour component of garlic was effective against a number of Gram-positive, Gram-negative and acid-fast bacteria (Cavallito *et al*., 1944). It inhibited the growth of some *Staphylococci*, *Streptococci, Vibrio* (including *Vibrio cholerae*), *Bacilli, Pseudomonas, Escherichia coli*, *Mycobacterium* and *Clostridium* (Rose *et al*., 2005). Allicin was tested against thirty clinical isolates of methicillin-resistant *Staphylococcus aureus* strains, and of the strains which were tested, 88 % had MICs of 16 µg/mL and all the strains were inhibited at 32 µg/mL (Cutler and Wilson, 2004).

Allicin is considerably more bacteriostatic than bactericidal in action and operates by destroying sulphydryl groups of bacterial enzymes which are essential to bacterial proliferation thus inhibiting growth. *Allium* plants have long been associated with the treatment of infections and the antimicrobial properties are due to constituents derived from the cysteine sulfoxides (Rattanachaikunsopon and Phumkhachorn, 2009).

Allium species are also reported to be effective in the prevention of numerous disease states in humans including cancer, cardiovascular and inflammatory

disorders and these are due to the ability of *Allium* sulphur compounds to positively modify the anti-oxidant, apoptotic inflammatory and cardiovascular systems in mammalian systems (Lazarevic *et al*., 2011). Pyridine-*N*-oxides disulfides from *Allium stipitatum* (O'Donnell *et al*., 2009) and canthin-6-one and 8-hydroxy-canthin-6-one from *Allium neapolitanum* (O'Donnell and Gibbons, 2007) have been reported to be active with MICs within the range of 2-20 µg/mL against various strains of *Mycobacterium*. Flowers of some of the species studied are shown in figures 3.1, 3.8 - 3.10.

Figure 3. 8 Flower of *Allium* "Ambassador".

Allium "Ambassador" is a new giant variety obtained from *Allium stipitatum* and *Allium giganteum*. It is an improved, more vigorous and larger form of *Allium giganteum* and comprises of tightly compacted, intense purple florets and large bulbs

of about 10 cm in height. The foliage is green and the flowers are purple. They produce flowers usually in June-July.

Figure 3. 9 Flower of *Allium karataviense*.

Allium karataviense has large star-shaped pinkish-white flowers on stocky stems with mottled greenish-purple leaves. They flower from May-June and the plant reaches a height of 25 cm.

Figure 3. 10 Flower of *Allium* “Gladiator”.

Allium “Gladiator” is a spectacular ornamental onion with round softball sized flowers. It is an herbaceous perennial which grows to be approximately 14 inches tall.

3.6 Antimycobacterial activity of the extracts

The preliminary screening of different species of *Allium* including *Allium* "Ambassador", *Allium vineale*, *Allium sphaerocephalon*, *Allium christophii* and *Allium karataviense* using the SPOTi assay against *Mycobacterium bovis* BCG with isoniazid as the positive control was carried out using hexane, chloroform and methanol.

The MICs were recorded, as the lowest concentration at which there was no growth. Growth inhibition was exhibited mostly by the chloroform extract with the rest of the MICs greater than 500 mg/L. The chloroform extract of *Allium vineale* produced the lowest MIC of 125 mg/L followed by *Allium* "Ambassador" with an MIC of 250 mg/L. Based on the fact that *Allium* "Ambassador" extract showed some antibacterial activity, the chloroform extract was further investigated by SPE fractionation to isolate the bioactive compounds responsible for the activity. The chloroform extract of *Allium* "Ambassador" (300 mg) was fractionated by normal phase SPE with 10 % incremented step gradient system from 100 % hexane to 100 % ethyl acetate to 100 % methanol. All the fractions were screened for antimycobacterial activity using the HT-SPOTi assay. However, the MICs obtained were greater than 500 mg/L.

3.7 Antibacterial activity using the Disc Diffusion Assay

The disc diffusion assay is a qualitative assay, which can be used as a preliminary screening technique to give an idea of possible inhibitory activity of extracts. In this experiment, the chloroform extract of *Allium* "Ambassador" having shown growth inhibition was fractionated using normal phase SPE as described in the method

section (Chapter 2) and the fractions were tested. Fraction 3 (100 µg/disc) exhibited inhibitory activity (figure 3.11) with the diameter of zone of inhibition being 12 mm, 10 mm and 11 mm respectively against the tested *Staphylococcus aureus* strains SA-1199B, MSSA-13373, and MRSA-12981 (table 3.1).

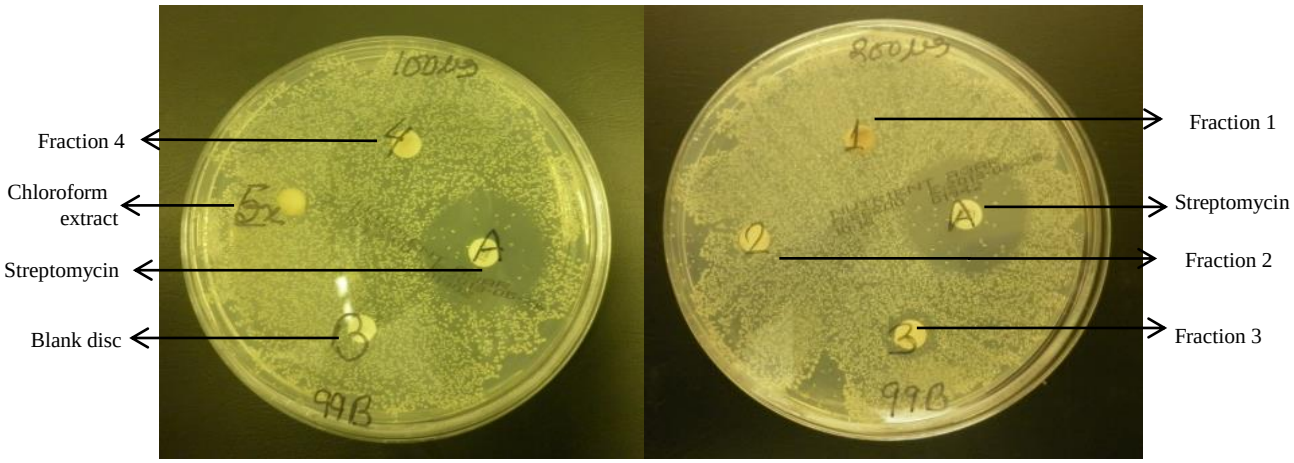

Figure 3. 11 Growth inhibition of SPE fractions of *Allium* "Ambassador" chloroform extract by disc diffusion assay using *Staphylococcus aureus* strain SA 1199B on nutrient agar.

Table 3. 1**.** Antibacterial activity of SPE fractions of *Allium* "Ambassador" chloroform extract by disc diffusion assay

	Staphylococcus aureus strains		
	SA-1199B	MSSA 13373	MRSA 12981
Test sample	Diameter of zones/mm		
Fractions 100 µg/disc			
Fraction 1	-	-	-
Fraction 2	-	-	-
Fraction 3	12	10	11
Fraction 4	-	-	-
Crude chloroform extract	-	-	-
Chloroform only	-	-	-
Streptomycin	24	35	27
Rifampicin	35	37	40
Fractions 200 µg/disc			
Fraction 1	-	-	-
Fraction 2	-	-	-
Fraction 3	12	11	11
Fraction 4	-	-	-
Crude chloroform extract	-	-	-
Chloroform only	-	-	-
Streptomycin	16	39	26
Rifampicin	24	40	40

No zone of inhibition depicted by (-)

3.8 Characterisation of a compound from *Allium* "Ambassador"

Compound **A1** was obtained as a brown solid from SPE fraction 5 of the chloroform extract of *Allium* "Ambassador". The quantity of compound **A1** was 4.95 mg and the percentage yield with respect to the plant material (40 g) was 0.012 %. The ^{1}H NMR spectrum showed the presence of one methoxyl singlet at δ 3.90 ppm (3H, s) and methylene protons at δ 4.30 (2H, t, J = 5.5 Hz). There were three aromatic protons in an ABD substituted system. An olefinic proton at δ 6.52 ppm and δ 6.24 ppm appeared as a doublet with a large J value of 16 Hz indicative of a trans orientation around the double bond. From the ^{13}C NMR spectrum there were three quaternary carbons and these were missing in the DEPT 135 NMR spectrum. The structure of Compound **A-1** is shown in figure 3.12.

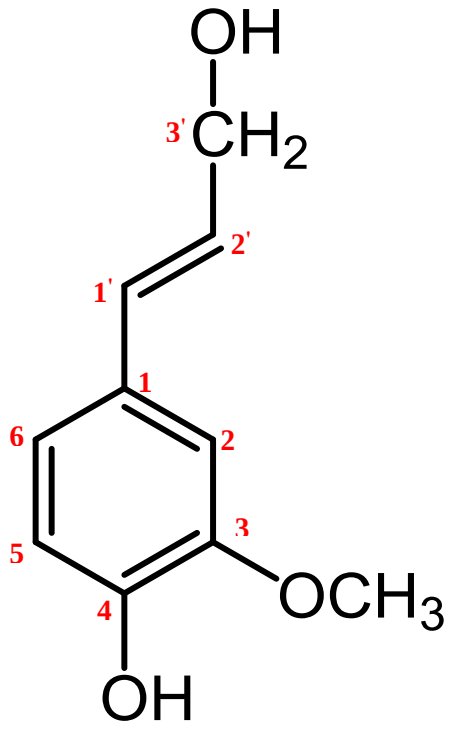

Figure 3. 12 Structure of Compound **A-1**.

Table 3. 2 ^{1}H NMR (500 MHz) and ^{13}C (125 MHz) data of compound **A1** in $CDCl_3$

Position	**A-1**		Heath *et al*, 2011	
	^{1}H	^{13}C	^{1}H	^{13}C
OMe	3.90 (3H, s)	56.0	3.78 (3H, s)	56.1
1		129.4		129.3
2	6.92 (1H, d, *J* = 1.5 Hz)	108.4	7.05 (1H, d, *J* = 2.2 Hz)	109.9
3		146.8		148.4
4		145.7		147.1
5	6.91 (1H, d, *J* = 8.0 Hz)	120.5	7.03 (1H, d, *J* = 8.0 Hz)	120.6
6	6.89 (1H, dd, *J* = 8.0 Hz, 1.5 Hz)	114.6	6.89 (1H, dd, *J* = 8.0 Hz, 2.2 Hz)	115.7
1’	6.52 (1H, d, *J* = 16 Hz)	129.4	6.50 (1H, d, *J* = 15.0 Hz)	130.2
2’	6.24 (1H, dt, *J* = 16 Hz, 5.5 Hz)	128.0	6.25 (1H, dt, *J* = 15.7 Hz, 5.0 Hz)	128.0
3’	4.30 (2H, t, *J* = 5.5 Hz)	63.5	4.07 (2H, t, *J* = 5.0 Hz)	63.4

Careful inspection of the ^{1}H and ^{13}C NMR spectra of **A-1** listed in Table 3.2, was in close agreement with NMR data of Heath *et al*. (2011) reported in literature. Based on this information compound **A-1** was identified as coniferyl alcohol, a cinnamyl alcohol derivative. There were however, some additional signals appearing in the NMR spectra of Compound **A-1** indicating the possibility of the presence of some impurities.

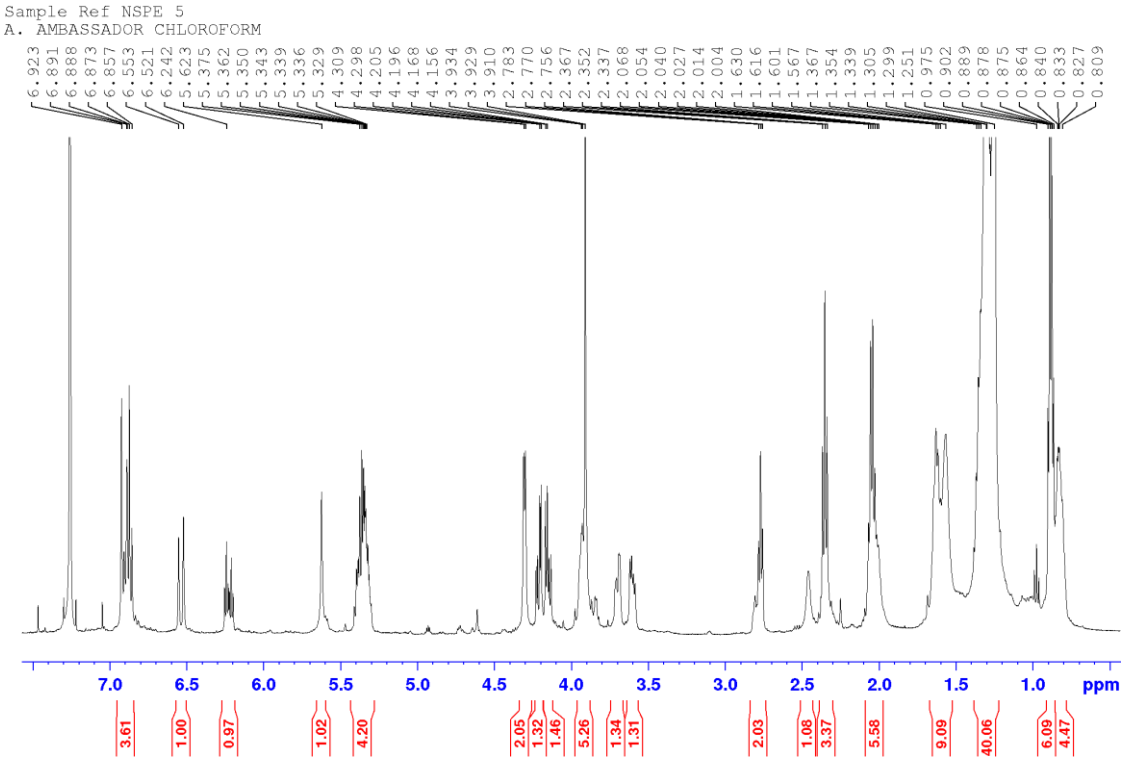

Figure 3. 13 ^{1}H NMR spectrum of **A-1** in $CDCl_3$ (500 MHz).

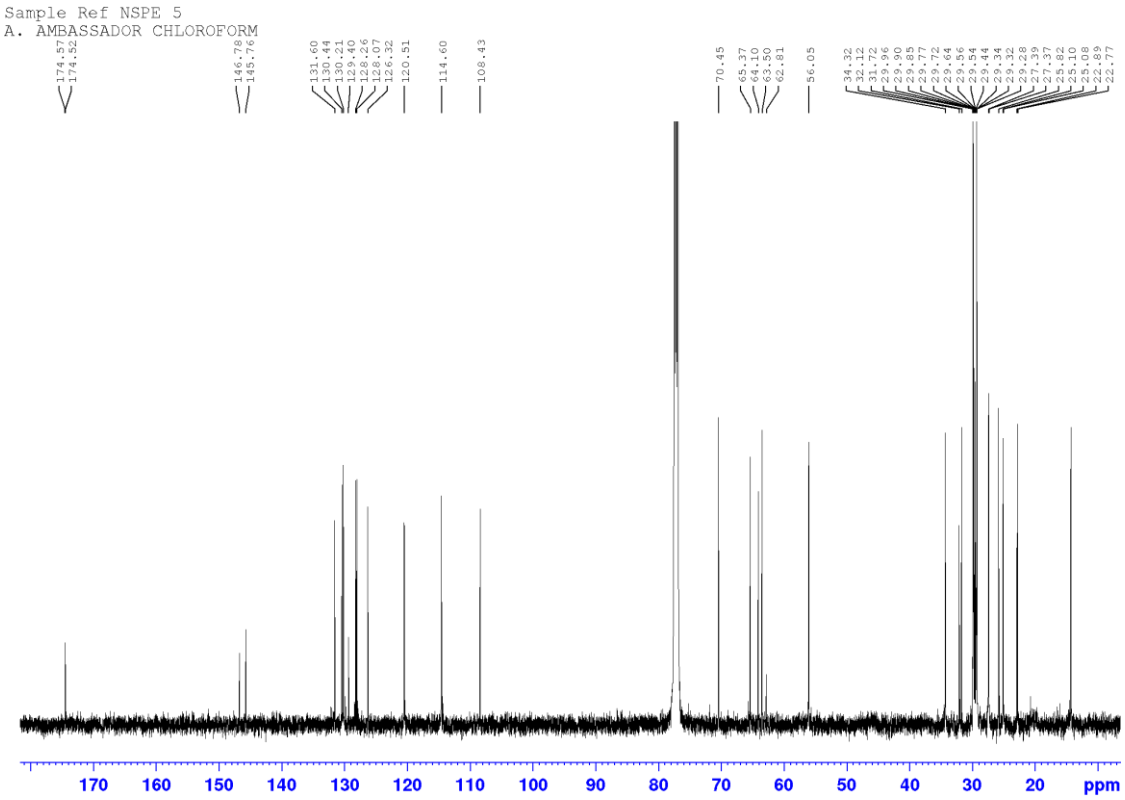

Figure 3. 14 ^{13}C NMR spectrum of **A-1** in $CDCl_3$ (125 MHz).

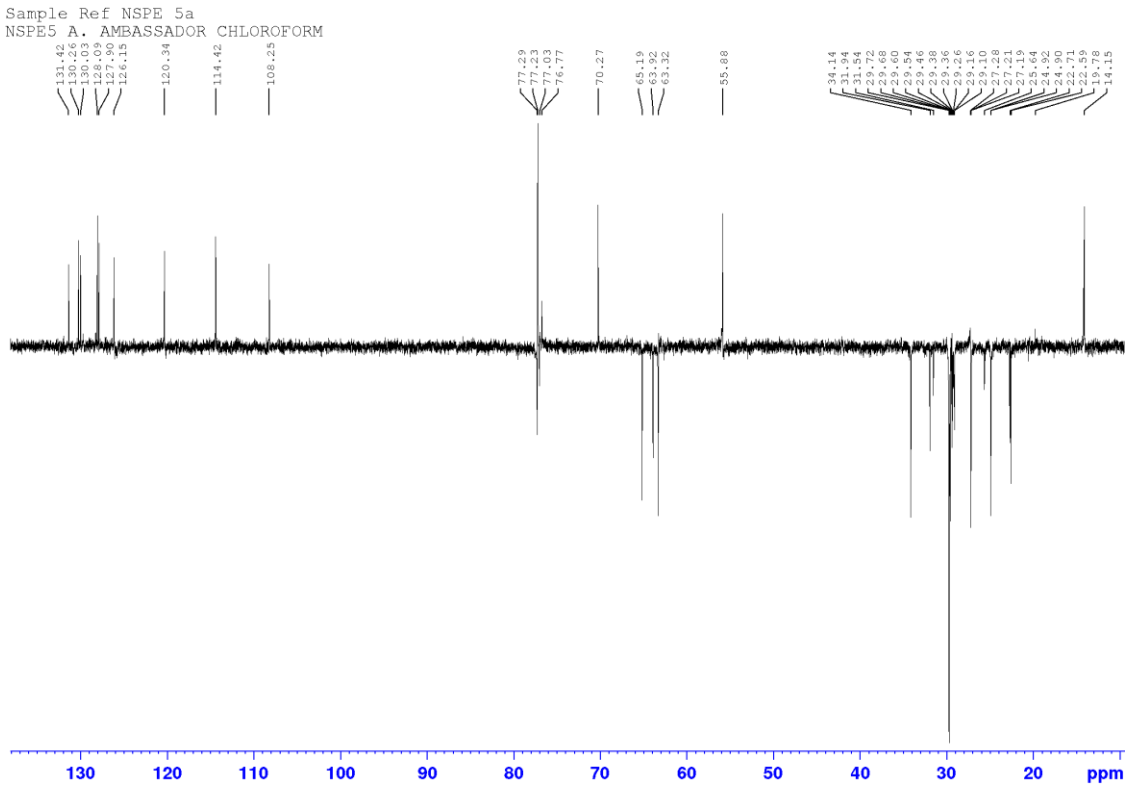

Figure 3. 15 DEPT 135 NMR spectrum of **A-1** in $CDCl_3$ (125 MHz).

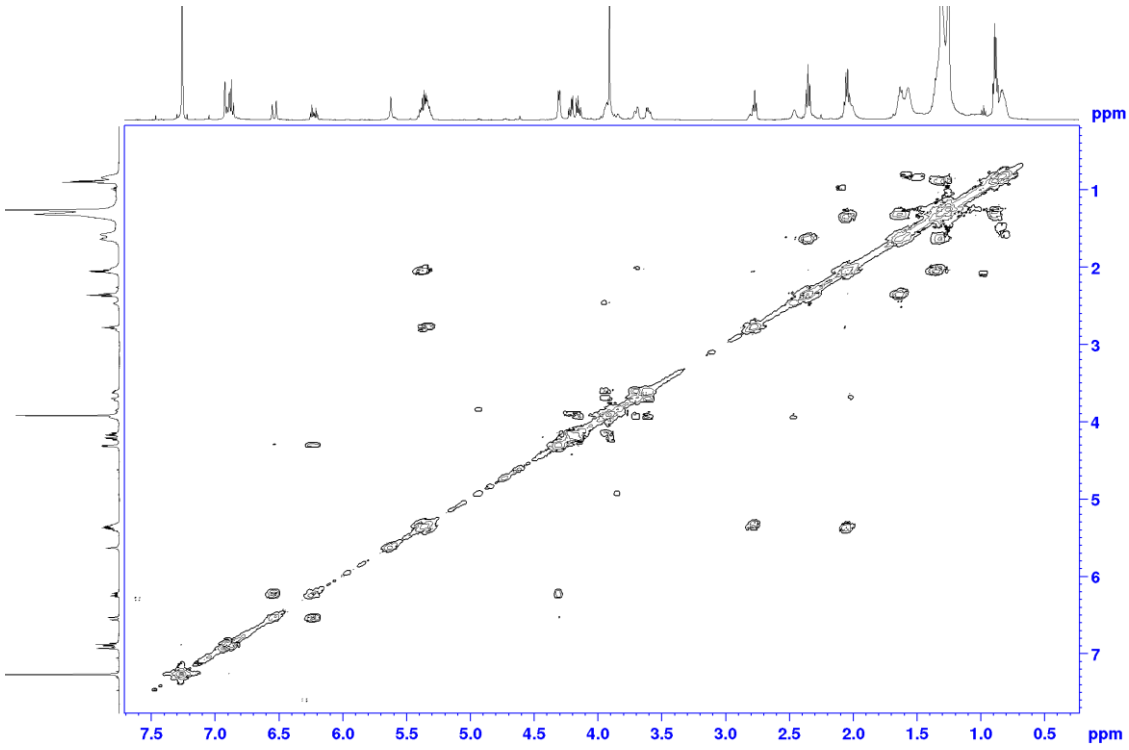

Figure 3. 16 ^{1}H-^{1}H COSY NMR spectrum of **A-1** in $CDCl_3$ (500 MHz).

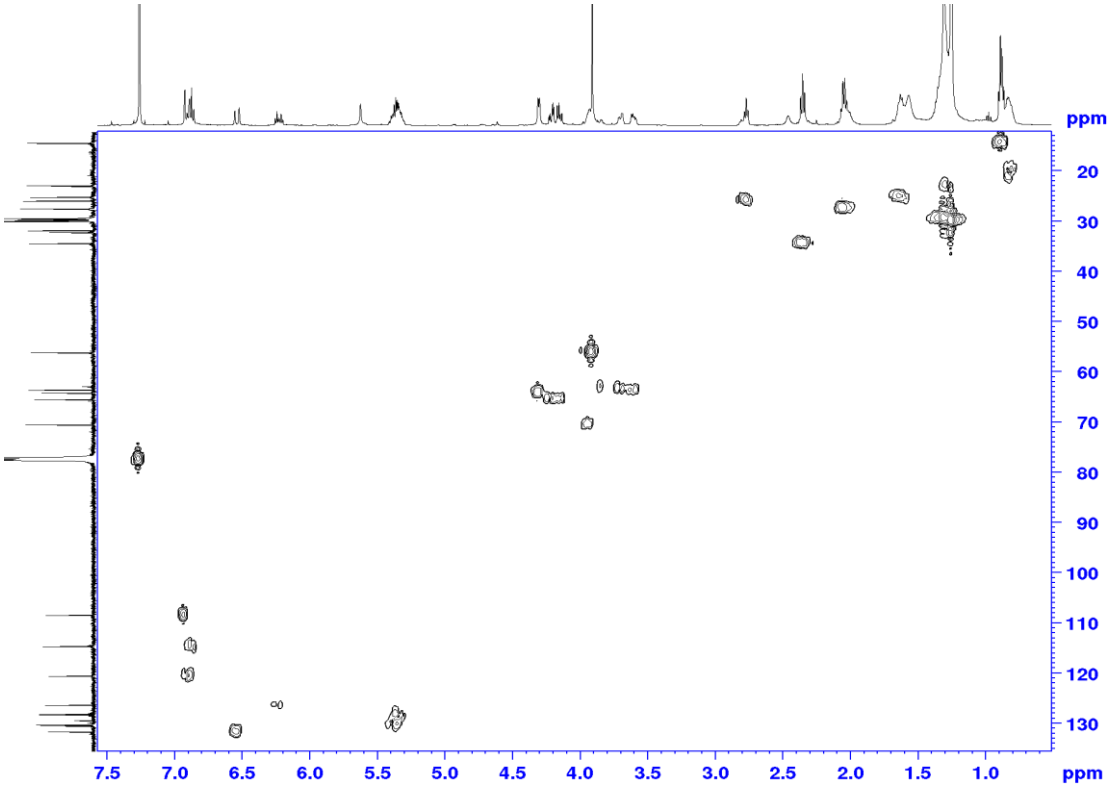

Figure 3. 17 HMQC spectrum of **A-1** in $CDCl_3$ (500 MHz).

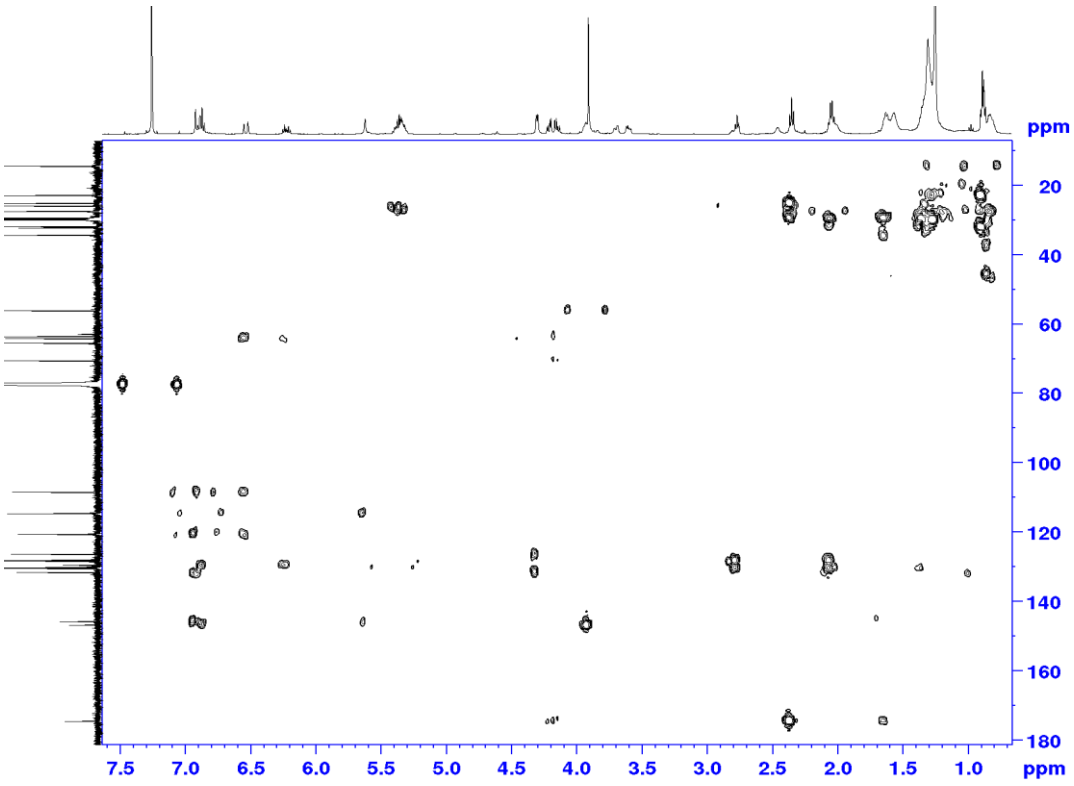

Figure 3. 18 HMBC spectrum of **A-1** in $CDCl_3$ (500 MHz).

Mass spectroscopy

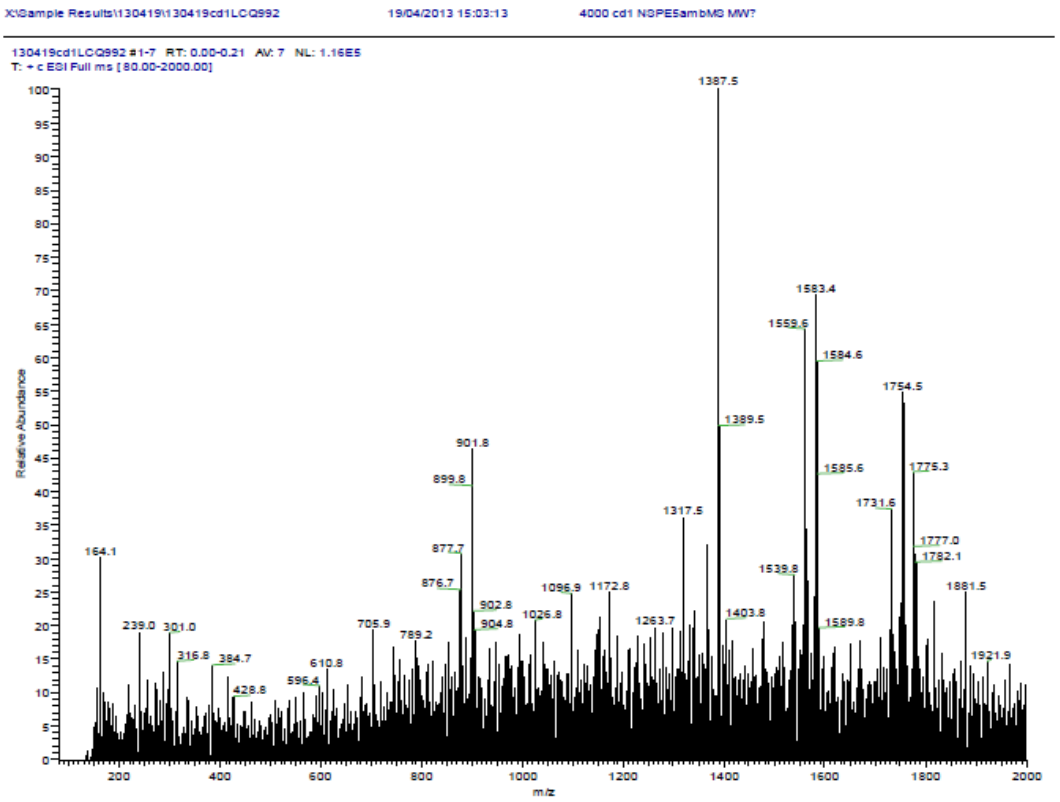

Figure 3. 19 ESI-MS spectrum of **A-1**.

The ESI-MS spectrum obtained for **A-1** (figure 3.19) does not show a clear evidence of adduct of the tentative compound coniferyl alcohol. The complexity of the mixture or the presence of impurities could possibly suppress ionisation of the components of the compound.

Chapter 4: Synthesis and biological evaluation of analogues of natural product disulfides from the genus *Allium*

4.1 Introduction

One *Allium* species recently studied for its antimicrobial properties is the Central Asian species *Allium stipitatum*. It was found to display outstanding potency towards slow-growing species of *Mycobacterium* (*including M. tuberculosis* H_{37}Rv *and M. bovis* BCG), fast-growing species of *Mycobacterium* (*including M. smegmatis, M. fortuitum and M. phlei)* and multidrug-resistant (MDR) variants of *Staphylococcus aureus* (*including SA 1199B, XU212 and EMRSA-15*).The minimum inhibitory concentrations (MIC) exhibited were clinically relevant and found to range between (0.5-8 mg/L). Subsequently, a series of structurally-related methyldisulfides were synthesized in an effort to optimize the exceptional antibacterial activity. Structure activity relationship (SAR) studies revealed that the presence of the disulfide moiety was not the only factor responsible for activity, and it is possible that the disulfide is strongly "activated" by the presence of electron-withdrawing functional groups such as pyridine, pyridine-*N*-oxide, pyrimidine, and quinoline, whereas phenyl and thiophene were poorly electron withdrawing. The findings indicated that synthetic compounds, structurally related to naturally-occurring disulfides can serve as leads for the development of effective new antibacterials for pathogenic bacteria. Hence, the rational structure-based design of compounds that will contain an electron-withdrawing group with the parallel preservation of the disulfide moiety may lead to the identification of novel scaffolds for combating multidrug resistance.

In line with these findings, analogues of natural product disulfides from *Allium stipitatum* were produced by *S*-methylthiolation of the appropriate aromatic thiol

using *S*-methylmethanethiosulfonate and back extraction with dichloromethane (O'Donnell *et al*., 2009, Kitson and Loomes, 1985). The synthesized compounds were characterized by the use of spectroscopic techniques. A number of whole-cell phenotypic bioassays including the spot-culture growth inhibition assay (SPOTi), drug efflux and biofilm assays which interrogate all of the endogenous drug targets simultaneously in specific physiological contexts, were used to evaluate these compounds. The products exhibited antimycobacterial activity at clinically-relevant concentrations and also inhibited mycobacterial drug efflux and biofilm mechanisms, which are reported here for the first time for this class of compounds. The results obtained suggest that the synthesized methyldisulfides are new scaffolds, which can lead to potentially new drugs against tuberculosis.

4.2 Procedure for synthesis

Aromatic thiols (Figure 4.1) were purchased from Sigma-Aldrich, Gillingham, UK and used as starting materials for the synthesis.

1. 4-amino-5-(benzylthio)-4H-1,2,4-triazole-3-thiol (CDS011027 ALDRICH) **(1')**
2. 4-aminothieno[2,3-d]pyrimidine-2-thiol (CDS011798 ALDRICH) **(2')**
3. 7-Fluorobenzo[d]thiazole-2-thiol (ANV00148 ALDRICH) **(3')**
4. 5-[(e)-2-phenylvinyl]-4H-1,2,4-triazole-3-thiol (CDS015509 ALDRICH) **(4')**
5. 4-ethyl-5-mercapto-4H-1,2,4-triazol-3-ol (CDS012290 ALDRICH) **(5')**

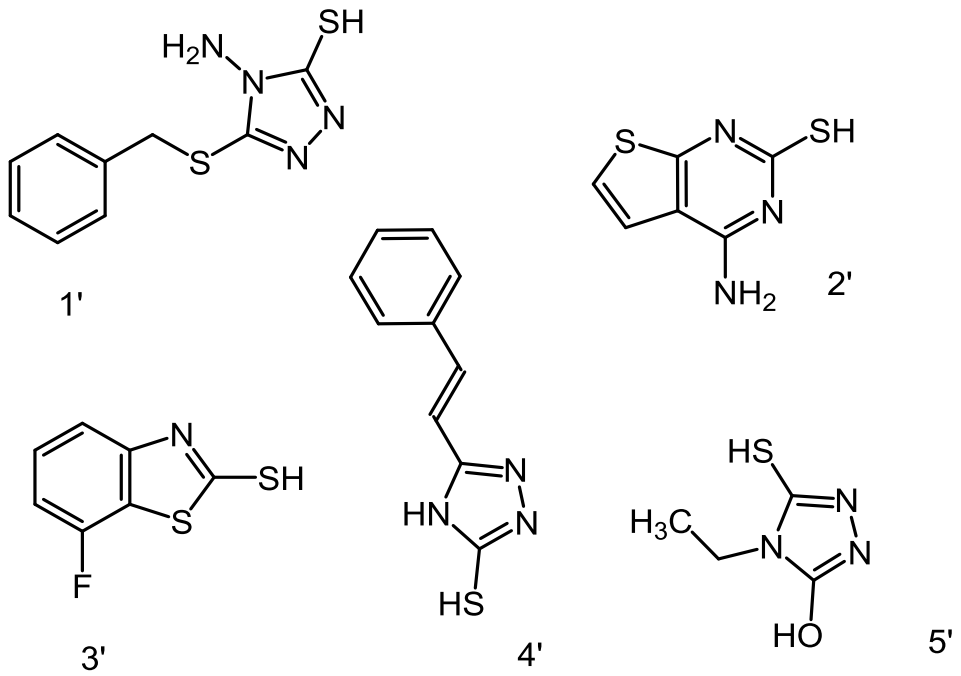

Figure 4. 1 Aromatic thiols used as starting materials.

Other reagents and chemicals used: *S*-methylmethanethiosulfonate (Fluka, 64306), Sodium hydroxide (Fisher Scientific UK Ltd, S/4920/53), Dichloromethane (VWR International SAS P25631) and Sodium sulfate (Sigma-Aldrich 746363).

The method of Kitson and Loomes (1985) was modified and adapted for the synthesis of the methyldisulfides. The appropriate thiol (1 mmol) was dissolved in water (2 mL) containing NaOH (0.040 g, 1 mmol, 1 equiv). *S*-methyl methanethiosulfonate (0.126 g, 1 mmol, 1 equiv) was then added, which formed a cloudy suspension and this suspension was stirred for 1 h at room temperature by using a magnetic stirrer (IKAMAG REO). The cloudy suspension was then extracted with dichloromethane twice (20 mL x2) and the resulting dichloromethane solution was dried with anhydrous sodium sulfate, filtered and concentrated by rotary evaporation (BUCHI Rotavapor R-200) under reduced pressure to afford the pure

disulfide (O'Donnell *et al*., 2009). The synthesised compounds were characterised by the use of spectroscopic techniques, namely NMR spectroscopy, UV-visible spectroscopy, IR spectroscopy and HRESIMS.

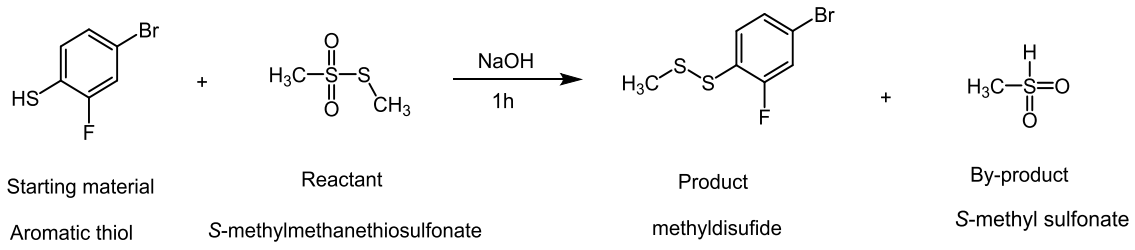

Figure 4. 2 Reaction scheme leading to methyldisulfides

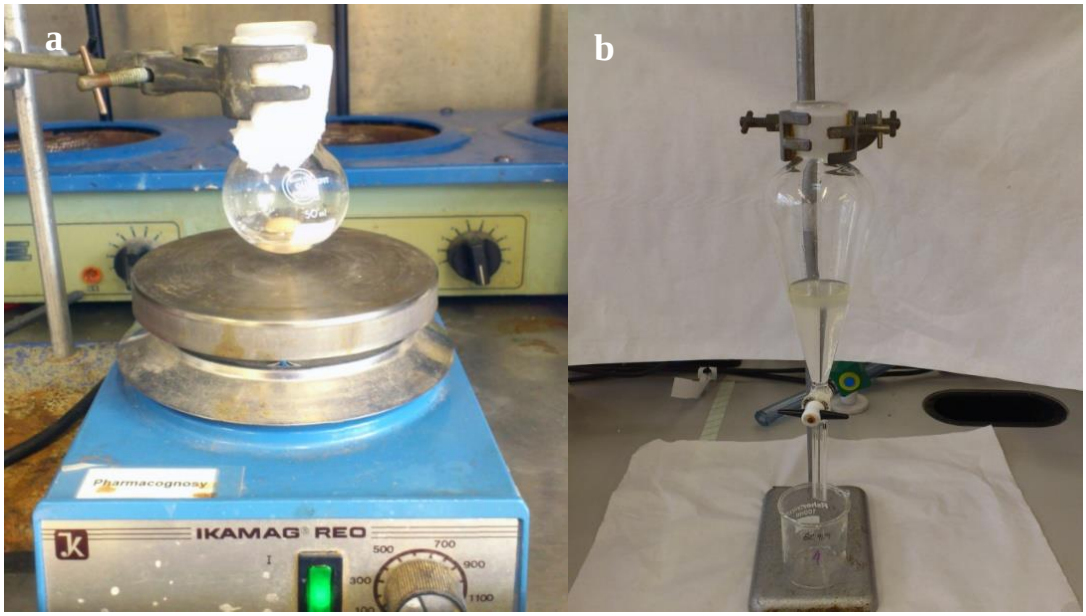

Figure 4. 3 (a) Process of synthesizing methyldisulfide using a magnetic stirrer and (b) Separation of the dichloromethane layer using a separating funnel.

4.3 Results

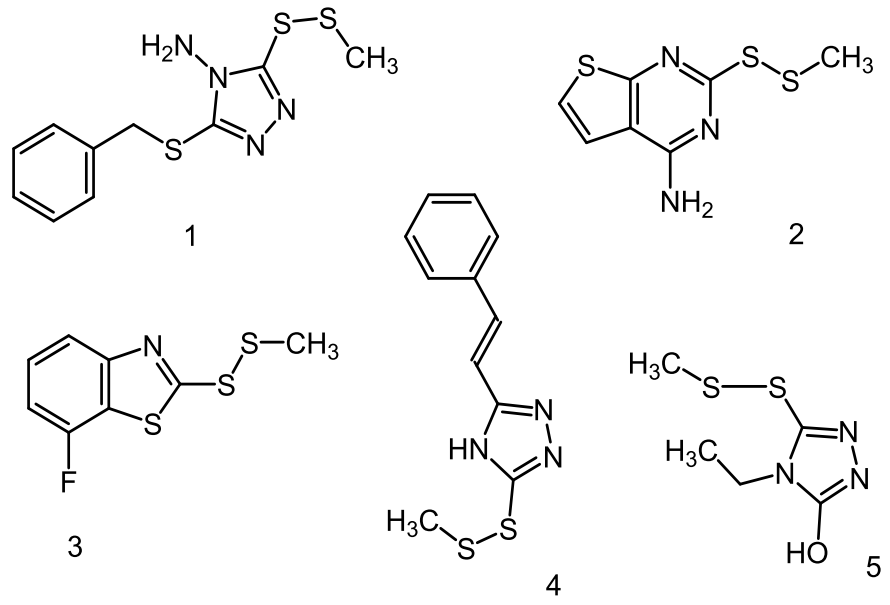

Figure 4. 4 Synthesized methyldisulfides.

4.3.1 Characterization of the methyldisulfides

The synthesized methyldisulfides were characterized by extensive NMR techniques; ^{1}H, ^{13}C, DEPT 135, HMQC, HMBC spectra of the compounds assisted in the confirmation of their identity. Infrared and ultraviolet spectroscopy provided insight about the functional groups of the molecules. The UV spectra revealed a common wavelength (λ_{max}) at 208-211 nm between compounds **1**, **4** and **5**, which demonstrated the presence of 1, 2, 4-triazole ring. The IR spectra revealed the C-H vibrations of the methyl group in the -S-S-CH_3 functional group. The characteristic frequency for the C-H bending vibration appeared in the fingerprint region at approximately 3000-3500 cm^{-1}.

The accurate mass measurement of the $[M+H]^+$ ion of each sample was performed with ESI-TOF and corresponded to the molecular formula of each methyldisulfide. The maximum allowed errors were within the limit range δ: 0-5ppm.

3-(benzylthio)-5-(methyldisulfanyl)-4*H*-1,2,4-triazol-4-amine (1)

White solid; Amount obtained 0.115 g (40 %). UV (MeOH) λ_{max} (logε) 208.0 (3.75), 255.0 (3.93) nm; IR ($CHCl_3$) ν_{max} 3247, 3142, 3025, 2973, 2918, 1413, 1382, 775, 697, 679 cm^{-1}; ^1H NMR (500 MHz, CD_3OD) δ 7.35 (2H, d), 7.29 (2H, t), 7.26 (1H, t), 4.38 (2H, s), 2.58 (3H, s); ^{13}C NMR (125 MHz, CD_3OD) δ 156.3, 154.1, 138.1, 130.1, 129.7, 128.9, 37.5, 23.4; HRESIMS *m/z* 285.0316 $[M+H]^+$ (calculated for $C_{10}H_{13}N_4S_3$ 285.0320).

2-(methyldisulfanyl)thieno[2,3-*d*]pyrimidin-4-amine (2)

Pale orange powder; Amount obtained 0.103 g (45 %). UV (MeOH) λ_{max} (logε) 228.0 (4.29), 281.0 (3.93); IR (film) ν_{max} 3068, 2983, 2912, 1556, 1470, 1408, 1271, 1238, 1032, 783 cm^{-1}; ^1H NMR (500 MHz, CD_3OD) δ 7.40 (1H, d), 7.33 (1H, t), 2.54 (3H, s); ^{13}C NMR (125 MHz, CD_3OD) δ 168.8, 166.0, 160.1, 122.6, 120.0, 115.3, 23.4; HRESIMS *m/z* 229.9888 $[M+H]^+$ (calculated for $C_7H_8N_3S_3$ 230.9880).

7-fluoro-2-(methyldisulfanyl)benzo[*d*]thiazole (3)

White fluffy solid; Amount obtained 0.109 g (47 %). UV (MeOH) λ_{max} (logε) 218.0 (4.42), 271.0 (3.86); IR (film) ν_{max} 3070, 2982, 2911, 1556, 1470, 1460, 1406, 1271, 1238, 1033, 781 cm^{-1}; ^1H NMR (500 MHz, $(CD_3)_2SO$) δ 7.55 (1H, d), 7.34 (1H, dd), 7.34 (1H, t), 2.75 (3H, s); ^{13}C NMR (125 MHz, $(CD_3)_2SO$) δ 176.2, 157.5, 154.4, 128.1, 123.2, 122.0, 110.5, 23.1; HRESIMS *m/z* 231.9736 $[M+H]^+$ (calculated for $C_8H_7FNS_3$ 231.9725).

(*E*)-3-(methyldisulfanyl)-5-styryl-4*H*-1,2,4-triazole (4)

Pale yellow powder; Amount obtained 0.110 g (44 %). UV (MeOH) λ_{max} (logε) 210.0 (4.13) 294.0 (4.29); IR (film) ν_{max} 3053, 2995, 2910, 2842, 2239, 1649, 1414, 970, 953, 753, 729, 696, 683 cm^{-1}; ^{1}H NMR (500 MHz, DMSO-d_6) δ 7.66 (2H, d), 7.42 (1H, t), 7.36 (2H, t), 7.12 (1H, d) 7.08 (1H, d), 2.63 (3H, d); ^{13}C NMR (125 MHz, DMSO) δ 159.6, 155.04, 150.1, 135.2, 129.2, 128.9, 127.2, 113.0, 23.2; HRESIMS *m/z* 250.0481 $[M+H]^+$ (calculated for $C_{11}H_{12}N_3S_2$ 250.0473).

4-ethyl-5-(methyldisulfanyl)-4*H*-1,2,4-triazol-3-ol (5)

Pale yellow powder; Amount obtained 0.079 g (41%). UV (MeOH) λ_{max} (logε) 210.0 (3.08); IR (film) ν_{max} 3087, 3016, 2950, 2860, 2770, 2617, 2312, 1686, 1489, 1305, 774, 749, 683 cm^{-1}; ^{1}H NMR (500 MHz, CD_3OD) δ 3.76 (2H, q), 2.50 (3H, s), 1.26 (3 H, t); ^{13}C NMR (125 MHz, CD_3OD) δ 156.9, 144.3, 38.1, 23.0, 14.5; HRESIMS *m/z* 192.0261 $[M+H]^+$ (calculated for $C_5H_{10}N_3OS_2$ 192.0265).

For reasons of limited space, thorough elaboration of the spectra of only compound **1** is shown. The ^{1}H NMR spectra of the other compounds (**2-5**) is presented in Appendix 2.

Characterisation of compound (1)

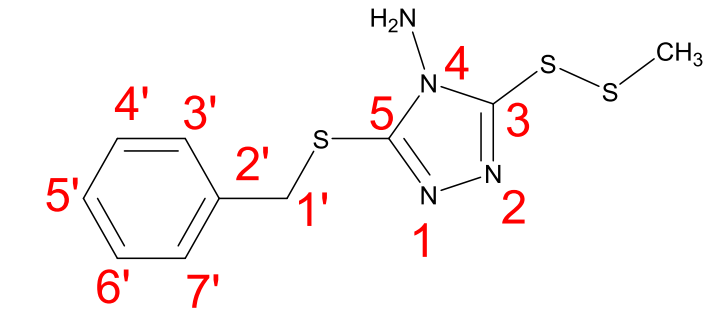

3-(benzylthio)-5-(methyldisulfanyl)-4*H*-1,2,4-triazol-4-amine

Figure 4. 5 Structure of compound **1**.

The examination of the ^{1}H NMR spectrum revealed the presence of 10 protons. The first peak, a singlet, appeared at δ 2.58 ppm in the spectrum and integrated for three protons. Therefore it corresponded to the three hydrogens of the methyl group. It was deshielded because of the neighbouring electron withdrawing sulphur group. There was a methylene at 4.38 (H-1') which integrated for two protons, while in the aromatic region the integration of the peaks proved the presence of five hydrogen atoms (protons H-3', H-7', H-4', H-6', H-5'). The ^{13}C-NMR spectrum (Figure 4.7) exhibited 10 signals which corresponded to 3 quaternary carbons, 5 methine, 1 methylene and 1 methyl carbon (Table 4.1). Analysis of the multiple patterns and the chemical shift of protons and carbons in the ^{1}H and ^{13}C NMR spectra, and by identifying the HMQC and HMBC correlations, the identity of compound **1** was confirmed (Table 4.1).

Table 4. 1 ^{1}H (500 MHz) and ^{13}C (125 MHz) spectral data and ^{1}H -^{13}C long-range correlations of Compound **1** in CD_3OD

			HMBC	
Position	**^{1}H**	**^{13}C**	**^{2}J**	**^{3}J**
3	-	154.1	-	-
5	-	156.3	-	-
1'	4.38, s	37.5	C-2'	C-5, C-3'/7'
2'	-	138.1	-	-
3', 7'	7.35, d, *J* = 7.0 Hz	130.1	C-2', 4'/6'	C-1', C-5'
4', 6'	7.29, t, *J* = 7.0 Hz	129.7	C-5', 3'/7'	C-2'
5'	7.26, t, *J* = 7.0 Hz	128.9	C-4'/6'	C-3'/7'
CH_3	2.58, s	23.4	-	-

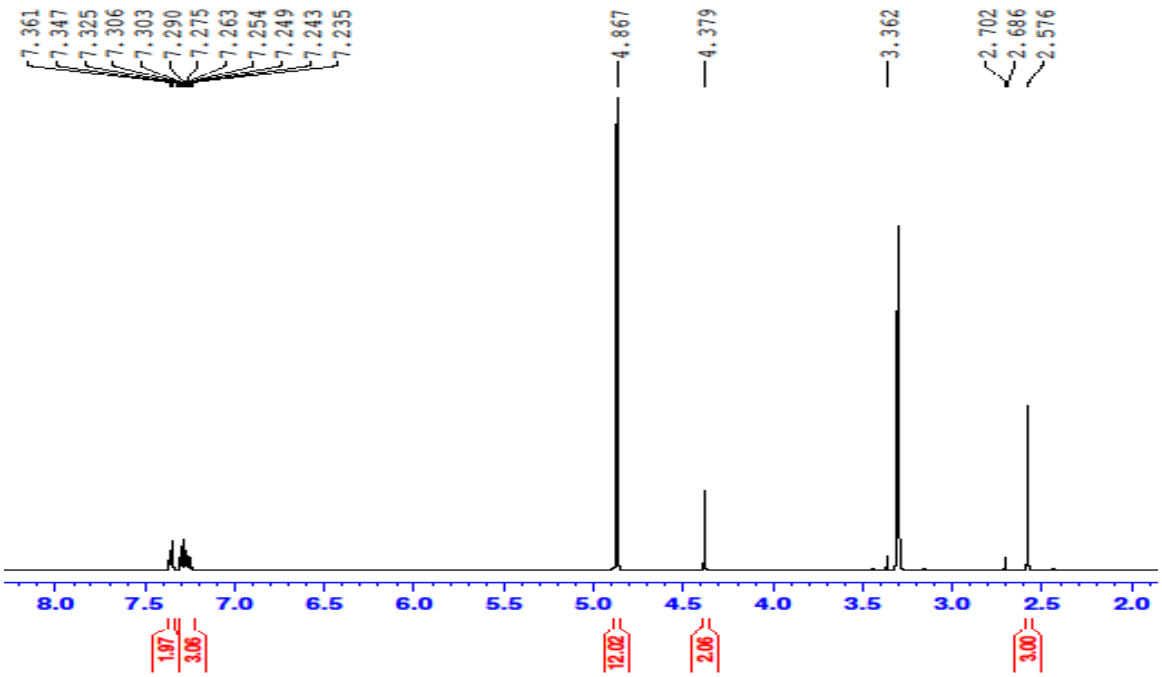

Figure 4. 6 ^{1}H NMR spectrum of compound **1** in CD_3OD (500 MHz).

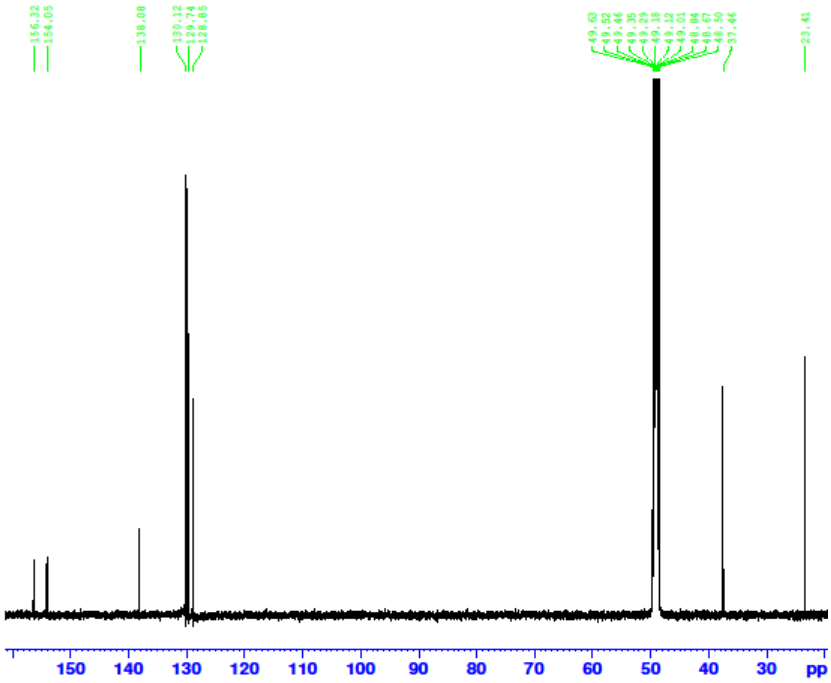

Figure 4. 7 ^{13}C NMR spectrum of compound **1** in CD_3OD (125 MHz).

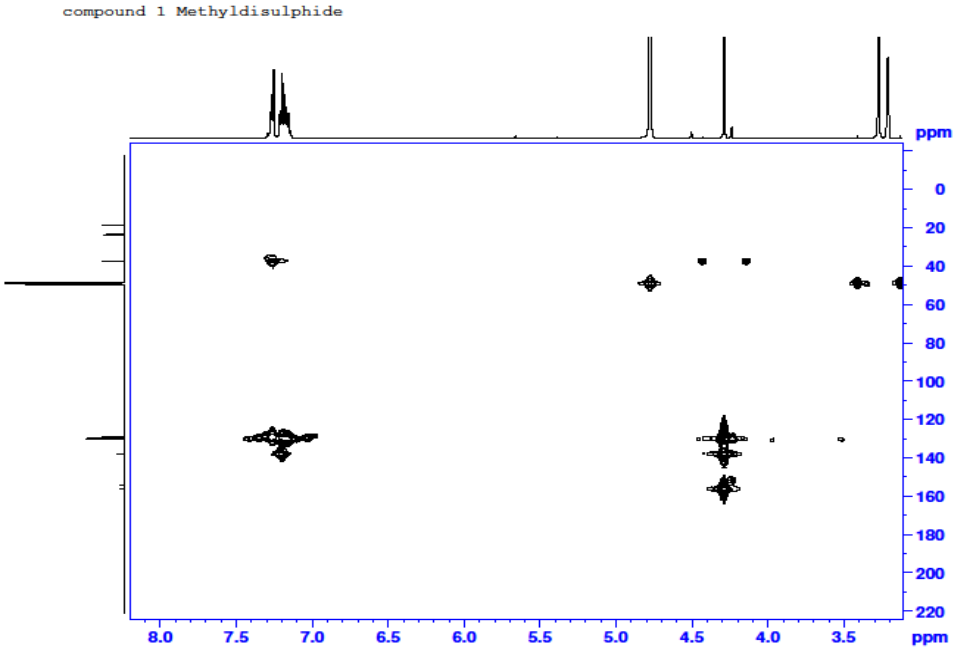

Figure 4. 8 HMBC spectrum of compound **1** in CD_3OD (500 MHz).

4.3.2 Biological evaluation

The drug susceptibility assays, cytotoxicity, efflux pump inhibition, biofilm and fungal assays as well as growth curve and CFU counting were carried out as described in Chapter 2 (Materials and Method section).

.

Table 4. 2 Minimum inhibitory concentration (MIC) mg/L of synthesized disulfides using different strains of bacteria

Compound	*M. smegmatis*	*M. aurum*	*M. bovis BCG*	*M. tuberculosis* $H_{37}Rv$	*E. coli* (NCTC 10418)	*Proteus mirabilis* (10830)	*K. pneu-moniae* (17)	*S. aureus* SA-1199B	*S. aureus* XU212	EMRSA-15	*E. faecalis*
1	**31.3**	**31.3**	**31.3**	**62.5**	**128**	**128**	**128**	**32**	**16**	**64**	**32**
2	**15.7**	**15.7**	**15.7**	**4.0**	**128**	**512**	**512**	**16**	**16**	**16**	**32**
3	**62.5**	**62.5**	**62.5**	**31.3**	**128**	**512**	**>512**	**32**	**16**	**16**	**16**
4	**15.7**	**15.7**	**15.7**	**31.3**	**32**	**512**	**512**	**16**	**8**	**8**	**8**
5	**15.7**	**15.7**	**15.7**	**31.3**	**16**	**64**	**64**	**16**	**16**	**8**	**16**
Norfloxacin	-	-	-	-	-	**>64**	**>64**	**64**	**8**	**0.5**	**2**
Isoniazid	**4**	**0.4**	**0.1**	**0.05**	-	-	-	-	-	-	-
Rifampicin	**8**	**0.1**	**0.5**	**0.1**	-	-	-	-	-	-	-

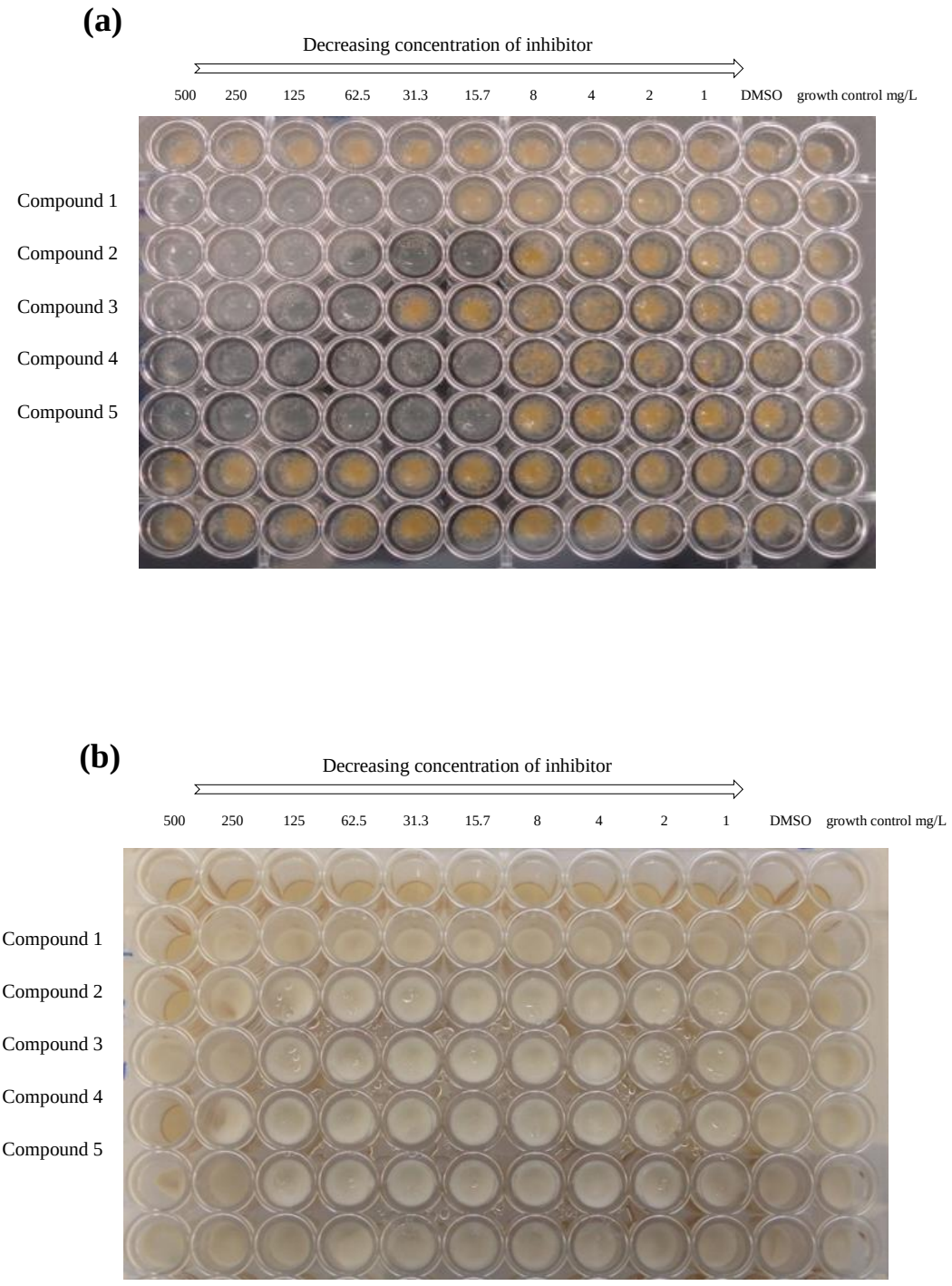

Figure 4. 9 Representative SPOTi plate showing minimum inhibitory concentration of methyldisulfides using (a) *M. aurum and* (b) *Trichophyton equinum respectively*.

Table 4. 3 Minimum Inhibitory Concentrations (MIC) mg/L of synthesized disulfides against fungi (dermatophytes)

Compound	*T. rubrum*	*T. mentagrophyte*	*T. equinum*	*T. tonsurans*
1	**500**	**62.5**	**500**	**250**
2	**500**	**62.5**	**500**	**250**
3	**>500**	**>500**	**>500**	**>500**
4	**500**	**250**	**500**	**250**
5	**>500**	**500**	**>500**	**>500**
Nystatin	**1**	**-**	**8**	**-**
Amorolfine	**0.008**	**1**	**0.008**	**-**
Terbinafine	**0.001**	**1**	**0.008**	**-**
Ciplox olamine	**0.008**	**31.3**	**15.7**	**-**
Ketoconazole	**0.125**	**-**	**0.016**	**-**
Itraconazole	**0.016**	**-**	**0.001**	**-**
Imidazole	**250**	**-**	**250**	**-**

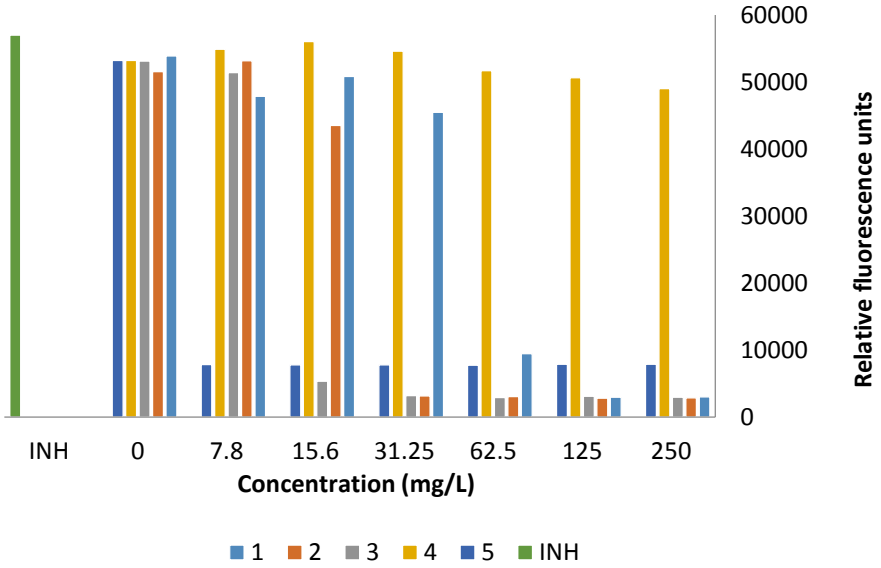

Figure 4. 10 Cell toxicity assay using murine macrophage RAW 264.7 cell line. The number of viable cells was quantified using the Trypan blue exclusion assay with the use of an haemocytometer and inverted microscope. The 50 % growth inhibitory concentration was determined based on the resazurin fluorescence assay and the SI calculated as SI = GIC_{50}/MIC.

Table 4. 4 Cytotoxicity profile of the compounds

Compound ID	MIC_{H37Rv}	GIC_{50}	$SI=GIC_{50}/ MIC_{H37Rv}$
Compound **1**	62.50	40.93	0.65
Compound **2**	4.00	18.23	4.56
Compound **3**	31.30	9.92	3.16
Compound **4**	31.30	>250	>7.99
Compound **5**	31.30	>250	>7.99

SI - Selectivity Index, GIC - Growth Inhibitory Concentration
MIC - Minimum Inhibitory Concentration

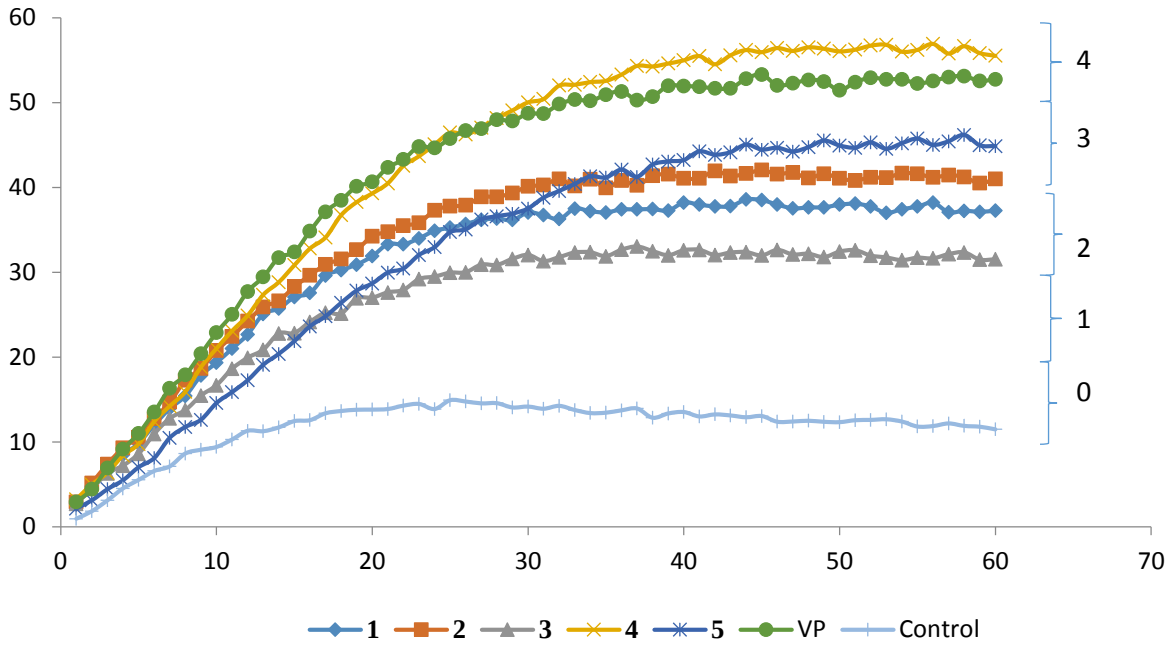

Figure 4. 11 Efflux pump inhibition effect of disulfide compounds. Ethidium bromide (EtBr) is an efflux pump substrate (used at a final concentration of 0.5 mg/L). Verapamil (VP) is a known efflux pump inhibitor and was used as the reference standard.

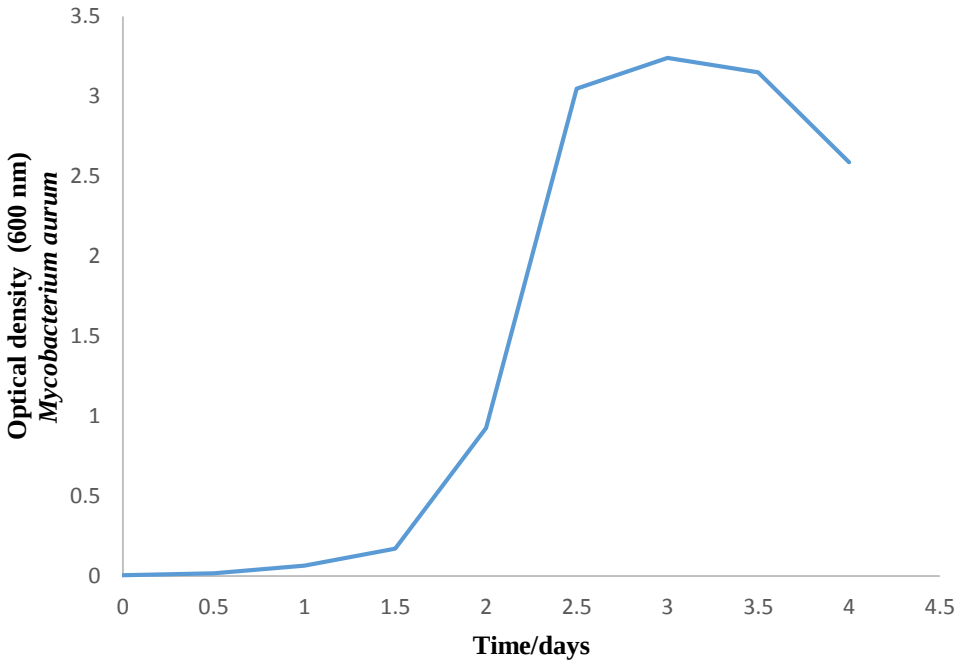

Figure 4. 12 Growth curve of *Mycobacterium aurum* (cells were grown at 180 rpm).

Table 4. 5 Optical density readings of *M. aurum* in the presence of different concentrations (MIC, 2x MIC, 4x MIC, 8x MIC) of disulfide compound **2** at different time points.

	Optical density			
Conc.(mg/L)	0	2 hr	4 hr	6 hr
0	0.685	0.866	1.002	1.194
15.7 (MIC)	0.685	0.854	0.964	1.066
31.4 (2x MIC)	0.685	0.846	0.902	0.98
62.8 (4x MIC)	0.685	0.786	0.774	0.744
125 (8x MIC)	0.685	0.704	0.662	0.68

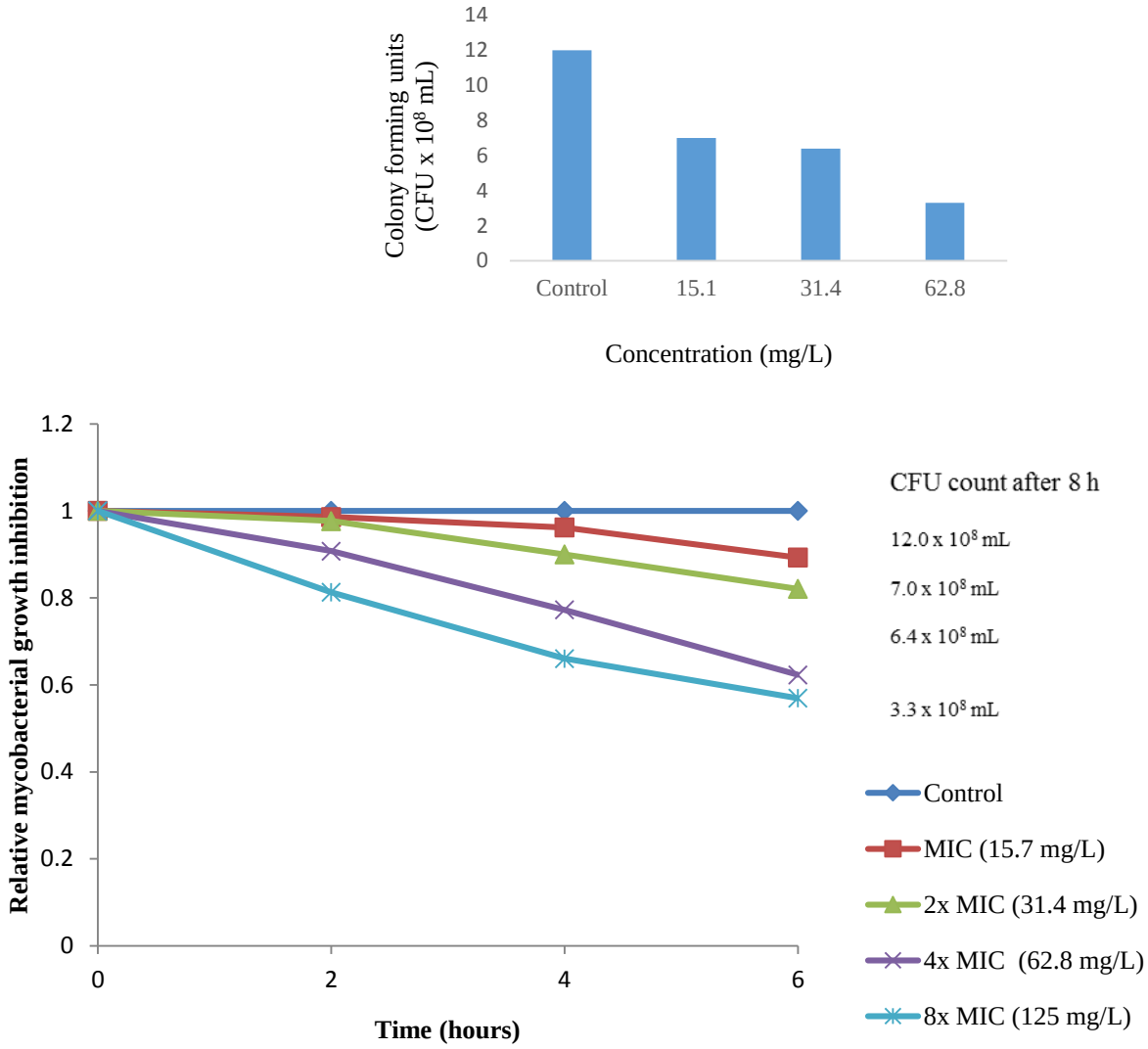

Figure 4. 13 Growth analysis of *M. aurum* in the presence of different concentrations (MIC, 2x MIC, 4x MIC, 8x MIC) of disulfide compound **2** at different time points. (Insert) Bar diagram of the number of Colony forming units (CFU) recorded at one time-point of liquid cultures of *M. aurum* treated with different concentrations of compound **2** MIC (15.17), 2x MIC (31.13), 4x MIC (62.5 mg/L). The aliquots were taken and plated on agar after 8 h.

Figure 4. 14 Dose-dependent inhibition of biofilm formation by compound **2** in (a) polypropylene tubes (b) 96-well plates (g) quantification of formed biofilm using the crystal violet technique, (c & d) SEM images and (e & f) light microscope images of *M. smegmatis* cells (planktonic form) and (biofilm form) at early stationary phase (OD 3.5) respectively by compound **2**. (h) SEM image of *M. smegmatis* cells (planktonic form) only at early stationary phase (OD_{600} 3.5) (i-n) dose-dependent SEM images of *M. smegmatis* (biofilm form) at early stationary phase (OD 3.5).

4.6 Discussion

Phenotypic screens have been used successfully to discover potent antibacterial drugs and the HT-SPOTi can help to identify new antimicrobial molecules with clinical relevance (Guzman *et al*., 2013). All of the synthesized methyldisulfides had antibacterial activity to a varying extent. They were tested against different species of *Mycobacterium*; *Mycobacterium aurum* (ATCC23366), *M. smegmatis* mc^2155 (ATCC700084), *M. bovis* BCG (ATCC35734), *M. tuberculosis* $H_{37}Rv$ and two multidrug-resistant strains of *M. tuberculosis* $H_{37}Rv$ clinical isolates as well as fungi, Gram-positive and Gram-negative organisms to establish whether these compounds were broad anti-bacterial inhibitors. All five compounds showed significant antimycobacterial activities when tested, with compound **2** having the lowest MIC of 4 mg/L, against the virulent *M. tuberculosis* $H_{37}R_V$ (table 4.2).

The synthesized methyldisulfides exhibited appreciable antibacterial activity against *E. coli* and particularly compounds **4** and **5** had good antibacterial activity with MIC values ranging from 16-32 mg/L. *Escherichia coli* was not susceptible to norfloxacin while *K. pneumoniae* and *Proteus mirabilis* were resistant to the antibiotic at the concentrations tested (MIC $\geq$ 64 mg/L). Interestingly, compound **5** inhibited *K. pneumoniae* and *Proteus mirabilis* at an MIC of 64 mg/L and whilst this is a moderate activity, it is rare to find compounds demonstrating any antibacterial activity toward these organisms. Compounds **1**-**5** exhibited antibacterial activity against the three *S. aureus* strains and the *E. faecalis* strain (MIC $\geq$64 mg/L) and in particular, compounds **2**, **4** and **5** were highly active against *S. aureus* strains with MIC values falling within 8-16 mg/L. *Staphylococcus aureus* strain SA-1199B and XU212 proved to be susceptible to the methyldisulfides. Overall, the

methyldisulfides exhibited a selective inhibitory effect against *Mycobacterium* species as compared to fungal strains, Gram-positive and Gram-negative bacteria.

Multidrug resistance due to the expression of efflux pump is a clinical problem rendering antibiotics redundant since it contributes to a reduction in drug accumulation. This could be circumvented by molecules that interfere or inhibit antibiotic efflux. Additionally, multidrug efflux pumps are often transmembrane proteins that secrete metabolites involved in quorum-sensing. This *cross-talk* between bacteria is believed to be essential for the formation and dispersion of bacterial biofilms. Therefore, inhibition of multidrug efflux pumps is also a strategy to prevent biofilm formation, which is a major contributor to antimicrobial resistance. Efflux mechanisms are involved in quorum-sensing that in turn plays a pivotal role in biofilm formation. *Mycobacterium smegmatis,* a non-pathogenic model for *M. tuberculosis,* forms stable biofilms at the liquid-air interface within 5 days and was used to test whether the impairment of drug efflux could also inhibit the formation of biofilm in mycobacteria. The synthetic compounds exhibited inhibition of multidrug-efflux pumps (figure 4.11). They also showed a dose-dependent inhibition in the biofilm formation (figure 4.12), which is reported here for the first time for this class of compounds.

In order to consider the therapeutic potential of a synthetic compound, it is recommended to determine the concentration range at which the compounds are active as inhibitors of the growth of pathogenic mycobacteria while being non-toxic to mammalian cells. The compounds were selectively more toxic towards mycobacterial cells as compared to murine macrophages. Compounds **2** and **3** had an SI of 4.5 and 3 respectively. The selectivity index indicates the therapeutic window offered by compounds when used in eukaryotic hosts. The efflux pump and

biofilm inhibitory effects demonstrated by these compounds suggests the probable mode of action of these drugs however, a molecular and biochemical investigation of the relevant genes and their products from resistant cells generated against these compounds needs to be followed up. The synthesized methyldisulfides are, however, new chemical scaffolds that have potential as templates for the design of new drugs against TB.

Chapter 5: Bioguided isolation and characterisation of compounds from *Andrographis paniculata*

5. 1 Introduction

Andrographis paniculata is an annual herbaceous plant belonging to the family Acanthaceae, commonly known as 'bitter herb' or 'King of bitters' because of its extremely bitter taste. The plant grows abundantly in Africa, Southern and Southeastern Asia, including India, Sri Lanka, Pakistan and Indonesia. *Andrographis paniculata* enjoys a reputation in traditional medicine and it has extensive ethnopharmacological use ranging from the treatment of upper respiratory tract infections, dysentery, dyspepsia, malaria, hypertension, diabetes and as an antidote for snakebite. It is antibacterial, antiviral, anthelmintic and anti-inflammatory (Zhang *et al*., 2015, Zhang and Tan, 1997, Visen *et al*., 1993, Wen *et al*., 2014).

Previous studies on the phytochemistry of *Andrographis paniculata* have established about 50 labdane diterpenoids and 30 flavonoids. Additionally, more than 30 novel phytochemicals have been isolated from the plant (Xu *et al*., 2010). Chemical explorations of *Andrographis paniculata* began by the end of the nineteenth century with the isolation of an extremely bitter lactone diterpene in 1896 for the first time. This was named andrographolide. The second non-bitter component namely neoandrographolide was discovered forty one years later followed by the isolation of the third relatively minor diterpene, 14-deoxy-11,12-didehydroandrographolide, along with three other diterpenes, including andrographiside, 14-deoxyandrographolide and 14-deoxyandrographiside (Matsuda *et al*., 1994).

The aerial part of the plant contains the highest proportion of available diterpene lactones of which the major ones contributing to pharmacological activity are andrographolide, 14-deoxy-11,12-didehydroandrographolide and neoandrographolide. The other lactones present in the plant are 14-deoxyandrographolide, 14-deoxy-11-andrographolide, andrographon, andragraphan, deoxyandrographiside, andrographiside and andrographosterol (Matsuda *et al*., 1994, Puri *et al*., 1993). In addition to the diterpene lactones, flavonones, oroxylin and wogonin were also isolated from the leaves of *Andrographis paniculata*. From the roots, more flavonones including andrographadines, andrographin and panicolin were isolated (Chao and Lin, 2010).

The presence of the active constituents from the diterpenoid group such as andrographolide, neoandrographolide and 14-deoxy-11,12-didehydroandrographolide has given incredible unique medicinal properties to the plant. *Andrographis paniculata* has been employed historically in epidemics, including the global flu epidemic of 1919. It was credited during that period as a wonder drug for arresting the spread of the contagious illness. It has antimicrobial and growth promoting function and may be used as an alternative to antibiotics and tonic (Wang *et al*., 2015, Koteswara Rao *et al*., 2004). Most importantly, *Andrographis paniculata* has also been included in the WHO monographs on selected medicinal plants.

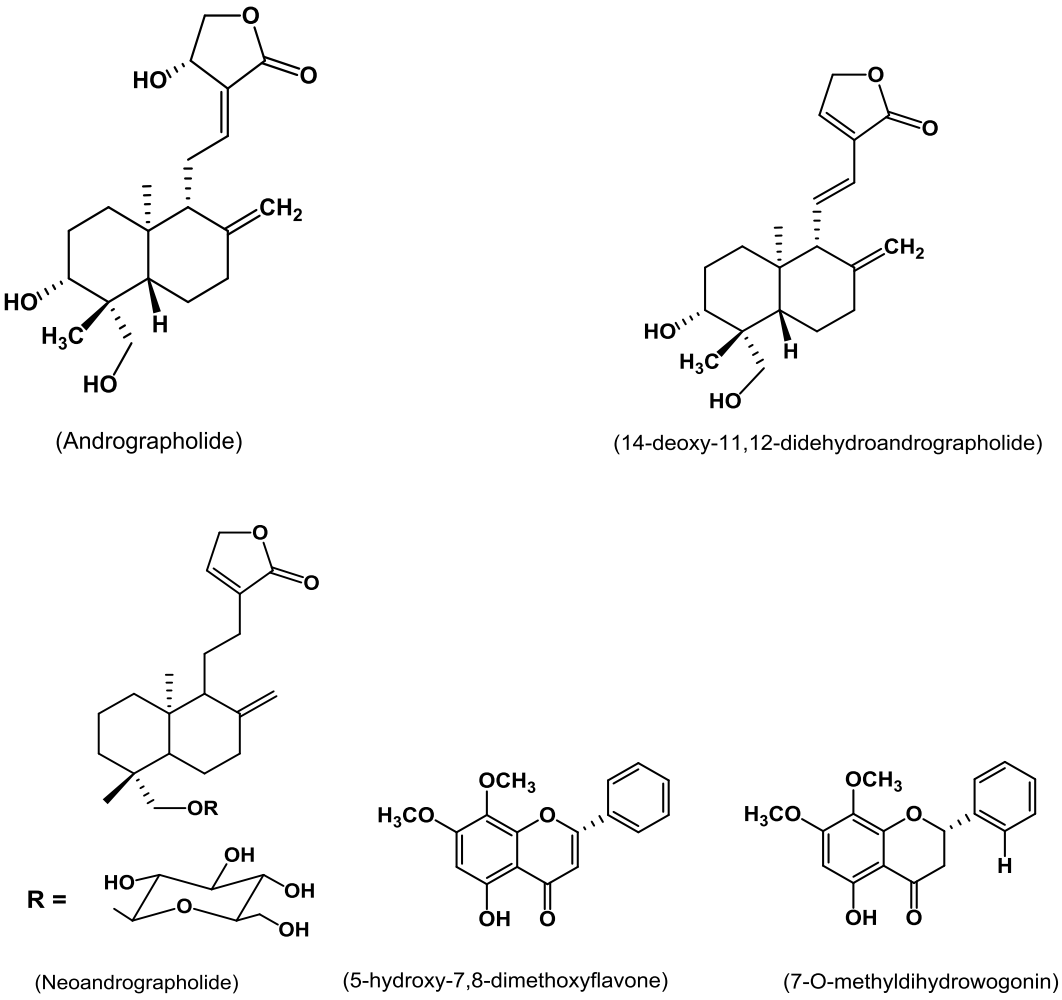

Figure 5. 1 Labdane diterpenoids and flavonoids from *Andrographis paniculata*.

In this research, different extraction and chromatographic techniques were employed to aid isolation of the compounds. The powdered leaves of *Andrographis paniculata* (2 Kg) were extracted sequentially using a Soxhlet apparatus with the organic solvents hexane, chloroform and methanol which yielded 14.1, 21.1 and 43.3 g of extracts respectively. Vacuum liquid chromatography was done using the MeOH extract with an increasingly polar gradient of 10 % solvent; from 100 % hexane to 100 % ethyl acetate through to 100 % MeOH (Figure 5.2). Thin layer Chromatography (TLC) of the fractions was performed on normal and reverse phase silica.

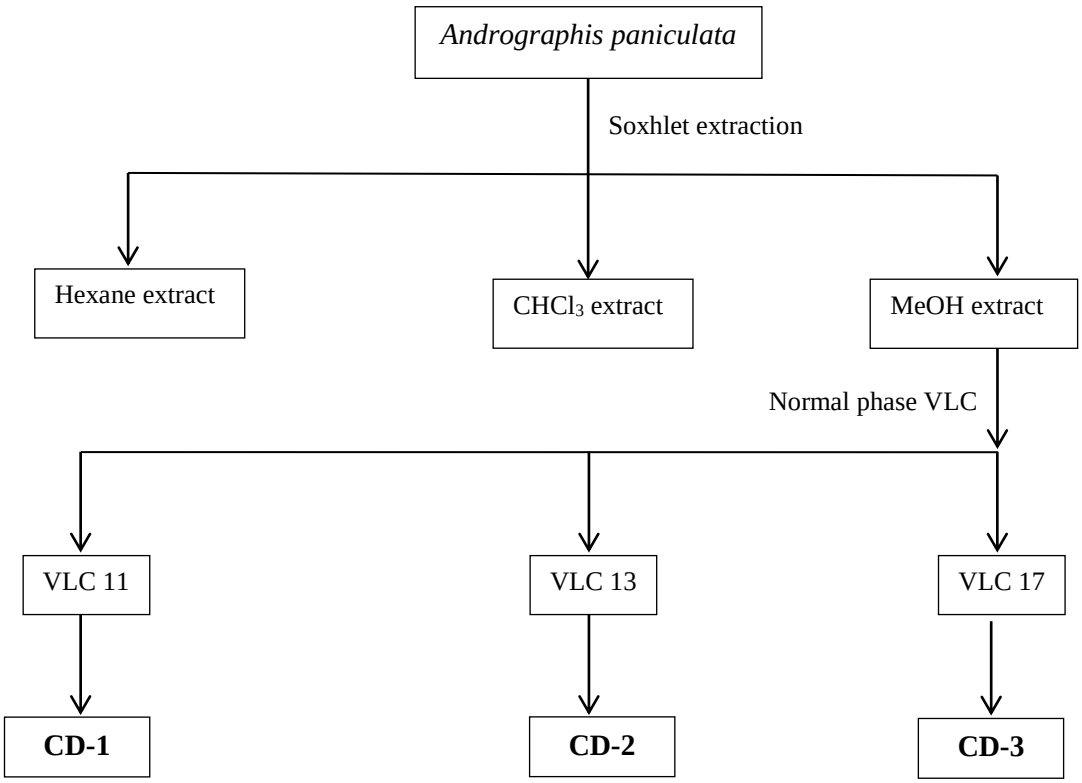

Figure 5. 2 Flow chart for the isolation of **CD-1**, **CD-2**, and **CD-3** from *Andrographis paniculata*.

The MeOH extract (20 g) obtained from Soxhlet extraction was dissolved in water and back extracted with butanol (BuOH). The BuOH was evaporated off and open column chromatography was carried out on 15 g of the BuOH extract using $CHCl_3$-MeOH gradient solvent system (Figure 5.3). Silica gel 60 (0.040-0.063 mm) was used and the analyte was mixed with silica to form a free flowing powder before it was packed. After performing TLC on all of the column fractions (1-60), similar fractions were pooled together and analysed.

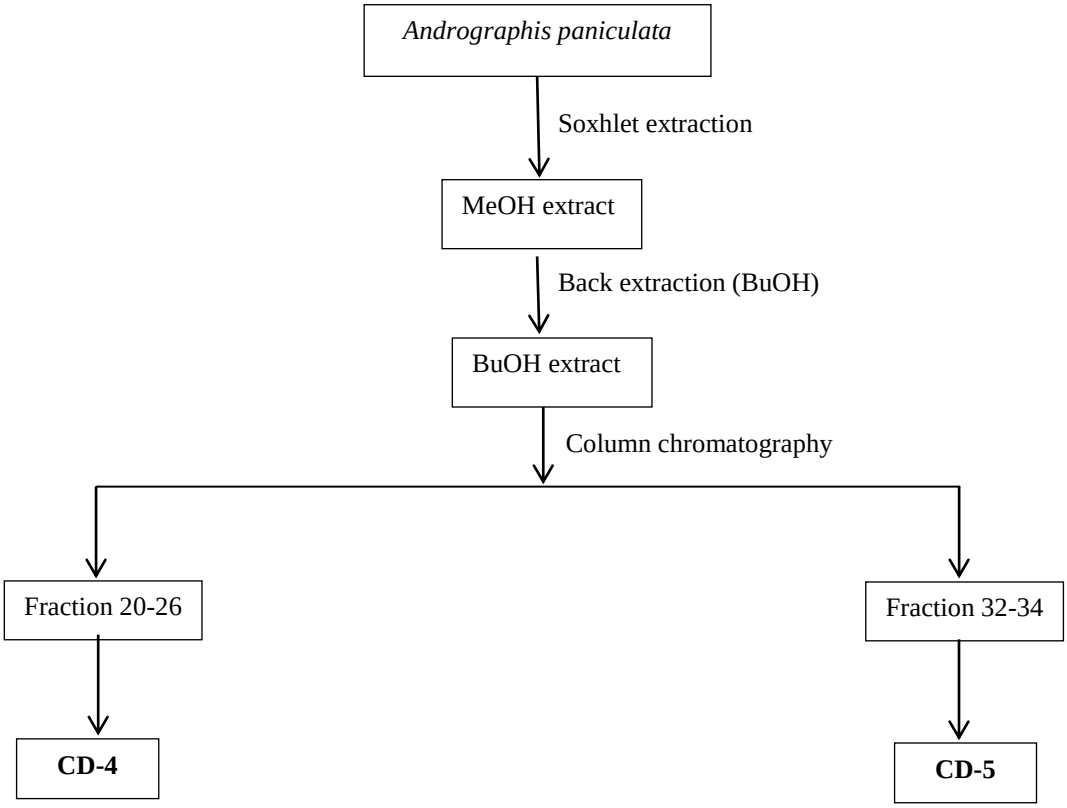

Figure 5. 3 Flow chart for the isolation of **CD-4** and **CD-5** from *Andrographis paniculata*.

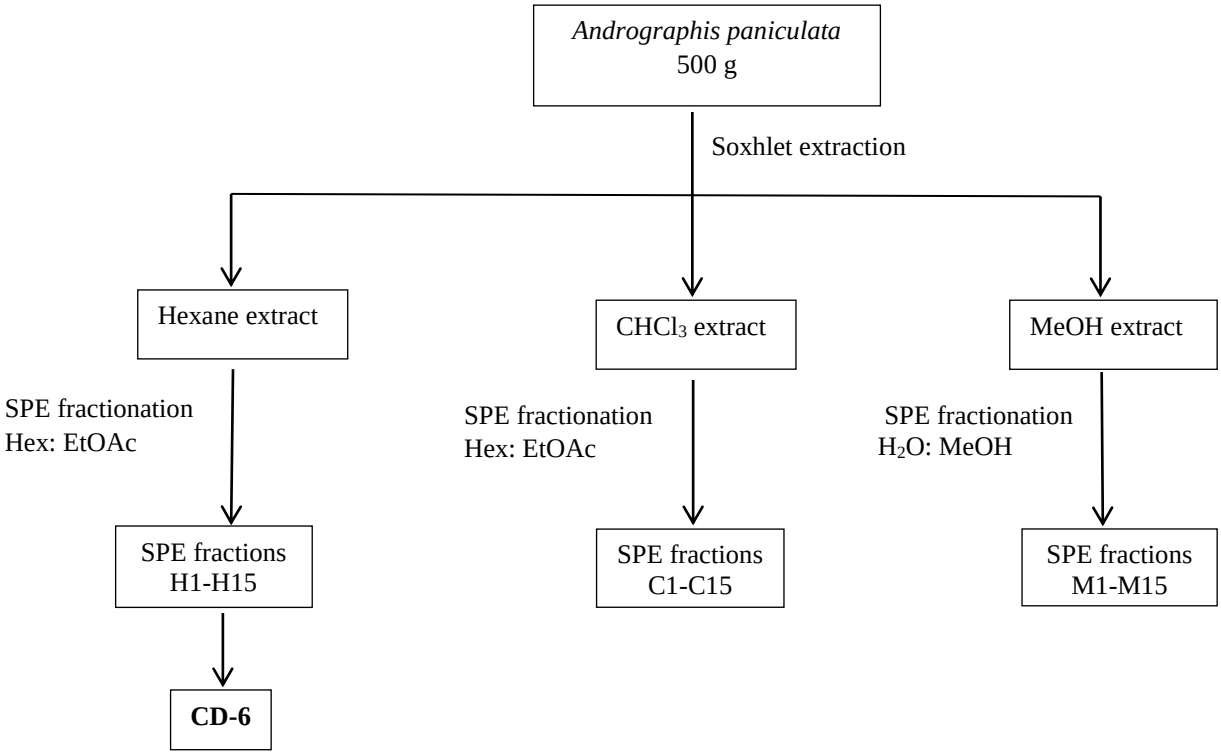

Figure 5. 4 Flow chart for the isolation of **CD-6** from *Andrographis paniculata*.

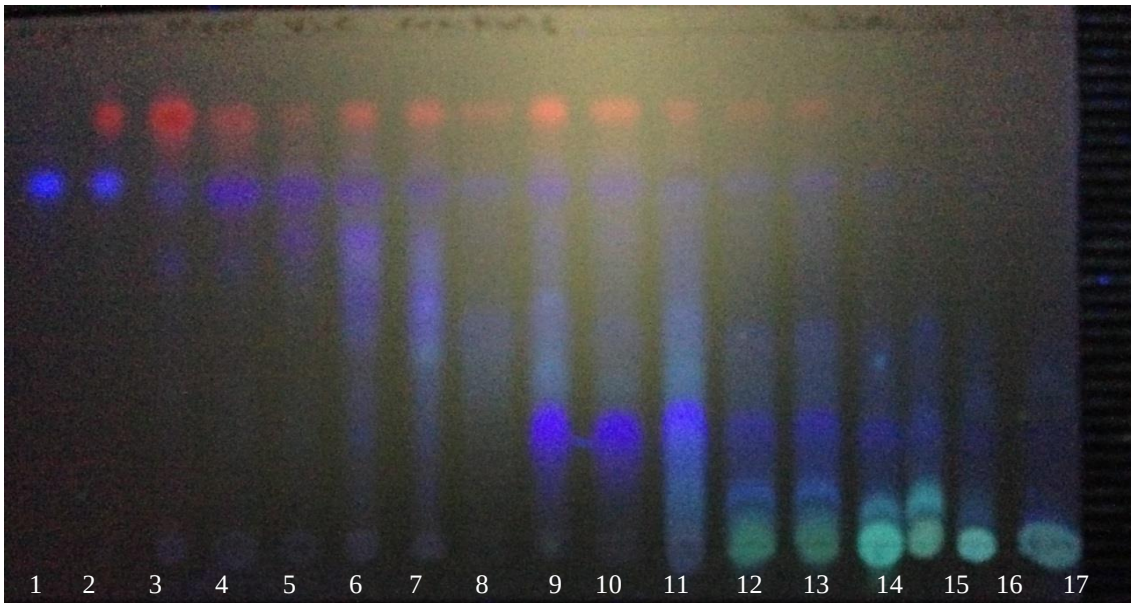

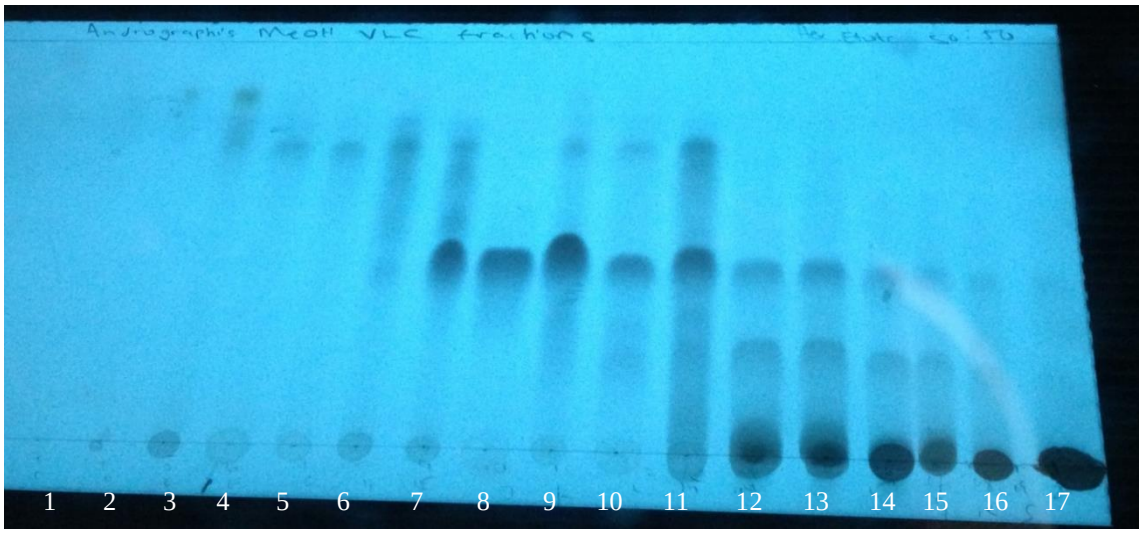

Figure 5. 5 The TLC profile of VLC fractions, solvent system Hexane: EtOAc 50:50.

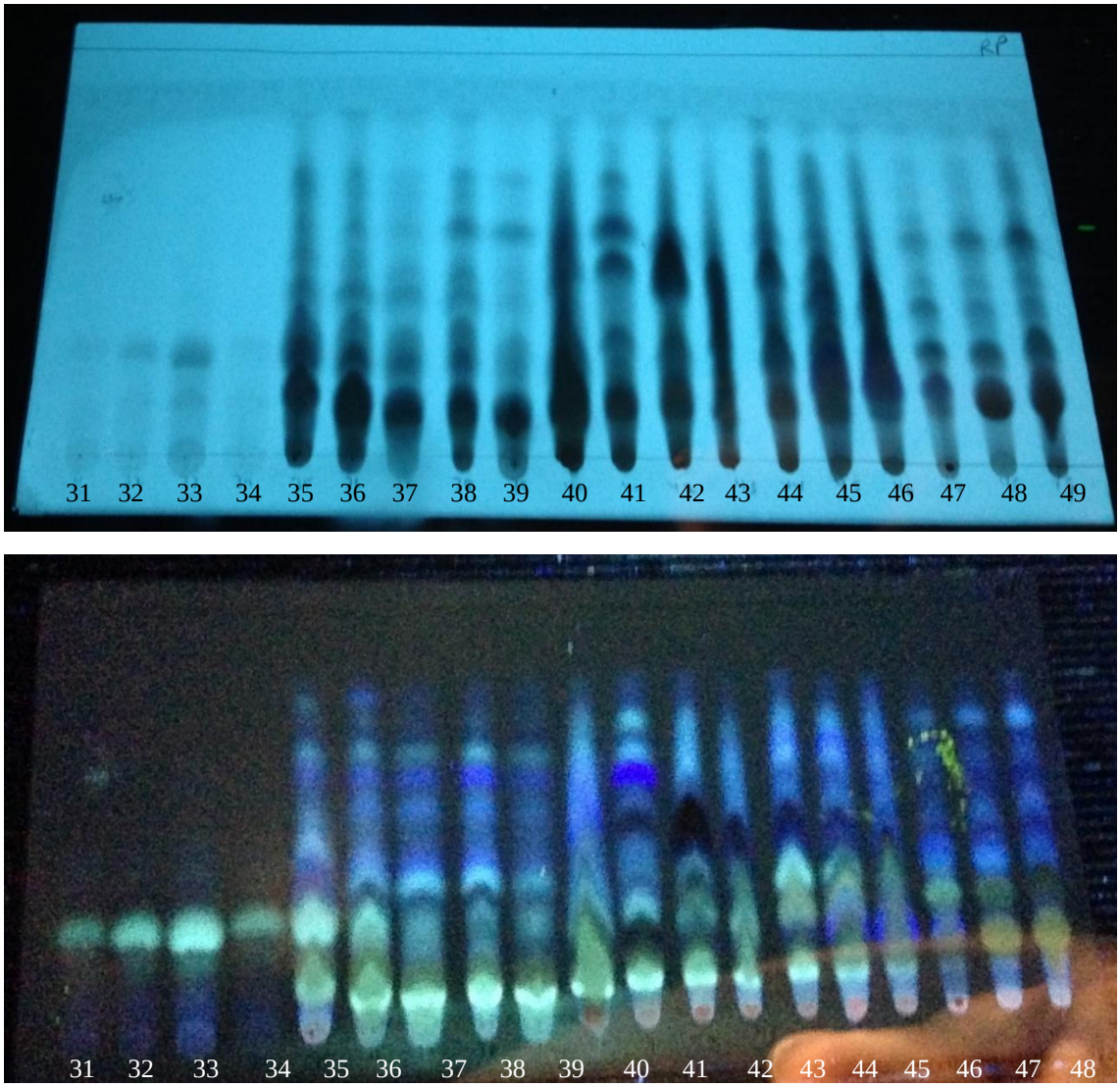

Figure 5. 6 The TLC profile of column chromatography fractions, solvent system Hexane: EtOAc 50: 50.

Selected images of TLC plates of the fractions from which the compounds were isolated are shown in Figures 5.5 and 5.6. These included the VLC fractions and column chromatography fractions.

5.2 Characterization of the isolated natural products.

5.2.1 Characterisation of **CD-1** as 14-deoxy-11,12-didehydroandrographolide

Compound **CD-1** was obtained as a white powder from VLC fraction 11 of the MeOH extract of *Andrographis paniculata*. The quantity of Compound **CD-1** isolated was 38.38 mg and the percentage yield with respect to the plant material (2 Kg) was 0.0019 %. In the ESI-MS data (Figure 5.12) the ion at m/z 355.3 is consistent with the $[M+Na]^+$ ion for 14-deoxy-11,12-didehydro andrographolide, with formula $C_{20}H_{28}NaO_4$. The ion at 687.4 is consistent with a dimeric $[2M+Na]^+$ ion, and the ions at m/z 315.2 and 297.2 could be fragmentation products from loss of one and two H_2O molecules respectively from the $[M+H]^+$ ion. The structure of the isolated compound was identified using ^1H and ^{13}C NMR Spectroscopy and the data obtained carefully compared with He *et al*., 2003 from literature which helped in the characterization of the compound.

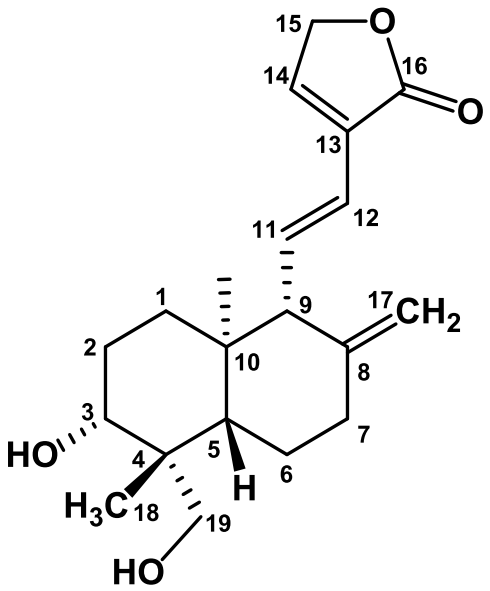

$[\alpha]^{25}_D$ = -18.14 (c=0.03)

Figure 5. 7 Structure of **CD-1** (14-deoxy-11,12-didehydroandrographolide).

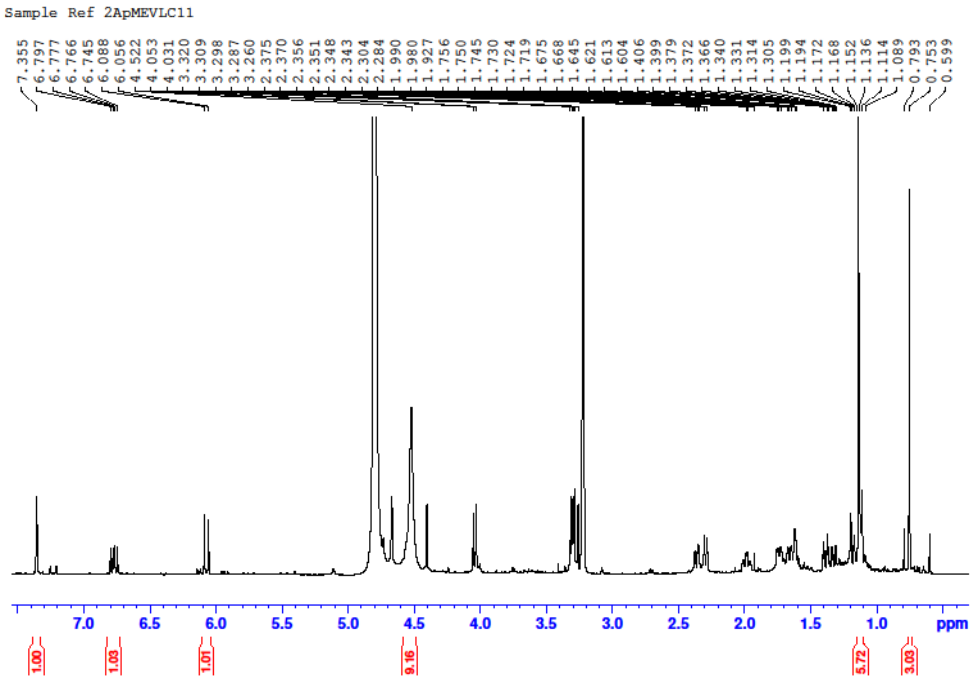

Figure 5. 8 ^{1}H NMR spectrum of **CD-1** in CD_3OD (500 MHz).

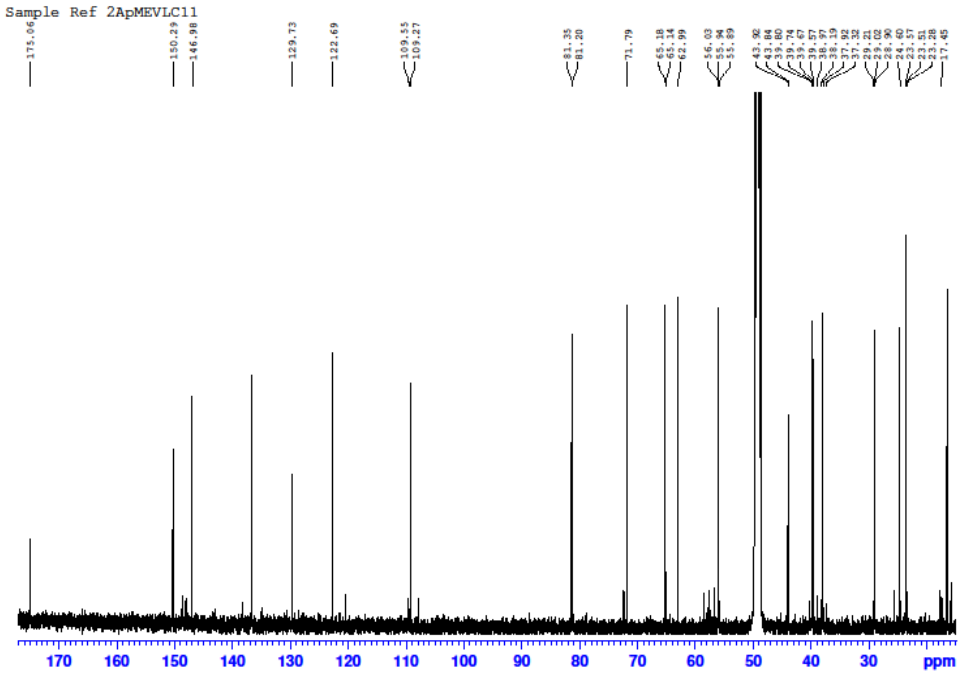

Figure 5. 9 ^{13}C NMR spectrum of **CD-1** in CD_3OD (125 MHz).

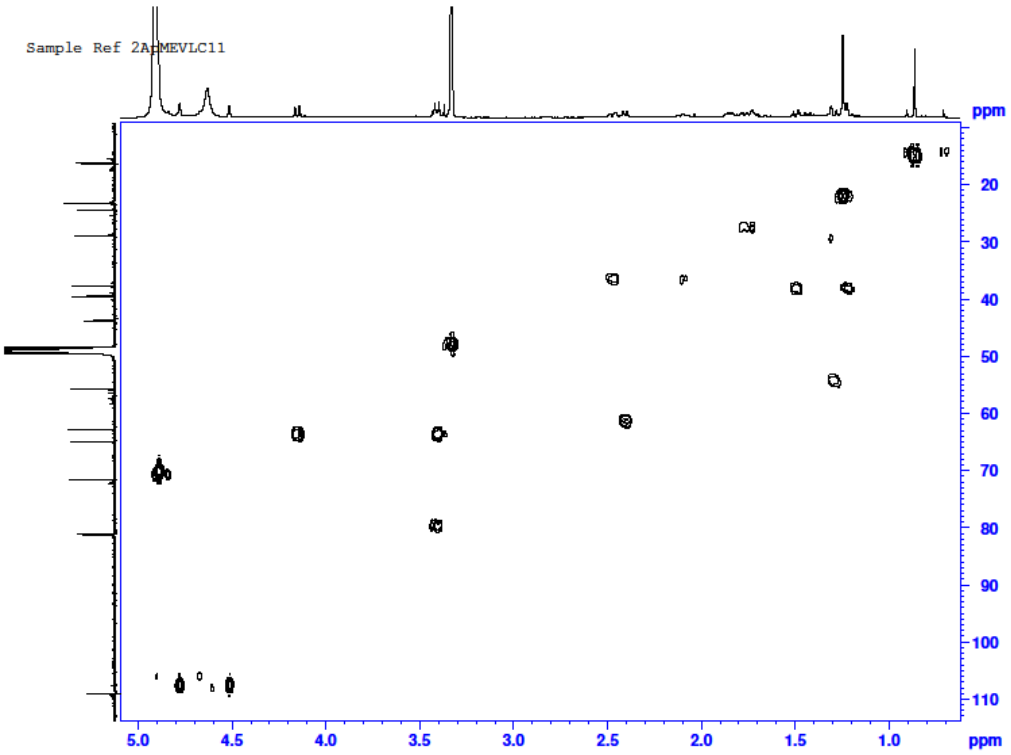

Figure 5. 10 HMQC spectrum for **CD-1** in CD_3OD (500 MHz).

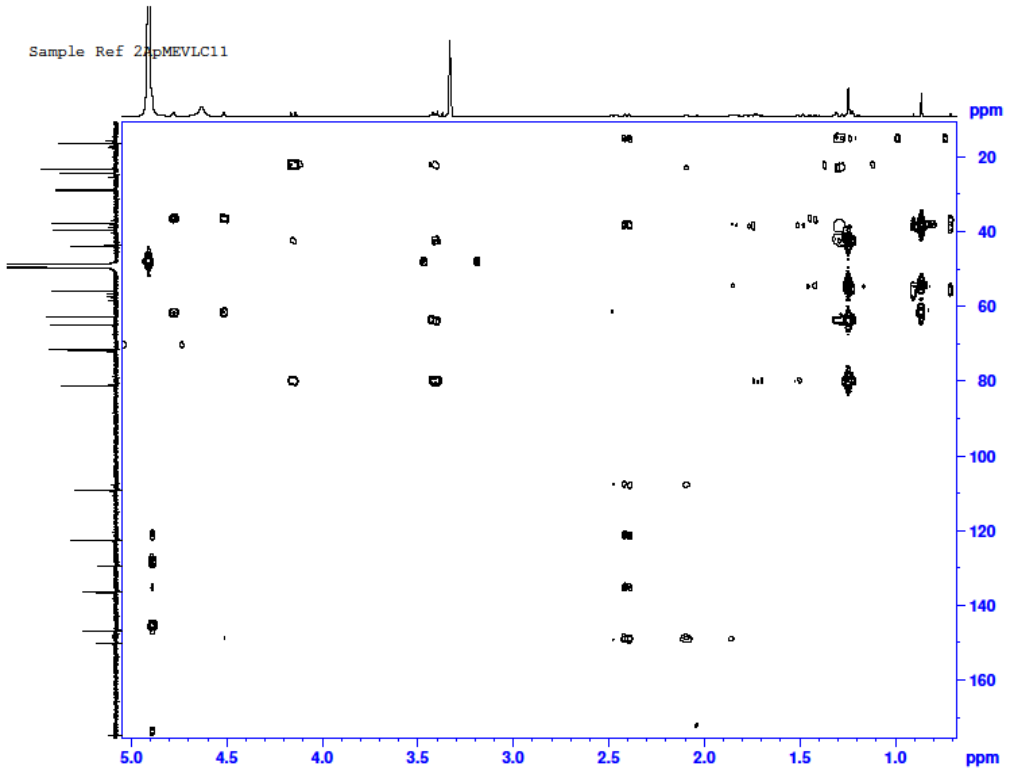

Figure 5. 11 HMBC spectrum for **CD-1** in CD_3OD (500 MHz).

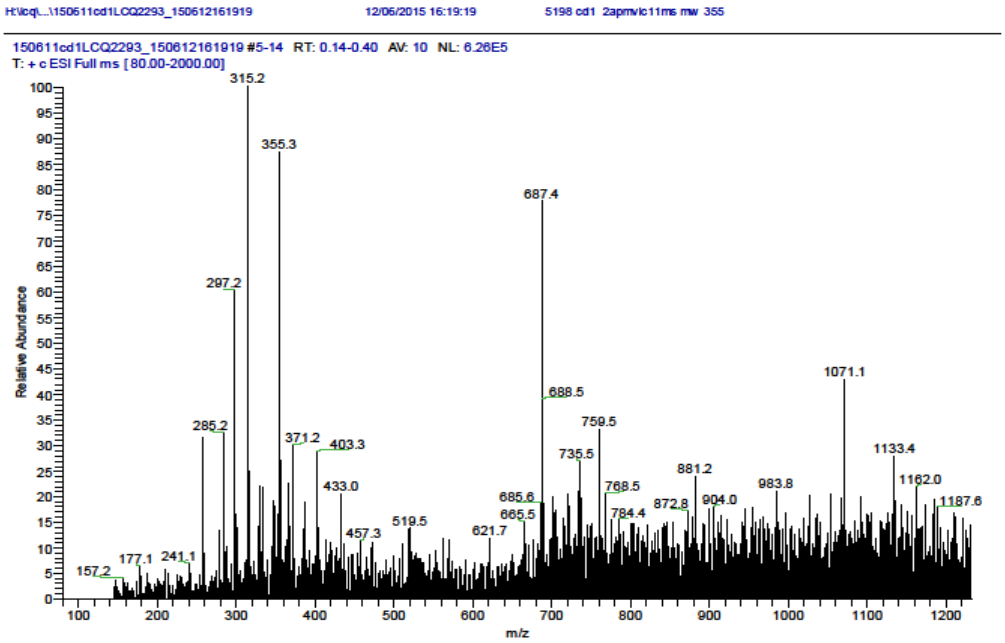

Figure 5. 12 ESI-MS spectrum of **CD-1**.

Table 5. 1 ^{1}H NMR (500 MHz) and ^{13}C NMR (125 MHz) data of **CD-1** in CD_3OD

Position	**CD-1** (CD_3OD)		He *et al*., 2003 (CD_3OD)	
	^{1}H	^{13}C	^{1}H	^{13}C
1		54.7	1.83, 1.34 (H, m)	39.5
2		29.0	1.75 (2H, m)	28.9
3		81.4	3.34 (H, m)	81.2
4		43.9		43.8
5		55.9	1.35 (H, m)	55.8
6		24.6	1.81 (2H, m)	24.4
7		37.8	2.34, 2.03 (H, m)	37.8
8		150.3		150.1
9		62.9	1.86 (H, m)	62.8
10		39.6		39.5
11	6.80 (H, dd, *J* = 8.0, 13.0 Hz)	136.6	6.85 (H, dd, *J* = 15.8, 10.1 Hz)	136.5
12	6.14 (H, d, *J* = 16 Hz)	122.7	6.15 (H, d, *J* = 15.8 Hz)	122.5
13		129.7		129.6
14	7.50 (H, t)	146.9	7.43 (H, t)	146.6
15		71.8	4.35 (2H, m)	71.6
16		175.0		174.8
17	4.75, 4.81 (H, d, *J* = 1.8 Hz)	109.3	4.75, 4.81 (H, d, *J* = 1.8 Hz)	109.1
18	1.28 (3H, s)	23.5	1.22 (3H, s)	23.3
19	3.37, 4.14 (H, d, *J* = 11.1 Hz)	65.0	3.38, 4.13 (H, d, *J* = 11.1 Hz)	65.0
20	0.86 (3H, s)	16.4	0.84 (3H, s)	16.3

The ^{1}H and ^{13}C NMR data of **CD-1** (Table 5.1) were compared with literature and a close examination revealed similarities with the NMR spectral data of He *et al*., 2003. In the ^{1}H NMR spectrum, the signals of δ 6.80 (H-11, H, dd, *J* = 8.0, 13.0 Hz) and δ 6.14 (H-12, H, d, *J* = 16 Hz) were a pair of trans-coupling olefinic signals assigned to position H-11 and H-12 respectively. The signal of δ 4.75 and δ 4.81 (H, d, *J* = 1.8 Hz) were a pair of olefinic protons at C-17. In the ^{13}C NMR spectrum, the signal at δ 175.0 belonged to an unsaturated ester carbonyl (C-16). Three carbon-carbon double bonds were present in the molecule. On the basis of the ^{1}H and ^{13}C NMR data which was in close agreement with He *et al*., 2003 presented in Table 5.1, **CD-1** was assigned as 14-deoxy-11,12-didehydroandrographolide.

5.2.2 Characterisation of **CD-2** as andrographolide

Structure elucidation and characterization of Compound **CD-2** was achieved using the information gathered from the ^{1}H and ^{13}C NMR spectral data in comparison with literature. Compound **CD-2** was obtained from VLC fraction 13 of the MeOH extract as colourless crystals. The quantity of Compound **CD-2** isolated was 55.12 mg and the percentage yield with respect to the plant material (2 Kg) was 0.0028 %. In the ESI-MS data (Figure 5.18) the ion at m/z 373.3 is consistent with the $[M+Na]^{+}$ ion for andrographolide, with formula $C_{20}H_{30}NaO_5$. The ion at 723.3 is consistent with a dimeric $[2M+Na]^{+}$ ion, and the ion at 1073.3 is consistent with a trimeric $[3M+Na]^{+}$ ion.

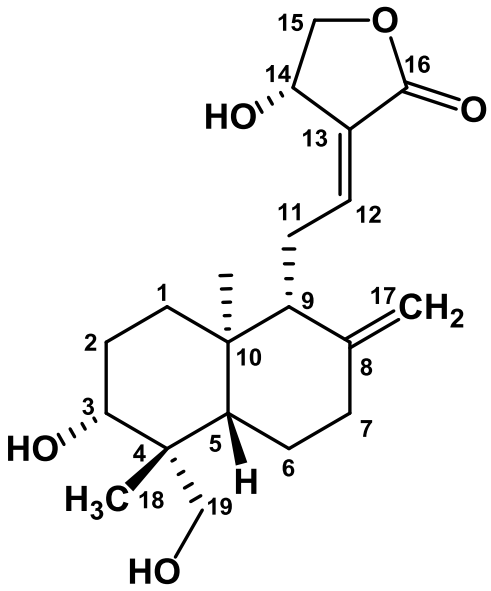

$[\alpha]^{25}_{D}$ = -72.22 (c = 0.03)

Figure 5. 13 Structure of **CD-2** (Andrographolide).

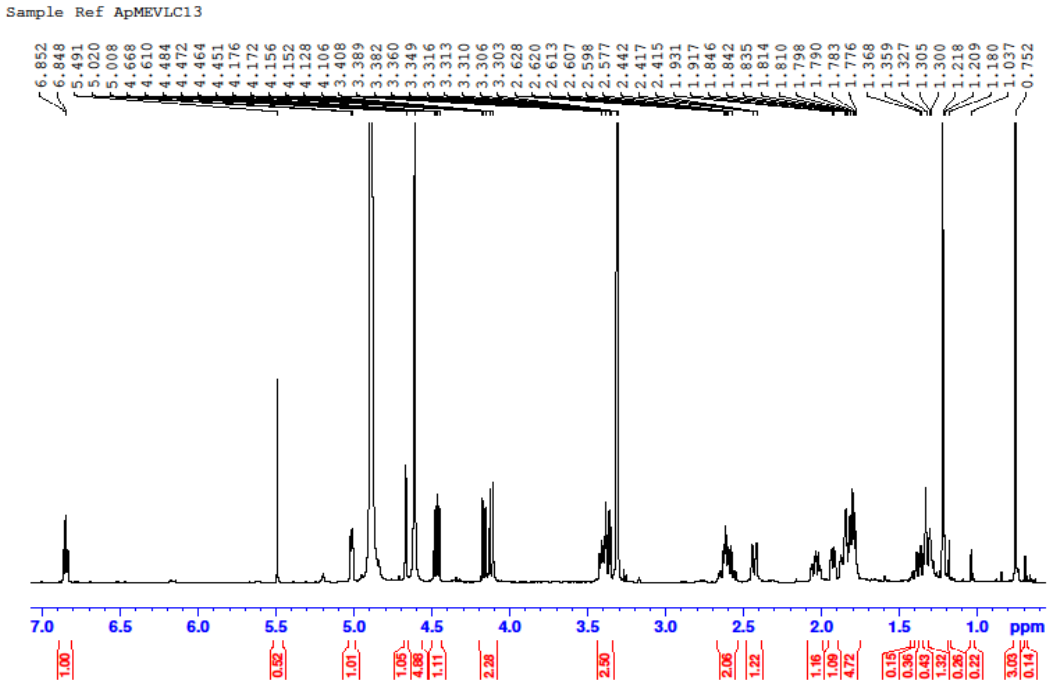

Figure 5. 14 ^{1}H spectrum of **CD-2** in $(CD_3)_2SO$ (500 MHz).

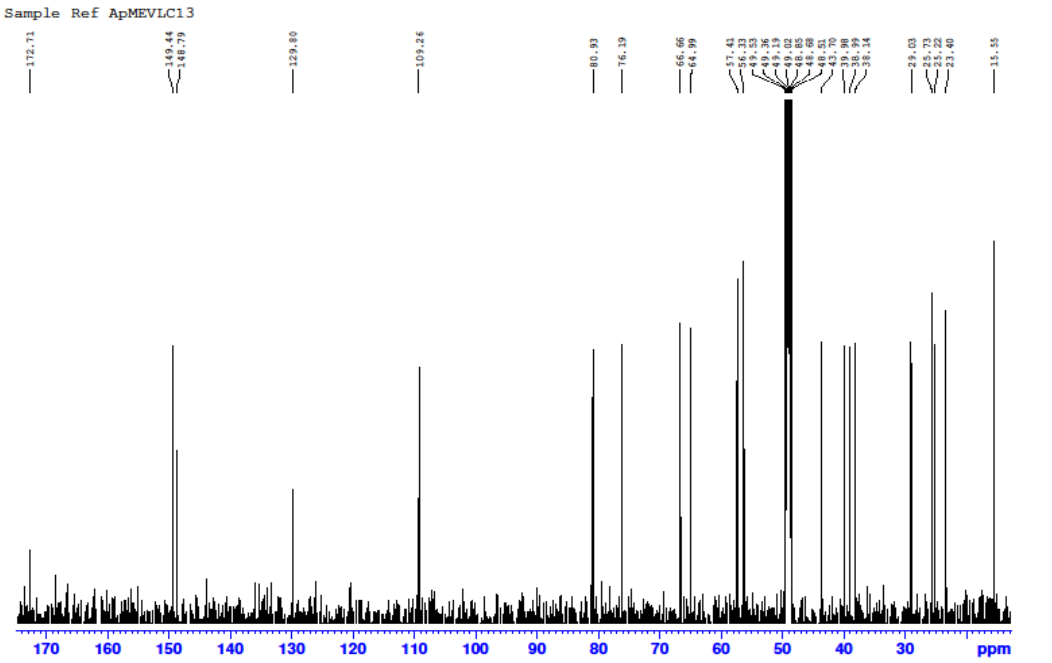

Figure 5. 15 ^{13}C spectrum for **CD-2** in $(CD_3)_2SO$ (125 MHz).

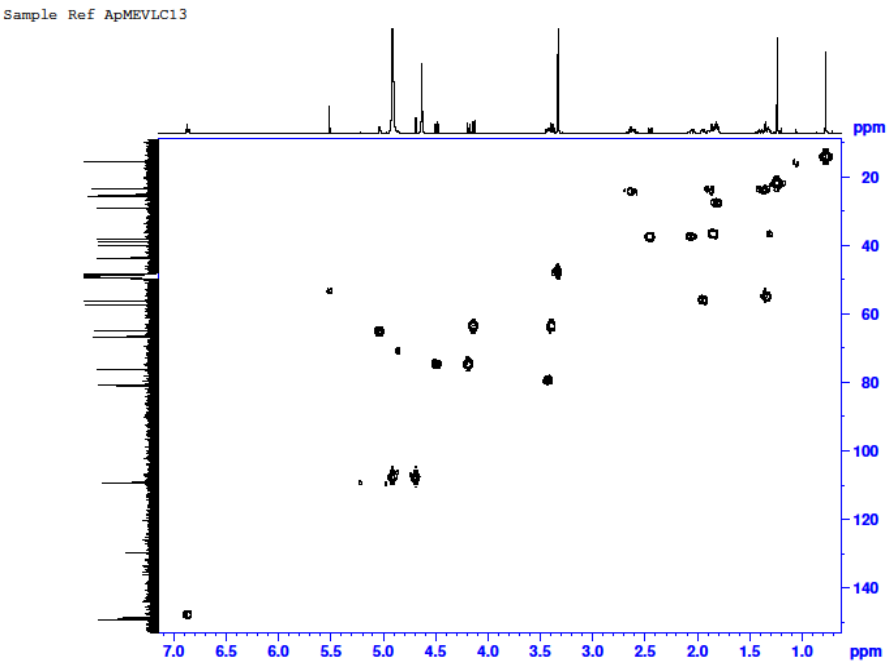

Figure 5. 16 HMQC spectrum of **CD-2** in $(CD_3)_2SO$ (500 MHz).

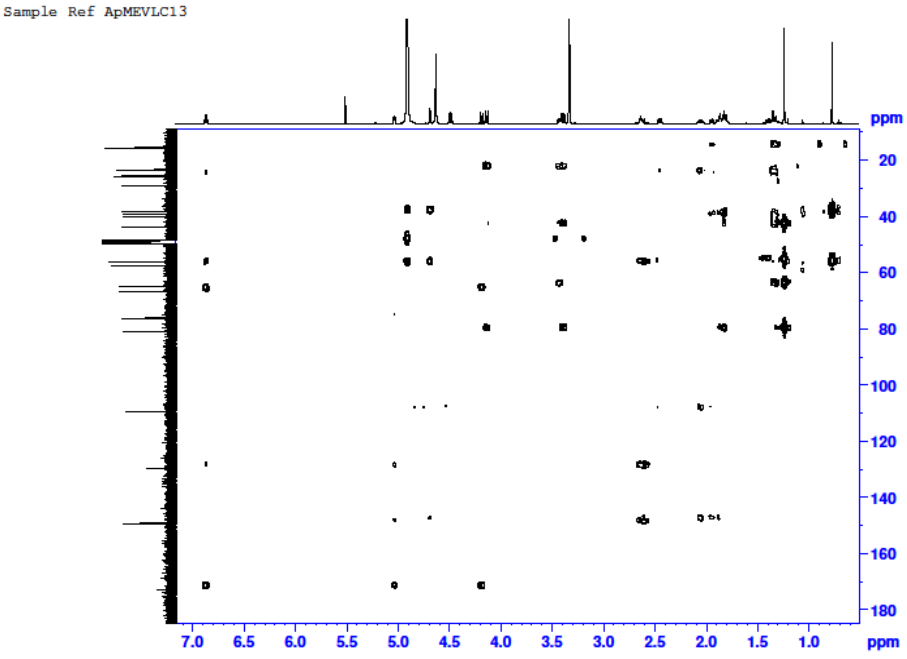

Figure 5. 17 HMBC spectrum of **CD-2** in $(CD_3)_2SO$ (500 MHz).

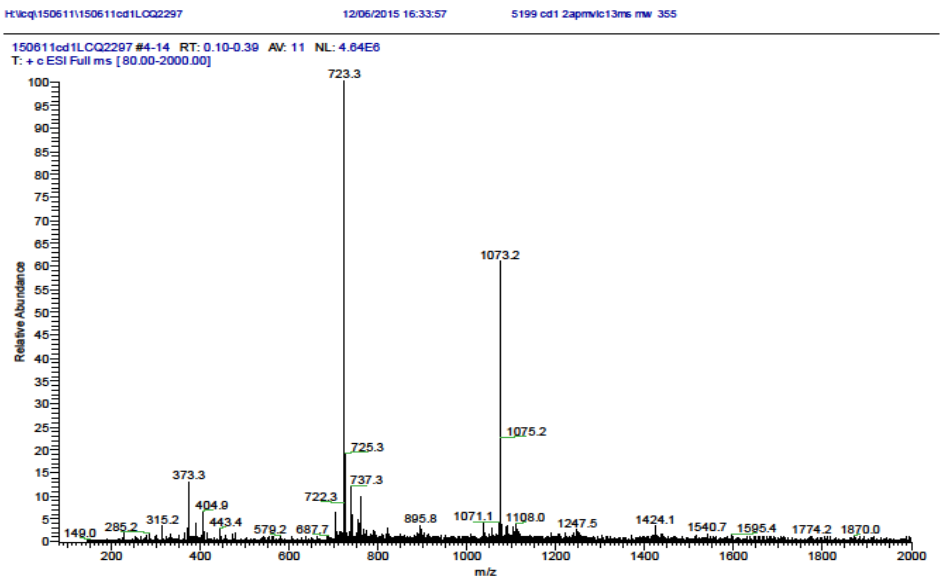

Figure 5. 18 ESI-MS spectrum of **CD-2**.

Table 5. 2 ^{1}H NMR (500 MHz) and ^{13}C NMR (125 MHz) data for **CD-2** in $(CD_3)_2SO$

Position	**CD-2** $(CD_3)_2SO$		Patra *et al*., 1981 $(CD_3)_2SO$	
	^{1}H	^{13}C	^{1}H	^{13}C
1		38.1		36.7
2		29.0		28.0
3	3.18 (1H, m)	80.9	3.18 (1H, m)	78.7
4		43.7		42.4
5		56.3		54.6
6		25.2		24.1
7		38.9		37.6
8		148.8		147.6
9		57.4		55.7
10		39.9		38.7
11		25.7		24.1
12	6.49 (1H, t, *J* = 8.0 Hz)	149.4	6.49 (1H, t, *J* = 8.0 Hz)	146.4
13		129.8		129.1
14	4.85 (1H, br d, *J* = 5.5 Hz)	66.7		64.7
15	3.98 (1H, dd, *J* = 2 and 10 Hz)	76.2		74.4
16		172.6		170.0
17	4.58, 4.77 (2H, d, *J* = 1.8 Hz)	129.8	4.88, 4.67(2H, d, *J* = 1.8 Hz)	108.4
18	1.07 (3H, s)	23.4	1.07 (3H, s)	23.1
19	3.23, 3.82 (1H d, *J* = 11.1 Hz)	65.0		62.9
20	0.86 (3H, s)	15.6	0.86 (3H, s)	14.9

Careful inspection of the ^{1}H and ^{13}C NMR spectra of **CD-2** showed a strong correlation with the spectra data of Patra *et al*., 1981 cited in literature. The ^{1}H NMR spectral data in Table 5.2 revealed a pair of olefinic protons at C-17 resonating at δ 4.58 and 4.77. Two tertiary methyl groups were present at δ 0.86 and 1.07 for C-20 and C-18 respectively. The ^{13}C NMR spectra showed the presence of a methylene carbon at position C-19, a methyl group attached to C-4 and a lactone carbonyl at C-16. A hydroxyl group was attached at positions C-3, C-14 and C-19 respectively. Based on the information gathered from the NMR spectral data, **CD-2** was assigned as andrographolide, a diterpene-lactone of the labdane group.

5.2.3 Characterisation of **CD-3** as andropanoside

The VLC fraction 17 of the MeOH extract of *Andrographis paniculata* produced pale yellow crystals named as Compound **CD-3**. The quantity of Compound **CD-3** isolated was 95.83 mg and the percentage yield with respect to the plant material (2 Kg) was 0.0048 %. The ^{1}H and ^{13}C NMR spectra obtained in comparison with NMR data of Fujita *et al*, 1983 in literature helped in the characterization of compound **CD-3** as a diterpene hexoside.

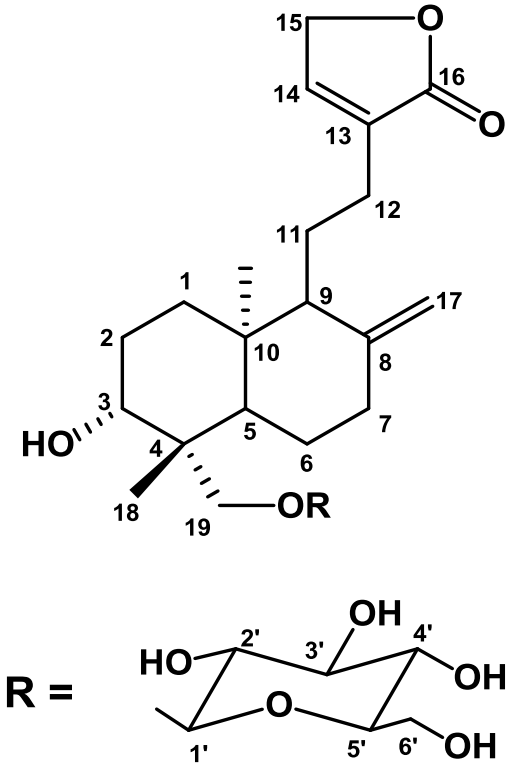

Figure 5. 19 Structure of **CD-3** as Andropanoside.

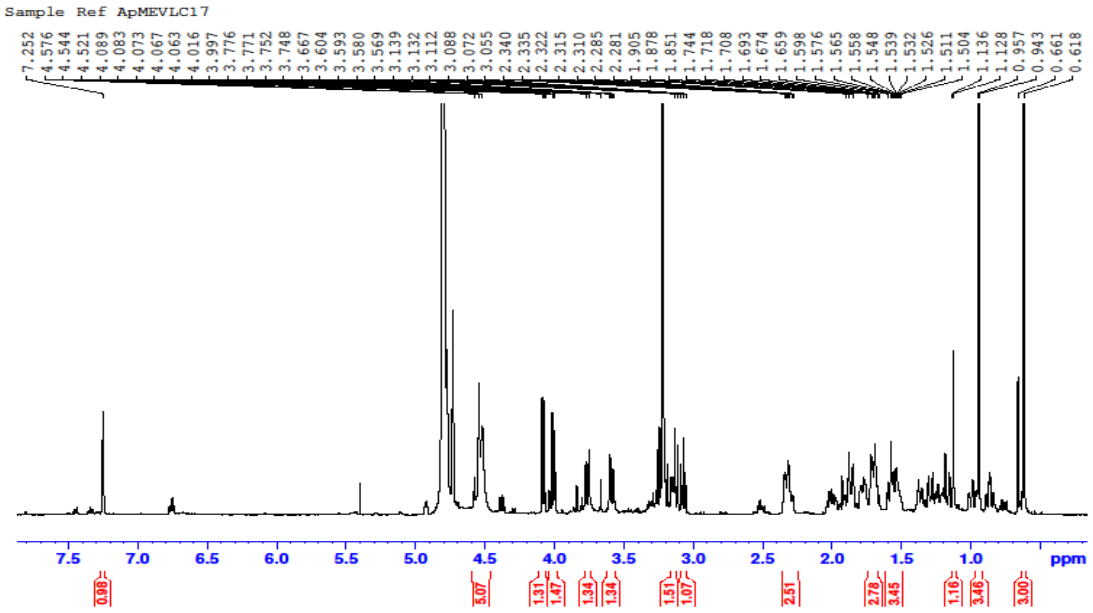

Figure 5. 20 ^{1}H spectrum for **CD-3** in CD_3OD (500 MHz).

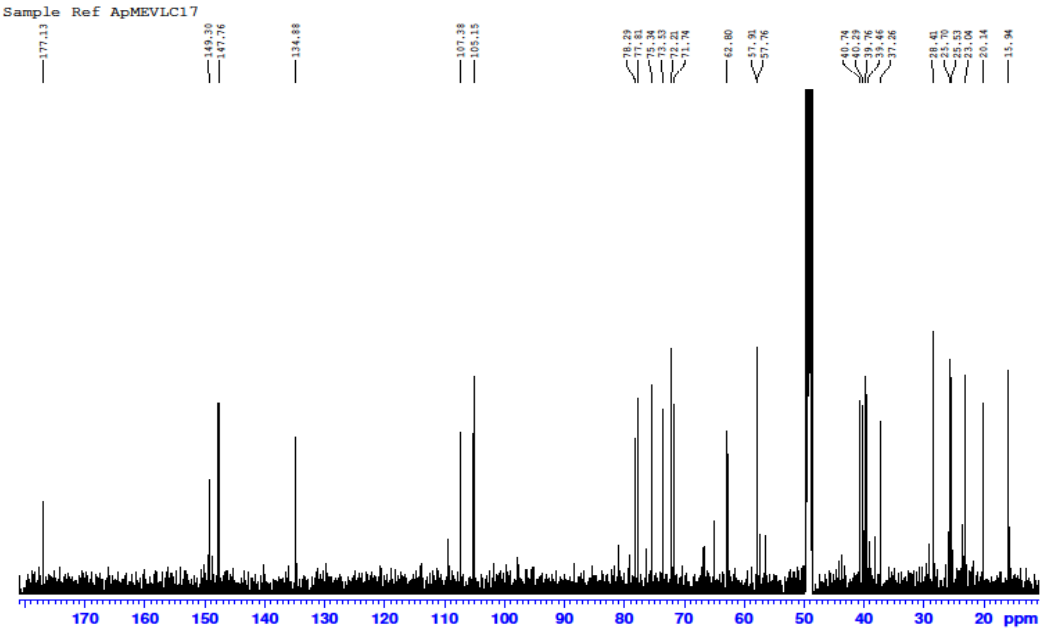

Figure 5. 21 ^{13}C NMR spectrum for **CD-3** in CD_3OD (125 MHz).

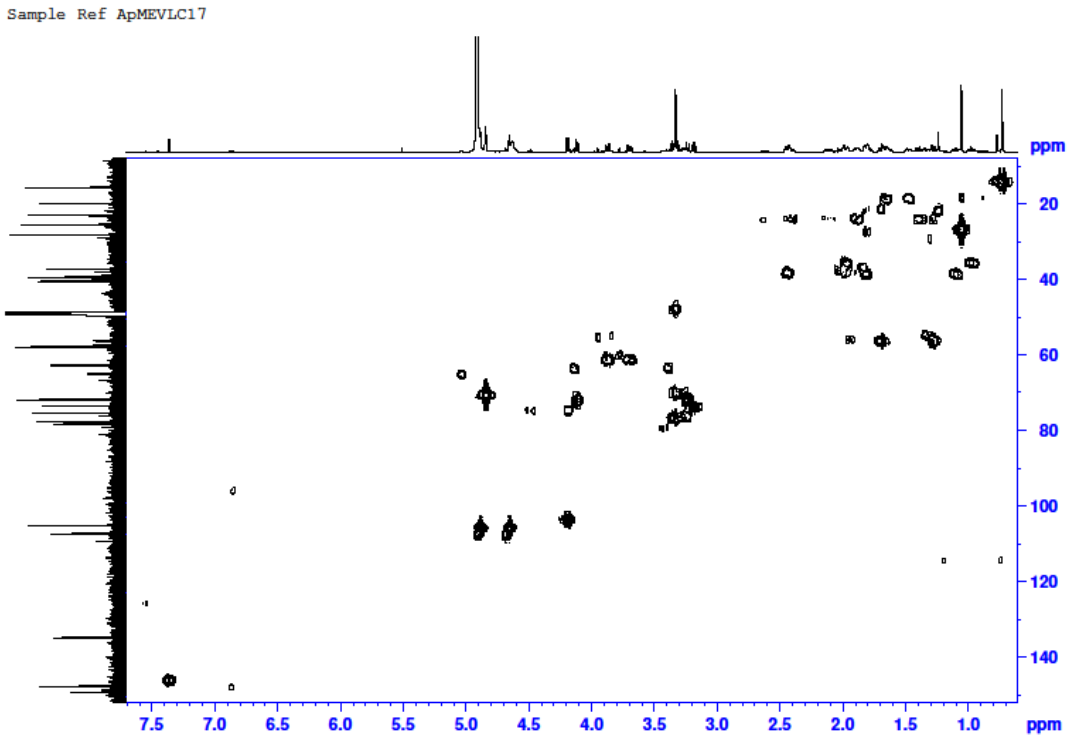

Figure 5. 22 HMQC NMR spectrum for **CD-3** in CD_3OD (500 MHz).

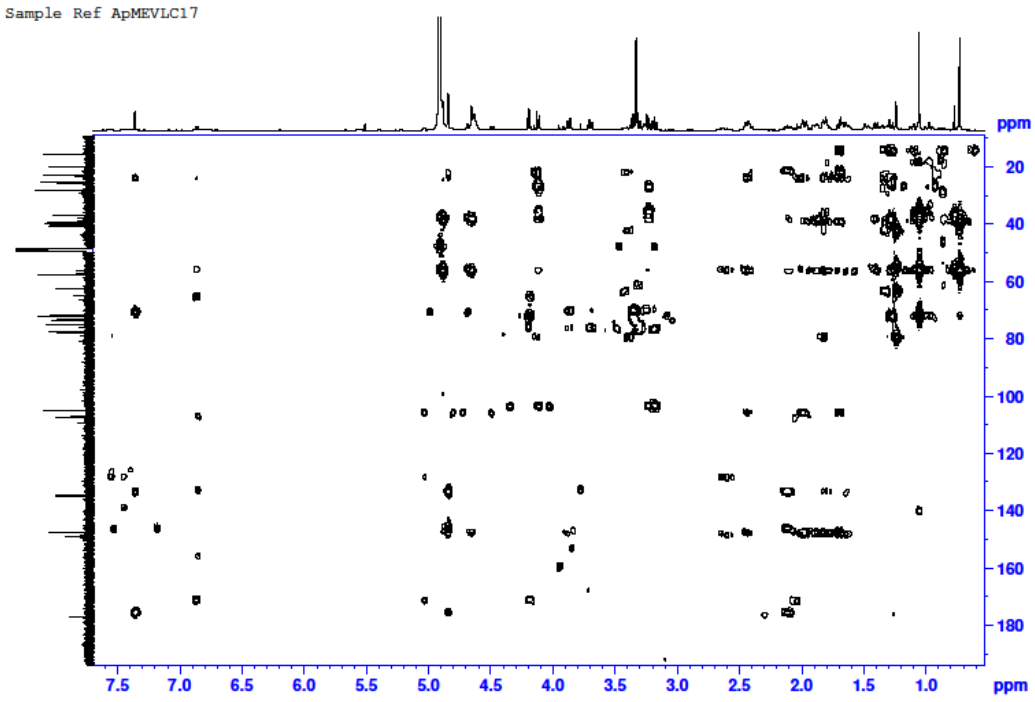

Figure 5. 23 HMBC NMR spectrum for **CD-3** in CD_3OD (500 MHz).

Table 5. 3 ^{1}H NMR (500 MHz) and ^{13}C NMR (125 MHz) data for **CD-3** in CD_3OD

Position	**CD-3** (CD_3OD)	Fujita *et al*, 1983	(CD_3OD)
	^{1}H	^{13}C	^{1}H	^{13}C
1		37.2		37.9
2		28.4		29.2
3		78.2		79.3
4		43.7		43.4
5		57.4		55.9
6		25.2		25.1
7		39.4		38.9
8		149.2		148.3
9		57.8		56.8
10		39.7		39.8
11		22.9		22.5
12		25.6		25.3
13		134.8		134.4
14	7.25 (1H, m)	147.8	7.10 (1H, m)	145.4
15		75.3		70.6
16		177.1		174.6
17	4.57, 4.77 (2H, d, J = 1.8 Hz)	107.3	4.57, 4.77 (2H, d, J = 1.8 Hz)	107.1
18	1.12 (3H, s, CH_3)	23.0	0.92 (3H, s, CH_3)	24.4
19		72.1		72.0
20	1.61 (3H, s, CH_3)	15.9	1.47 (3H, s, CH_3)	15.0
1’		105.1		105.4
2’		75.3		74.8
3’		77.8		78.7
4’		71.7		71.8
5’		78.2		78.4
6’		62.8		62.9

Inspection of the ^{1}H and ^{13}C NMR spectral data of compound **CD-3** showed a close correlation when compared to the NMR data of Fujita *et al*, 1983 in literature. The ^{1}H NMR spectral data (Table 5.3) indicated the presence of two methyl groups with three-proton singlet at δ 1.12 and δ 1.61 for C-18 and C-20 respectively, the exomethylene group at C-17 resonating at δ 4.58 and 4.77, a methine at δ 7.25 (1H, m) for C-14 and a methylene carbon at C-19.

The ^{13}C NMR data revealed a carbonyl at C-16, five non-protonated carbons and glucose were present. Compound **CD-3** was therefore assigned as andropanoside, a diterpenoid hexoside based on the ^{1}H and ^{13}C NMR spectral data in Table 5.3.

5.2.4 Characterisation of **CD-4** as neoandrographolide

Compound **CD-4** was obtained as colourless crystals from a column chromatography fraction of the BuOH extract of *Andrographis paniculata*. The quantity of Compound **CD-4** isolated was 88.55 mg and the percentage yield with respect to the plant material (2 Kg) was 0.0044 %. Using ^{1}H and ^{13}C NMR Spectroscopy, the structure of the isolated compound was identified by carefully comparing the data obtained with literature and it showed similarities with Du *et al* 2003 suggesting a diterpene hexoside.

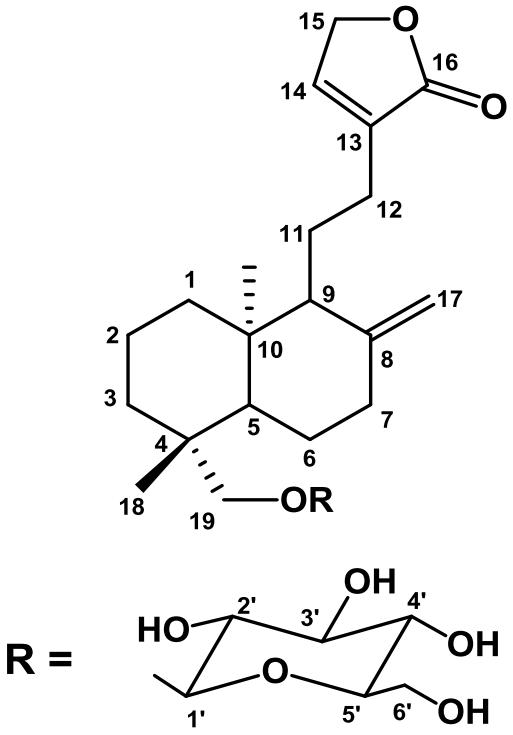

Figure 5. 24 Structure of **CD-4** as neoandrographolide.

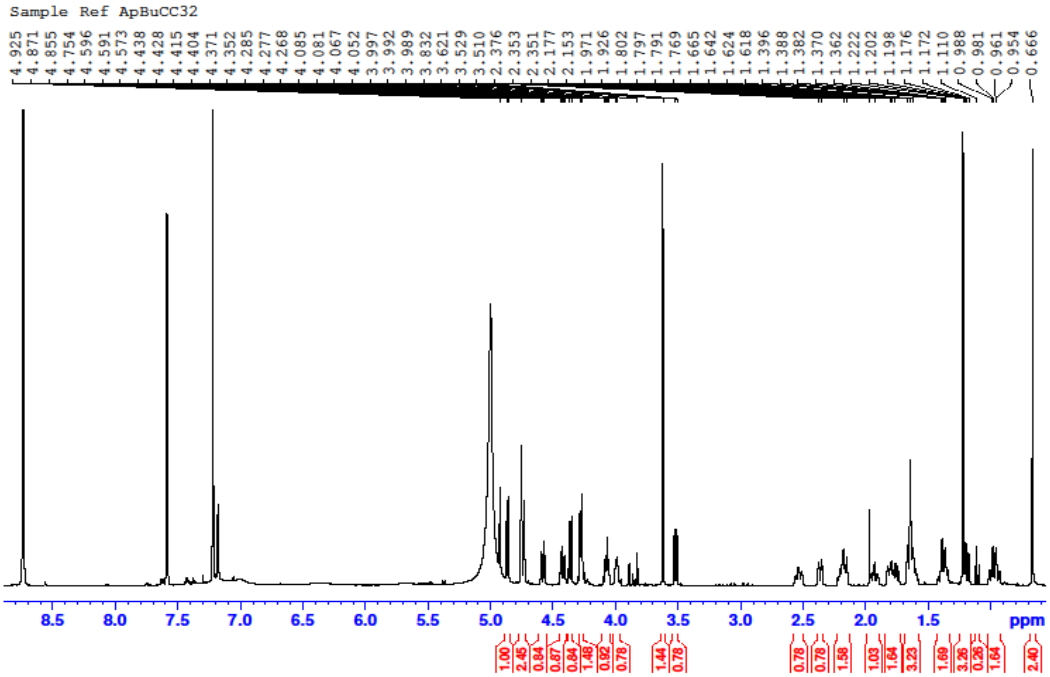

Figure 5. 25 ^{1}H NMR spectrum of **CD-4** in C_5D_5N (500 MHz).

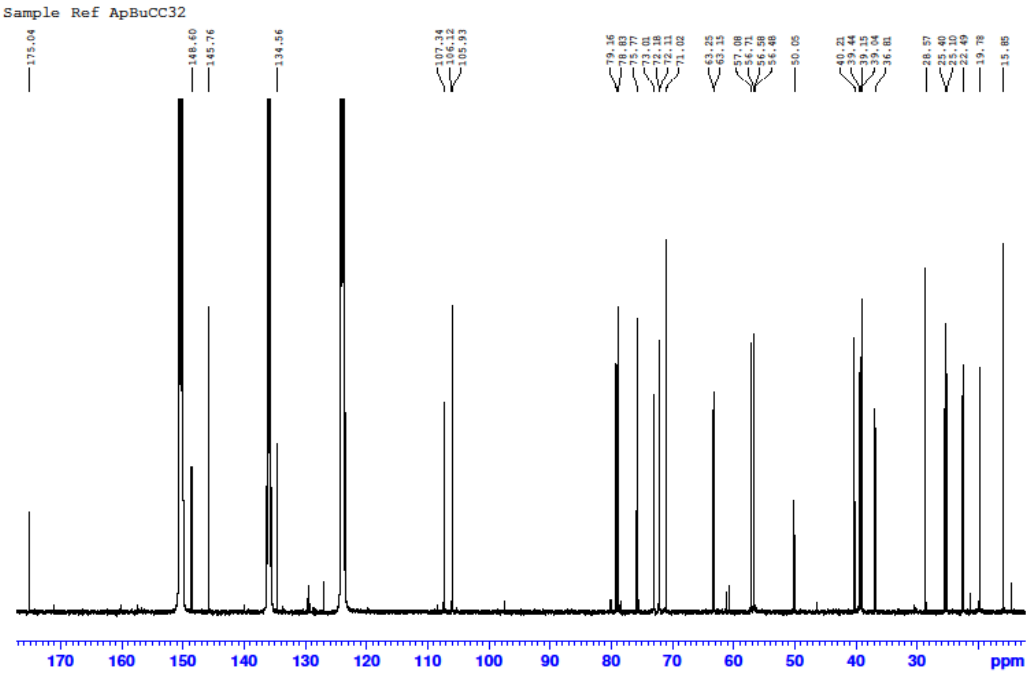

Figure 5. 26 ^{13}C NMR spectrum of **CD-4** in C_5D_5N (125 MHz).

Table 5. 4 ^{1}H NMR (500 MHz) and ^{13}C NMR (125 MHz) data for **CD-4** in C_5D_5N

Position	**CD-4** (C_5D_5N)		Du *et al*., 2003	C_5D_5N
	^{1}H	^{13}C	^{1}H	^{13}C
1		39.1		39.2
2		19.7		19.5
3		36.8		36.6
4		40.2		39.9
5		56.5		56.3
6	4.39 (1H, dd, *J* = 12.0, 5.5 Hz)	25.1	4.39 (1H, dd, *J* = 12.0, 5.5 Hz)	25.1
7		39.0		38.9
8		148.5		148.3
9		57.0		56.8
10		50.0		38.7
11		22.4		22.2
12	2.15, 2.35 (1H, m)	25.3	2.20, 2.50 (1H, m)	24.8
13		134.5		134.3
14	7.15 (H, t, *J* = 1.5)	145.7	7.15 (H, t, *J* = 1.5)	145.3
15		71.0		70.6
16		175.0		174.0
17	4.75,4.92 (1H, s)	107.3	4.75, 4.92 (1H, s)	107.0
18	1.17 (3H, s, CH_3)	28.5	1.18 (3H, s, CH_3)	28.2
19	3.52, 4.35 (1H, d, *J* = 9.5)	73.0	3.52, 4.32 (1H, d, *J* = 9.5)	72.7
20	0.66 (3H, s, CH_3)	15.8	0.63 (3H, s, CH_3)	15.5
1’	4.85 (1H, d, *J* = 7.5 Hz)	105.9	4.82 (1H, d, *J* = 7.5 Hz)	105.5
2’	4.05 (1H, m)	75.7	4.03 (1H, m)	75.4
3’	4.09 (1H, m)	79.1	4.19 (1H, m)	78.8
4’	4.26 (1H, m)	72.2	4.24 (1H, m)	72.0
5’	3.98 (1H, m)	78.8	3.95 (1H, m)	78.4
6’	4.37, 4.54 (1H, dd, *J* = 12.0, 5.5 Hz)	63.2	4.39, 4.54 (1H, dd, *J* = 12.0, 5.5 Hz)	63.0

Detailed observation of the ^{1}H and ^{13}C NMR data of **CD-4** in Table 5.4., shows that the aglycone comprises of two tertiary methyl groups at position C-18 and C-20 at δ 1.17 (3H, s, CH_3) and 0.66 (3H, s, CH_3) respectively, a methylene at 3.52, 4.35 (1H, d, *J* = 9.5) and a methine at 7.15 (H, t, *J* = 1.5). The glucose moiety comprises of δ 4.85 (1H, d, *J* = 7.5 Hz) at position 1’, δ 4.05 (1H, m), δ 4.09 (1H, m), δ 4.26 (1H, m), δ 3.98 (1H, m) at positions 2’, 3’, 4’, 5’ and δ 4.37, 4.54 (1H, dd, *J* = 12.0, 5.5 Hz) at position 6’. This information was in agreement with Du *et al* 2003; **CD-4** was therefore assigned as neoandrographolide based on the NMR data.

5.2.5 Characterisation of **CD-5** as andrographolide

Compound CD-**5** was obtained as colourless crystals from column chromatograph fraction of the BuOH extract of *Andrographis paniculata*. The quantity of Compound **CD-5** isolated was 80.13 mg and the percentage yield with respect to the plant material (2 Kg) was 0.0040 %. The structure of the isolated compound was identified and characterized using ^{1}H and ^{13}C NMR Spectroscopy and was compared with the NMR data of Cui *et al*., 2005.

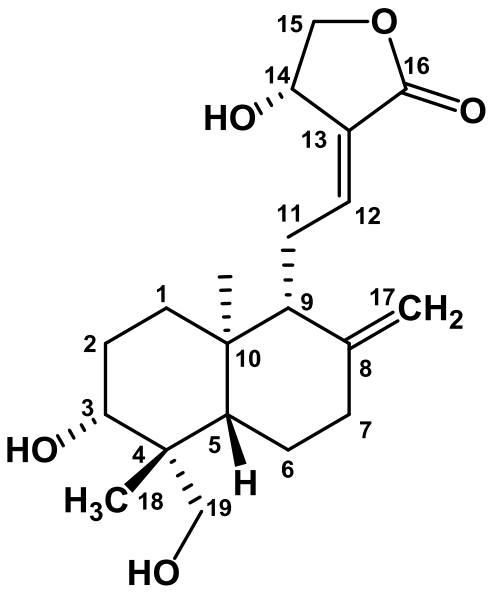

Figure 5. 27 Structure of **CD-5** as Andrographolide.

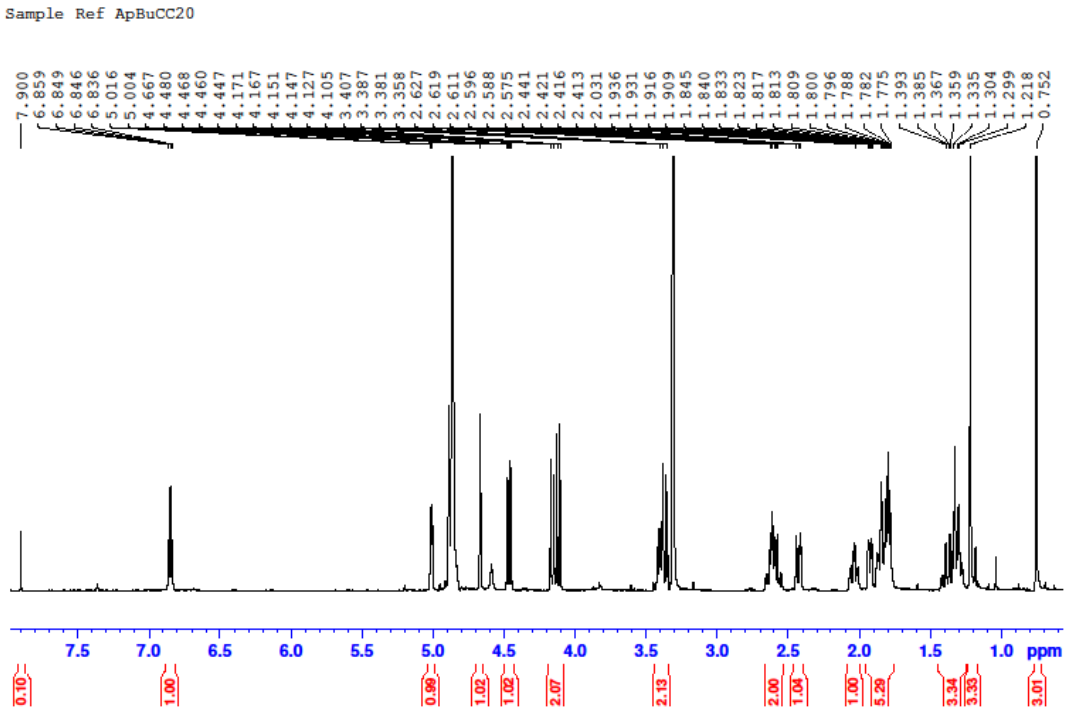

Figure 5. 28 ^{1}H NMR spectrum for **CD-5** in CD_3OD (500 MHz).

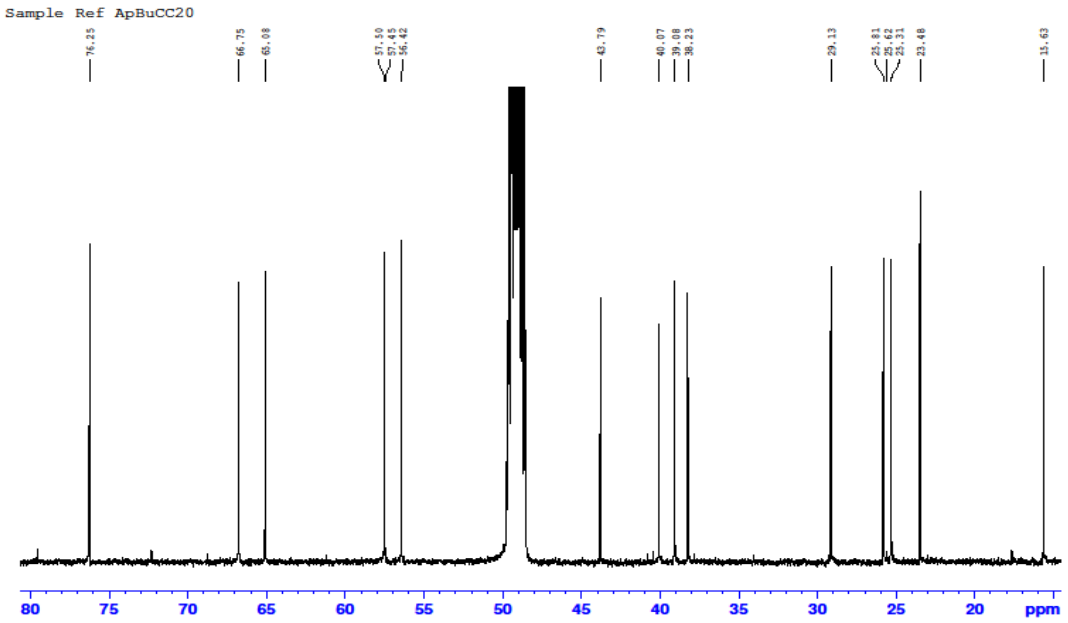

Figure 5. 29 ^{13}C NMR spectrum for **CD-5** in CD_3OD (125 MHz).

Table 5. 5 ^{1}H NMR (500 MHz) and ^{13}C NMR (125 MHz) data for CD-5 in CD_3OD

Position	**CD-5** (CD_3OD)		Cui *et al*., 2005 (CD_3OD)	
	^{1}H	^{13}C	^{1}H	^{13}C
1		38.2	1.83, 1.28 (H, m)	38.1
2	1.79 (H, m)	29.1	1.79 (H, m)	29.0
3		81.0	3.40 (H, m)	80.9
4		43.8		43.6
5		56.4	1.32 (H, m)	56.3
6		25.3	1.87, 1.36 (H, m)	25.2
7	2.41, 2.03 (H, m)	38.2	2.41, 2.03 (H, m)	38.9
8		148.9		148.7
9		57.5	1.91 (H, m)	57.4
10		39.1		39.9
11	2.61 (2H, m)	25.8	2.60 (2H, m)	25.7
12	6.84 (H, t, *J* = 6.7, 1.7 Hz)	149.5	6.84 (H, t, *J* = 6.7, 1.7 Hz)	149.3
13		129.9		129.8
14	5.00 (H, d, *J* = 6.0 Hz)	66.8	5.00 (H, dd, *J* = 4.2, 1.7 Hz)	66.6
15	4.45 (H, dd, *J* = 10.2, 6.1 Hz) 4.14 (H, dd, *J* = 10.2, 2.0 Hz)	76.3	4.45 (H, dd, *J* = 10.2, 6.1 Hz)	76.1
16		172.8		172.6
17	4.88, 4.67 (1H, s)	109.3	4.87, 4.65 (H, d, *J* = 11.7 Hz)	109.2
18	1.2 (3H, s)	23.5	1.20 (3H, s)	23.3
19	4.10 (1H, d, *J* = 11.0 Hz)	65.1	4.10 (H, d, *J* = 11.0 Hz)	64.9
20	0.75 (3H, s)	15.5	0.74 (3H, s)	15.5

A thorough literature search revealed that the ^{1}H and ^{13}C NMR data presented by Cui *et al*., 2005, matches very well with the ^{1}H and ^{13}C NMR data of **CD-5** presented in Table 5.5. The ^{1}H NMR spectral data revealed a pair of olefinic protons at C-17 resonating at δ 4.88 and 4.67. Two tertiary methyl groups were present at δ 0.75 and 1.20 for C-20 and C-18 respectively. The ^{13}C NMR spectra showed the presence of a methylene carbon at position C-19, a methyl group attached to C-4 and a lactone carbonyl at C-16. A hydroxyl group was attached at positions C-3, C-14 and C-19 respectively. On the basis of the NMR spectral data, **CD-5** was assigned as andrographolide.

5.2.6 Characterisation of **CD-6** as stigmasterol

Compound **CD-6** was obtained as a dark green solid from SPE fraction 4 of the methanol extract of *Andrographis paniculata*. The quantity of Compound **CD-6** isolated was 96.93 mg and the percentage yield with respect to the plant material (2 Kg) was 0.0048 %. The ^{1}H and ^{13}C NMR spectral data helped in the structure elucidation and characterization of the isolated compound when compared with Siripong *et al*., 1992 NMR data.

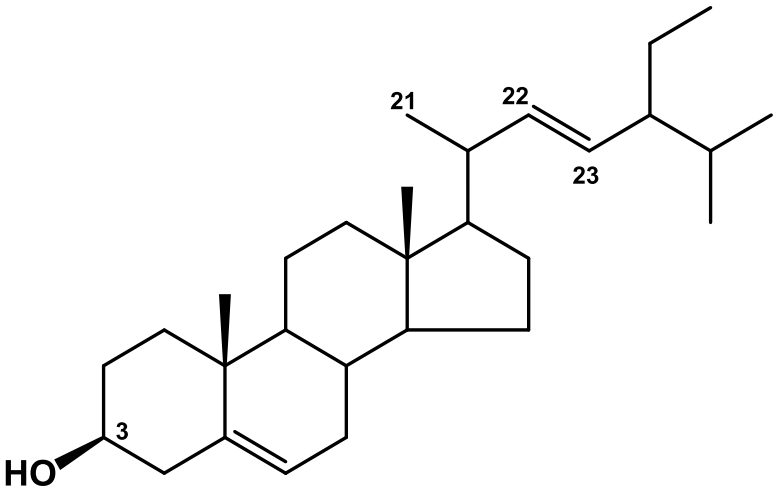

Figure 5. 30 Structure of **CD-6** as Stigmasterol

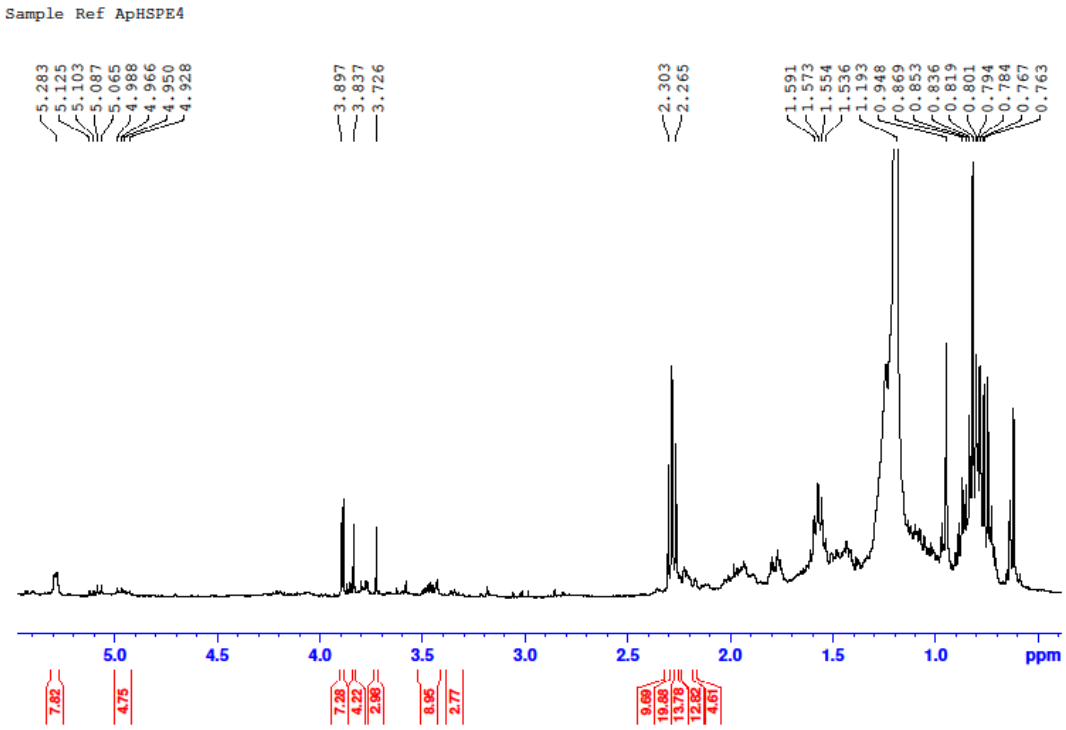

Figure 5. 31 ^{1}H spectrum for **CD-6** in $CDCl_3$ (500 MHz).

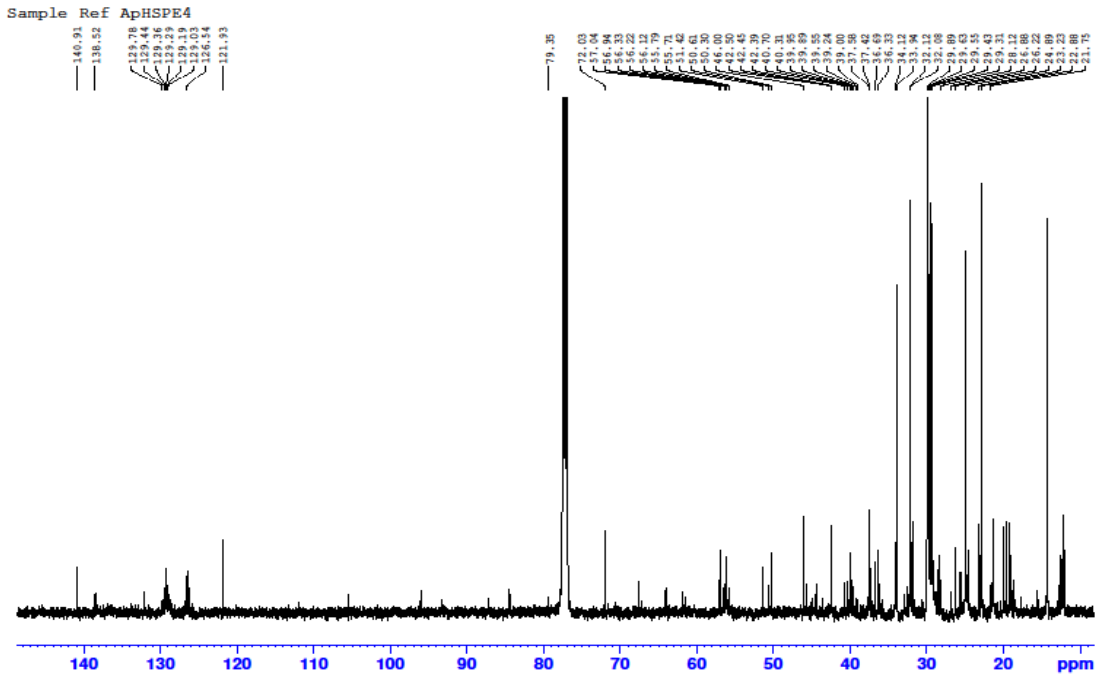

Figure 5. 32 ^{13}C spectrum for **CD-6** in $CDCl_3$ (125 MHz).

Table 5. 6 ^{1}H NMR (500 MHz) and ^{13}C (125 MHz) NMR data for CD-6 in $CDCl_3$

Position	**CD-6** ($CDCl_3$)		Siripong, *et al* 1992	($CDCl_3$)
	^{1}H	^{13}C	^{1}H	^{13}C
1		37.4		37.1
2		29.3		28.4
3	3.52 (1H, m)	79.3	3.52 (1H, m)	79.0
4		38.9		38.9
5		140.9		145.2
6	5.36 (1H, d, *J* = 4.8 Hz)	121.9	5.34 (1H, d, *J* = 4.8 Hz)	121.7
7		34.1		34.2
8		36.3		36.3
9		50.3		50.4
10		37.4		37.1
11		26.2		26.1
12		40.3		40.1
13		39.2		39.2
14		56.2		55.3
15		28.1		28.1
16		29.6		29.7
17		55.7		55.1
18	1.29 (3H, d)	15.5	1.29 (3H, d)	15.6
19	0.74 (3H, d)	19.2	0.74 (3H, d)	19.3
20		40.7		40.8
21		17.7		17.7
22	5.04 (1H, dd, *J* = 15.2, 8.4 Hz)	140.9	5.02 (1H, dd, *J* = 15.2, 8.4 Hz)	139.8
23	5.17 (1H, dd, *J* = 15.2, 8.4 Hz)	129.8	5.15 (1H, dd, *J* = 15.2, 8.4 Hz)	129.8
24		21.7		21.6
25		26.8		27.4
26	0.84 (3H, d)	21.1	0.80 (3H, d)	21.1
27	0.97 (3H, d)	19.4	0.90 (3H, d)	19.4
28		25.4		25.4
29	1.04 (3H, t)	12.1	1.04 (3H, t)	12.1

The ^{13}C spectral data shows twenty nine carbon atoms including six methyl groups indicated by high intensity peaks between δ 0.60 -1.20, nine methylene, eleven methine and three quaternary carbons. The structure comprises of a steroid skeleton with a side chain containing ten carbons attached at C-17. The signal for the C-5 and C-6 double bond appears at δ 140.9 and 121.9 respectively. The hydroxyl group was attached to C-3 at δ 71.9 and the proton at H-3 appeared at δ 3.52. The angular methyl groups at C-18 and C-19 resonates at δ 1.29 and 0.74 while the C-22 and C-23 double bond resonates at δ 5.17 and 5.04 respectively. As a result of the similarities between the NMR data of **CD-6** and Siripong, *et al* 1992, **CD-6** was assigned as Stigmasterol, a phytosterol.

5.3 Antibiotic susceptibility testing

Screening of ethnobotanical plants is a pre-requisite to evaluate their therapeutic potential which can lead to the isolation of new bioactive compounds. Two types of antibiotic susceptibility testing were used, the microtitre plate broth dilution assay and the high-throughput spot-culture growth inhibition assay (HT-SPOTi).

The hexane, chloroform, methanol and water extracts of *Andrographis paniculata* were tested against multidrug-resistant *S. aureus* strains (SA-1199B, XU212, RN4220 and EMRSA-15). All the extracts had an MIC > 512 mg/L with the exception of the chloroform extract which had an MIC of 256 mg/L. When tested against *E.coli*, the MIC was > 512 mg/L for all the extracts.

Fifteen Solid Phase Extraction (SPE) fractions each of the hexane, chloroform and methanol extracts as well as the original extracts were tested using the HT-SPOTi assay against *M. aurum*. Majority of the fractions and crude extracts had MICs greater than or equal to 500 mg/L. The lowest MIC was 125 mg/L for hexane SPE fraction 1 and methanol SPE fraction 6.

5.4 Discussion

Medicinal plants contain physiologically active principles that over the years have been exploited in traditional medicine for the treatment of various ailments. *Andrographis paniculata* is one of the highly used medicinal plants in the world. The plant is traditionally used for the treatment of several infectious diseases ranging from malaria to dysentery; it is antibacterial, antipyretic, antioxidant, antidiabetic, anticancer and hepatoprotective (Zhang *et al*., 2015). It has efficacy in treating upper respiratory tract infections, bronchitis, cough, flu and sinusitis. It has also been used traditionally to treat tuberculosis. Ethnobotanical use of a plant is an important criteria

in the choice of plant and our rationale for the selection of *A. paniculata* was based on its popularity in the treatment of upper respiratory tract infections and tuberculosis. This is in line with the objective of discovering new drugs to tackle multidrug-resistant tuberculosis.

A number of active constituents have been found in the plant including diterpenoid lactones, flavonoids and polyphenols, however, the therapeutic properties of the plant have been attributed to its prime constituent andrographolide (Wen *et al*., 2014). In this study, using different extraction techniques led to the isolation and characterization of andrographolide, neoandrographolide and 14-deoxy-11,12-didehydroandrogapholide. Further studies on the phytoconstituents are required even though the crude extracts and SPE fractions did not show significant activity. Other phenotypic assays such as the efflux pump inhibition and anti-biofilm assays could also be explored.

Chapter 6: Overall discussion and future direction

Natural products remain an outstanding source of novel chemical scaffolds that have served as useful leads in the development of drugs. Most pharmaceutical companies had neglected natural products preferring to utilise combinatorial chemistry libraries as a source of chemical diversity. Unfortunately such libraries lack the true chemical diversity that natural products display (extensive functional group chemistry and chirality) and these libraries are poor for discovery purposes but have potential in lead optimisation. However, there has been a renewed interest in natural products (Guzman et al., 2012, Gibbons, 2004, Wright, 2014). Plants in particular are a rich source of bioactive compounds and there are reasons that make compelling and convincing argument for the evaluation of plants as a source of new antibacterial agents.

Firstly, in terms of plant chemical ecology, it is logical that plants produce antibacterial metabolites as part of their chemical defence strategy to protect themselves against microbes in their environment. Soil is rich in bacteria, fungi and viruses and it is likely that plants contain latent antimicrobials or synthesise them *de novo* as part of a phytoalexic response on microbial invasion. Some species of soil bacteria such as *Streptomyces* are plant pathogens and these are taxonomically related to *Mycobacterium* species and this opportunity or taxonomic "closeness" and specificity is worth exploitation. Secondly, there are countless examples of plants which are used topically and systemically to treat bacterial infections in the ethnobotanical setting. There have to be opportunities to investigate ethnobotanical antibacterials to discover new drugs, particularly given the long association and plethora of herbal materials which are used in this area. Before the advent of antibiotic therapy and even topical synthetic antibacterials, plants were widely accepted as a resource of antiseptic materials, with fresh plants of certain taxa producing an array of

volatile natural products with antibacterial activity. Thirdly, it is the extensive functional group chemistry, chirality and ultimately chemical diversity of phytochemicals, and natural products in general, which mark them out as a valuable pool of bioactive molecules. Approximately one-quarter of all prescription medicines owe their origin either directly or indirectly to natural products. It is therefore highly probable that research in this area will yield new antibacterials. Finally, phytochemicals are structurally distinct from microbially derived antibiotic natural products such as the tetracyclines and macrolides. It is likely that this chemical uniqueness will give rise to classes of antibacterials with modes of action which are distinct from existing compounds (Gibbons, 2004).

Tuberculosis remains a challenging health problem worldwide due to the rapid spread of tuberculosis strains resistant to the major anti-tuberculosis drugs on the market. Tuberculosis control is hampered by the emergence of multidrug-resistance (MDR), defined as resistance to at least rifampicin and isoniazid, two key drugs in the treatment of the disease. The recent emergence of XDR-TB (strains, that are resistant to isoniazid or rifampicin, in addition to any fluoroquinolone and to at least one of the three second line injectable drugs amikacin, capreomycin or kanamycin) has greatly contributed to the control of TB becoming harder because there is virtually no effective drug available for its treatment. Enormous effort by all concerned to combat the disease is utterly necessary and this explains why this research is timely. New antimycobacterial entities with novel mechanisms of action are clinically needed for treating resistant forms of tuberculosis. This was the rationale for exploring new avenues such as plants for anti-tuberculosis drug discovery in this research.

The antibacterial activity of both naturally isolated and synthesized analogues of the naturally isolated compounds were investigated. Additionally, possible mode or mechanism of action of the synthesized compounds was investigated by testing their ability to inhibit multidrug efflux pumps or anti-biofilm activity.

Two important genera *Allium* and *Andrographis* which both have extensive ethnopharmacologic use for respiratory tract infections and tuberculosis were studied.

The genus *Allium* is worth phytochemical and antimicrobial studies because it comprises of over 750 species with a wide range of secondary metabolites (Keusgen et al., 2006). Members of the genus *Allium* such as garlic (*Allium sativum*) have a long history of usage as an antibacterial and been renowned as 'Russian penicillin' and have even found clinical utility in the United States as a treatment for TB with some success. *Allium sativum* chemistry is sulphur dominant with classic examples such as allicin, ajoene and a range of other sulphides which may be cyclic or linear. However, the chemistry of the family Alliaceae as a whole is diverse with examples of indole alkaloids, highly oxygenated and complex steroidal triterpenes of the furostane and spirostane type and anthocyanindins. It is highly likely that some of these compounds also have antibacterial activity. Some of these compounds have been demonstrated to show significant antibacterial and antimycobacterial activity (O'Donnell et al., 2009, O'Donnell and Gibbons, 2007).

In this study we investigated the phytochemistry and antibacterial properties of different species from the genus *Allium*. Even though some of the species showed favourable activity with MIC 125 mg/L, small quantities of fractions however prevented full chemical and biological characterisation.

Studies on the genus *Andrographis* also led to the isolation and characterization of major and minor compounds from the aerial parts of *Andrographis paniculata*. These

included andrographolide, 14-deoxy-11,12-didehydroandrographolide, neoandrographolide and andropanoside.

The antibacterial action of the compounds outlined throughout this study is a great contribution to the on-going search for antimicrobial drug leads. This is of prime importance since multidrug-resistance in *Mycobacterium* and other clinically relevant bacterial pathogens such as methicillin-resistant *Staphylococcus aureus* (MRSA) have emerged as a major threat to public health (Grundmann et al., 2006, Ventola, 2015, Abubakar et al., 2013). Studies are required to further unravel mechanism of action, improve toxicity and druggability which are necessary for the development of novel drugs.

Future studies

1. Bioassay-guided isolation of compounds from other *Allium* species on a large scale will be useful in discovering novel scaffolds.

2. Further studies on the biofilm inhibition of all the other synthesized disulfides to establish their effect will be useful.

3. Generating drug resistant mutants and performing whole genome sequencing of the mutants and analysing the altered genes will be useful in understanding the mechanism of action of the synthesized compounds.

4. Antibacterial, anti-biofilm and multidrug efflux pump inhibition assays on the purely isolated compounds from *Andrographis paniculata* will advance knowledge on these compounds.

References

ABUBAKAR, I., ZIGNOL, M., FALZON, D., RAVIGLIONE, M., DITIU, L., MASHAM, S., ADETIFA, I., FORD, N., COX, H., LAWN, S. D., MARAIS, B. J., MCHUGH, T. D., MWABA, P., BATES, M., LIPMAN, M., ZIJENAH, L., LOGAN, S., MCNERNEY, R., ZUMLA, A., SARDA, K., NAHID, P., HOELSCHER, M., PLETSCHETTE, M., MEMISH, Z. A., KIM, P., HAFNER, R., COLE, S., MIGLIORI, G. B., MAEURER, M. & SCHITO, M. 2013. Drug-resistant tuberculosis: time for visionary political leadership. *Lancet Infectious Diseases*, 13, 529-39.

ALMEIDA DA SILVA, P. E. & PALOMINO, J. C. 2011. Molecular basis and mechanisms of drug resistance in *Mycobacterium tuberculosis*: classical and new drugs. *Journal of Antimicrobial Chemotherapy*, 66, 1417-30.

ANDERSEN, C. L., HOLLAND, I. B. & JACQ, A. 2006. Verapamil, a Ca2+ channel inhibitor acts as a local anesthetic and induces the sigma E dependent extra-cytoplasmic stress response in *E. coli*. *Biochimica et Biophysica Acta*, 1758, 1587-95.

ANISHETTY, S., PULIMI, M. & PENNATHUR, G. 2005. Potential drug targets in *Mycobacterium tuberculosis* through metabolic pathway analysis. *Computational Biology and Chemistry*, 29, 368-378.

BAUGH, S., EKANAYAKA, A. S., PIDDOCK, L. J. & WEBBER, M. A. 2012. Loss of or inhibition of all multidrug resistance efflux pumps of *Salmonella enterica* serovar Typhimurium results in impaired ability to form a biofilm. *Journal of Antimicrobial Chemotherapy*, 67, 2409-17.

BAUGH, S., PHILLIPS, C. R., EKANAYAKA, A. S., PIDDOCK, L. J. & WEBBER, M. A. 2014. Inhibition of multidrug efflux as a strategy to prevent biofilm formation. *Journal of Antimicrobial Chemotherapy*, 69, 673-81.

BEGG, E. J. & BARCLAY, M. L. 1995. Aminoglycosides--50 years on. *British Journal of Clinical Pharmacology*, 39, 597-603.

BELARD, S., HEUVELINGS, C. C., JANSSEN, S. & GROBUSCH, M. P. 2015. Bedaquiline for the treatment of drug-resistant tuberculosis. *Expert Review of Anti-infective Therapy*, 13, 535-53.

BENOIT, M. R., CONANT, C. G., IONESCU-ZANETTI, C., SCHWARTZ, M. & MATIN, A. 2010. New device for high-throughput viability screening of flow biofilms. *Applied Environmental Microbiology*, 76, 4136-42.

BHAKTA, S., BESRA, G. S., UPTON, A. M., PARISH, T., SHOLTO-DOUGLAS-VERNON, C., GIBSON, K. J., KNUTTON, S., GORDON, S., DASILVA, R. P., ANDERTON, M. C. & SIM, E. 2004. Arylamine *N*-acetyltransferase is required for synthesis of mycolic acids and complex lipids in Mycobacterium bovis BCG and represents a novel drug target. *Journal of Experimental Medicine*, 199, 1191-9.

BLAIR, J. M., RICHMOND, G. E. & PIDDOCK, L. J. 2014. Multidrug efflux pumps in Gram-negative bacteria and their role in antibiotic resistance. *Future Microbiology*, 9, 1165-77.

BLAIR, J. M., WEBBER, M. A., BAYLAY, A. J., OGBOLU, D. O. & PIDDOCK, L. J. 2015. Molecular mechanisms of antibiotic resistance. *Nature Reviews Microbiology*, 13, 42-51.

BLOCK, E. 1985. The chemistry of garlic and onions. *Scientific American*. 252(3):114-9. PMID: 3975593

BRAGGINTON, E. C. & PIDDOCK, L. J. 2014. UK and European Union public and charitable funding from 2008 to 2013 for bacteriology and antibiotic research in the UK: an observational study. *Lancet Infectious Diseases*, 14, 857-68.

BRANDA, S. S., VIK, S., FRIEDMAN, L. & KOLTER, R. 2005. Biofilms: the matrix revisited. *Trends in Microbiology*, 13, 20-6.

BRENNAN, P. J. 2003. Structure, function, and biogenesis of the cell wall of *Mycobacterium tuberculosis*. *Tuberculosis (Edinburgh)*, 83, 91-7.

BROCK, I., WELDINGH, K., LILLEBAEK, T., FOLLMANN, F. & ANDERSEN, P. 2004. Comparison of tuberculin skin test and new specific blood test in tuberculosis contacts. *American Journal of Respiratory and Critical Care Medicine*, 170, 65-9.

CAMINERO, J. 2007. [The old battle between the human species and Koch's bacillae. Can one dream of eradicating tuberculosis?]. *Anales del sistema sanitario de Navarra*, 30 Suppl 2, 163-80.

CAMINERO, J. A., SOTGIU, G., ZUMLA, A. & MIGLIORI, G. B. 2010. Best drug treatment for multidrug-resistant and extensively drug-resistant tuberculosis. *Lancet Infectious Diseases*, 10, 621-9.

CARLET, J., PULCINI, C. & PIDDOCK, L. J. 2014. Antibiotic resistance: a geopolitical issue. *Clinical Microbiology and Infection*, 20, 949-53.

CHALKE, H. D. 1962. The Impact of Tuberculosis on History, Literature and Art. *Medical History*, 6, 301-18.

CHAO, W. W. & LIN, B. F. 2010. Isolation and identification of bioactive compounds in *Andrographis paniculata* (Chuanxinlian). *Chinese Medicine*, 5, 17.

COOK, G. M., BERNEY, M., GEBHARD, S., HEINEMANN, M., COX, R. A., DANILCHANKA, O. & NIEDERWEIS, M. 2009. Physiology of mycobacteria. *Advances in Microbial Physiology*, 55, 81-182, 318-9.

CREWS, P., RODRıGUEZ, J. & JASPARS, M. 1998. *Organic structure analysis*, New York ; Oxford : Oxford University Press.

CRICK, D. C., MAHAPATRA, S. & BRENNAN, P. J. 2001. Biosynthesis of the arabinogalactan-peptidoglycan complex of *Mycobacterium tuberculosis*. *Glycobiology*, 11, 107R-118R.

D'COSTA, V. M., KING, C. E., KALAN, L., MORAR, M., SUNG, W. W., SCHWARZ, C., FROESE, D., ZAZULA, G., CALMELS, F., DEBRUYNE, R., GOLDING, G. B., POINAR, H. N. & WRIGHT, G. D. 2011. Antibiotic resistance is ancient. *Nature*, 477, 457-61.

DA SILVA, P. E., VON GROLL, A., MARTIN, A. & PALOMINO, J. C. 2011. Efflux as a mechanism for drug resistance in *Mycobacterium tuberculosis*. *FEMS Immunology and Medical Microbiology*, 63, 1-9.

DAVIES, S. C., FOWLER, T., WATSON, J., LIVERMORE, D. M. & WALKER, D. 2013. Annual Report of the Chief Medical Officer: infection and the rise of antimicrobial resistance. *Lancet*, 381, 1606-9.

DE KIEVIT, T. R., PARKINS, M. D., GILLIS, R. J., SRIKUMAR, R., CERI, H., POOLE, K., IGLEWSKI, B. H. & STOREY, D. G. 2001. Multidrug efflux pumps: expression patterns and contribution to antibiotic resistance in *Pseudomonas aeruginosa* biofilms. *Antimicrobial Agents and Chemotherapy*, 45, 1761-70.

DE ROSSI, E., AÍNSA, J. A. & RICCARDI, G. 2006. Role of mycobacterial efflux transporters in drug resistance: an unresolved question. *FEMS Microbiology Reviews*, 30, 36-52.

DEBARBER, A. E., MDLULI, K., BOSMAN, M., BEKKER, L. G. & BARRY, C. E., 3RD 2000. Ethionamide activation and sensitivity in multidrug-resistant *Mycobacterium tuberculosis*. *Proceedings of the National Academy of Sciences U S A*, 97, 9677-82.

DI PERRI, G. & BONORA, S. 2004. Which agents should we use for the treatment of multidrug-resistant *Mycobacterium tuberculosis*? *Journal of Antimicrobial Chemotherapy*, 54, 593-602.

DMITRIEV, B. A., EHLERS, S., RIETSCHEL, E. T. & BRENNAN, P. J. 2000. Molecular mechanics of the mycobacterial cell wall: from horizontal layers to vertical scaffolds. *International Journal of Medical Microbiology*, 290, 251-8.

DOUGLAS, A. S. & SKOOG, D. A. 2007. *Principles of instrumental analysis / Douglas A. Skoog, F. James Holler, Stanley R. Crouch*, Belmont, CA, Belmont, CA : Brooks/Cole.

EISENSTADT, J. & HALL, G. S. 1995. Microbiology and classification of mycobacteria. *Clinical Dermatology*, 13, 197-206.

EVANGELOPOULOS, D. & BHAKTA, S. 2010. Rapid methods for testing inhibitors of mycobacterial growth. *Methods in Molecular Biology*, 642, 193-201.

FERNÁNDEZ, L. & HANCOCK, R. E. 2012. Adaptive and mutational resistance: role of porins and efflux pumps in drug resistance. *Clinical Microbiology Reviews*, 25, 661-81.

FINE, P. E. 1995. Bacille Calmette-Guerin vaccines: a rough guide. *Clinical Infectious Diseases*, 20, 11-4.

FLEMMING, H. C. & WINGENDER, J. 2010. The biofilm matrix. *Nature Reviews Microbiology*, 8, 623-33.

GIBBONS, S. 2004. Anti-staphylococcal plant natural products. *Natural Product Reports*, 21, 263-77.

GIBBONS, S., MOSER, E., HAUSMANN, S., STAVRI, M., SMITH, E. & CLENNETT, C. 2005. An anti-staphylococcal acylphloroglucinol from *Hypericum foliosum*. *Phytochemistry*, 66, 1472-5.

GIBBONS, S. & UDO, E. E. 2000. The effect of reserpine, a modulator of multidrug efflux pumps, on the in vitro activity of tetracycline against clinical isolates of methicillin resistant *Staphylococcus aureus* (MRSA) possessing the tet(K) determinant. *Phytotherapy Research*, 14, 139-40.

GILLESPIE, S. H. 2002. Evolution of drug resistance in *Mycobacterium tuberculosis*: clinical and molecular perspective. *Antimicrobial Agents and Chemotherapy*, 46, 267-74.

GLOBAL RISKS 2014. World Economic Forum. Global Risks 2014 Report.

GORDON, R. E. & SMITH, M. M. 1955. Rapidly growing, acid fast bacteria. II. Species' description of *Mycobacterium fortuitum* Cruz. *Journal of Bacteriology*, 69, 502-7.

GRANGE, J. M. & ZUMLA, A. 1999. Paradox of the global emergency of tuberculosis. *Lancet*, 353**,** 996.

GRANGE, J. M. & ZUMLA, A. 2002. The global emergency of tuberculosis: what is the cause? *Journal of Royal Society for the Promotion of Health*, 122, 78-81.

GRUNDMANN, H., AIRES-DE-SOUSA, M., BOYCE, J. & TIEMERSMA, E. 2006. Emergence and resurgence of meticillin-resistant *Staphylococcus aureus* as a public-health threat. *Lancet*, 368, 874-85.

GUPTA, A. & BHAKTA, S. 2012. An integrated surrogate model for screening of drugs against *Mycobacterium tuberculosis*. *Journal of Antimicrobial Chemotherapy*, 67, 1380-91.

GUZMAN, J. D., EVANGELOPOULOS, D., GUPTA, A., BIRCHALL, K., MWAIGWISYA, S., SAXTY, B., MCHUGH, T. D., GIBBONS, S., MALKINSON, J. & BHAKTA, S. 2013. Antitubercular specific activity of ibuprofen and the other 2-arylpropanoic acids using the HT-SPOTi whole-cell phenotypic assay. *British Medical Journal Open*, 3.

GUZMAN, J. D., GUPTA, A., BUCAR, F., GIBBONS, S. & BHAKTA, S. 2012. Antimycobacterials from natural sources: ancient times, antibiotic era and novel scaffolds. *Frontiers in Bioscience*, 17, 1861-81.

GUZMAN, J. D., GUPTA, A., EVANGELOPOULOS, D., BASAVANNACHARYA, C., PABON, L. C., PLAZAS, E. A., MUNOZ, D. R., DELGADO, W. A., CUCA, L. E., RIBON, W., GIBBONS, S. & BHAKTA, S. 2010. Anti-tubercular screening of natural products from Colombian plants: 3-methoxynordomesticine, an inhibitor of MurE ligase of *Mycobacterium tuberculosis*. *Journal of Antimicrobial Chemotherapy*, 65, 2101-7.

HAAS, M., BIDDLECOME, S., DAVIES, J., LUCE, C. E. & DANIELS, P. J. 1976. Enzymatic modification of aminoglycoside antibiotics: a new 6'-N-acetylating enzyme from a *Pseudomonas aeruginosa* isolate. *Antimicrobial Agents and Chemotherapy*, 9, 945-50.

HAMPTON, T. 2013. Report reveals scope of US antibiotic resistance threat. *Jounal of the American Medical Association*, 310, 1661-3.

HEINRICH, M., BARNES, J., GIBBONS, S. & WILLIAMSON, W. M. 2012. Fundamentals of Pharmacognosy and Phytotherapy. London: Elsevier Churchill Livingstone.

HERNANDEZ-PANDO, R., JEYANATHAN, M., MENGISTU, G., AGUILAR, D., OROZCO, H., HARBOE, M., ROOK, G. A. & BJUNE, G. 2000. Persistence of DNA from *Mycobacterium tuberculosis* in superficially normal lung tissue during latent infection. *Lancet*, 356, 2133-8.

HERZOG, H. 1998. History of tuberculosis. *Respiration*, 65, 5-15.

HIGGINS, P. G., FLUIT, A. C. & SCHMITZ, F. J. 2003. Fluoroquinolones: structure and target sites. *Current Drug Targets*, 4, 181-90.

IVANOV, A. R., NAZIMOV, I. V. & BARATOVA, L. 2000. Determination of biologically active low-molecular-mass thiols in human blood. I. Fast qualitative and quantitative, gradient and isocratic reversed-phase high-performance liquid chromatography with photometric and fluorescence detection. *Jounal of Chromatography A*, 895, 157-66.

JANIN, Y. L. 2007. Antituberculosis drugs: ten years of research. *Bioorganic and Medicinal Chemistry Letters*, 15, 2479-513.

JARLIER, V. & NIKAIDO, H. 1994. Mycobacterial cell wall: structure and role in natural resistance to antibiotics. *FEMS Microbiology Letters*, 123, 11-8.

JONAS, K., TOMENIUS, H., KADER, A., NORMARK, S., RÖMLING, U., BELOVA, L. M. & MELEFORS, O. 2007. Roles of curli, cellulose and BapA in *Salmonella* biofilm morphology studied by atomic force microscopy. *BioMed Central Microbiology*, 7, 70.

JOSHI, J. M. 2011. Tuberculosis chemotherapy in the 21 century: Back to the basics. *Lung India*, 28, 193-200.

JOVANOVIC, D. 2004. [The role of chemoprophylaxis in prevention of tuberculosis]. *Medicinski pregled*, 57, Suppl 1**,** 49-52.

JUGHELI, L., BZEKALAVA, N., DE RIJK, P., FISSETTE, K., PORTAELS, F. & RIGOUTS, L. 2009. High Level of Cross-Resistance between Kanamycin, Amikacin, and Capreomycin among *Mycobacterium tuberculosis* Isolates from Georgia and a Close Relation with Mutations in the rrs Gene. *Antimicrobial Agents and Chemotherapy*, 53, 5064-5068.

JUNUTULA, J. R., FLAGELLA, K. M., GRAHAM, R. A., PARSONS, K. L., HA, E., RAAB, H., BHAKTA, S., NGUYEN, T., DUGGER, D. L., LI, G., MAI, E., LEWIS PHILLIPS, G. D., HIRARAGI, H., FUJI, R. N., TIBBITTS, J., VANDLEN, R., SPENCER, S. D., SCHELLER, R. H., POLAKIS, P. & SLIWKOWSKI, M. X. 2010. Engineered thio-trastuzumab-DM1 conjugate with an improved therapeutic index to target human epidermal growth factor receptor 2-positive breast cancer. *Clinical Cancer Research*, 16, 4769-78.

KAATZ, G. W., SEO, S. M. & RUBLE, C. A. 1993. Efflux-mediated fluoroquinolone resistance in *Staphylococcus aureus*. *Antimicrobial Agents and Chemotherapy*, 37, 1086-94.

KEUSGEN, M., FRITSCH, R. M., HISORIEV, H., KURBONOVA, P. A. & KHASSANOV, F. O. 2006. Wild *Allium* species (Alliaceae) used in folk medicine of Tajikistan and Uzbekistan. *Journal of Ethnobiology and Ethnomedicine*, 2, 18.

KITSON, T. M. & LOOMES, K. M. 1985. Synthesis of methyl 2- and 4-pyridyl disulfide from 2- and 4-thiopyridone and methyl methanethiosulfonate. *Analytical Biochemistry*, 146, 429-430.

KOCHI, A., VARELDZIS, B. & STYBLO, K. 1993. Multidrug-resistant tuberculosis and its control. *Research in Microbiology*, 144, 104-10.

KOJIMA, S. & NIKAIDO, H. 2013. Permeation rates of penicillins indicate that Escherichia coli porins function principally as nonspecific channels. *Proceedings of the National Academy of Science of the United States of America*, 110, E2629-34.

KOTESWARA RAO, Y., VIMALAMMA, G., RAO, C. V. & TZENG, Y. M. 2004. Flavonoids and andrographolides from *Andrographis paniculata*. *Phytochemistry*, 65, 2317-21.

KOZA, P., GONNOT, V. & PELLETER, J. 2012. Right-first-time isocratic preparative liquid chromatography-mass spectrometry purification. *American Chemical Society Combinatorial Science*, 14, 273-9.

KUMAR, N., BHARGAVA, S. K., AGRAWAL, C. S., GEORGE, K., KARKI, P. & BARAL, D. 2005. Chest radiographs and their reliability in the diagnosis of tuberculosis. *Journal of Nepal Medical Association*, 44, 138-42.

KVIST, M., HANCOCK, V. & KLEMM, P. 2008. Inactivation of efflux pumps abolishes bacterial biofilm formation. *Applied and Environmental Microbiology*, 74, 7376-82.

LARSEN, M. H., VILCHEZE, C., KREMER, L., BESRA, G. S., PARSONS, L., SALFINGER, M., HEIFETS, L., HAZBON, M. H., ALLAND, D., SACCHETTINI, J. C. & JACOBS, W. R., JR. 2002. Overexpression of inhA, but not kasA, confers resistance to isoniazid and ethionamide in *Mycobacterium smegmatis, M. bovis* BCG and *M. tuberculosis*. *Molecular Microbiology*, 46, 453-66.

LAWN, S. D. & ZUMLA, A. I. 2011. Tuberculosis. *Lancet*, 378, 57-72.

LAXMINARAYAN, R., DUSE, A., WATTAL, C., ZAIDI, A. K., WERTHEIM, H. F., SUMPRADIT, N., VLIEGHE, E., HARA, G. L., GOULD, I. M., GOOSSENS, H., GREKO, C., SO, A. D., BIGDELI, M., TOMSON, G., WOODHOUSE, W., OMBAKA, E., PERALTA, A. Q., QAMAR, F. N., MIR, F., KARIUKI, S., BHUTTA, Z. A., COATES, A., BERGSTROM, R., WRIGHT, G. D., BROWN, E. D. & CARS, O. 2013. Antibiotic resistance-the need for global solutions. *Lancet Infectious Diseases*, 13, 1057-98.

LECHNER, D., GIBBONS, S. & BUCAR, F. 2008. Plant phenolic compounds as ethidium bromide efflux inhibitors in *Mycobacterium smegmatis*. *Journal of Antimicrobial Chemotherapy*, 62, 345-8.

LEE, O. Y., WU, H. H., DONOGHUE, H. D., SPIGELMAN, M., GREENBLATT, C. L., BULL, I. D., ROTHSCHILD, B. M., MARTIN, L. D., MINNIKIN, D. E. & BESRA, G. S. 2012. *Mycobacterium tuberculosis* complex lipid virulence factors preserved in the 17,000-year-old skeleton of an extinct bison, Bison antiquus. *Public library of science One*, 7, e41923.

LEMIEUX, G., DAVIGNON, A. & GENEST, J. 1956. Treatment of arterial hypertension with rescinnamine, a new alkaloid isolated from *Rauwolfia serpentina*. *Canadian Medical Association Journal*, 74, 144-5.

LEWIS, K. 2007. Persister cells, dormancy and infectious disease. *Nature Reviews Microbiology*, 5, 48-56.

LING, L. L., SCHNEIDER, T., PEOPLES, A. J., SPOERING, A. L., ENGELS, I., CONLON, B. P., MUELLER, A., SCHÄBERLE, T. F., HUGHES, D. E., EPSTEIN, S., JONES, M., LAZARIDES, L., STEADMAN, V. A., COHEN, D. R., FELIX, C. R., FETTERMAN, K. A., MILLETT, W. P., NITTI, A. G., ZULLO, A. M., CHEN, C. & LEWIS, K. 2015. A new antibiotic kills pathogens without detectable resistance. *Nature*, 517, 455-9.

LOMOVSKAYA, O. & BOSTIAN, K. A. 2006. Practical applications and feasibility of efflux pump inhibitors in the clinic--a vision for applied use. *Biochemical Pharmacology*, 71, 910-8.

MATSUDA, T., KUROYANAGI, M., SUGIYAMA, S., UMEHARA, K., UENO, A. & NISHI, K. 1994. Cell differentiation-inducing diterpenes from *Andrographis paniculata* Nees. *Chemical and Pharmaceutical Bulletin (Tokyo)*, 42, 1216-25.

MABRY, T. J., MARKHAM, K. R. & THOMAS, M. B. 1970. *The Systematic Identification of Flavonoids*, New York, Springer Berlin Heidelberg.

MACHADO, D., COUTO, I., PERDIGÃO, J., RODRIGUES, L., PORTUGAL, I., BAPTISTA, P., VEIGAS, B., AMARAL, L. & VIVEIROS, M. 2012. Contribution of efflux to the emergence of isoniazid and multidrug resistance in *Mycobacterium tuberculosis*. *Public Library of Science One*, 7, e34538.

MATTEELLI, A., ROGGI, A. & CARVALHO, A. C. 2014. Extensively drug-resistant tuberculosis: epidemiology and management. *Clinical Epidemiology*, 6, 111-8.

MCSHANE, H., PATHAN, A. A., SANDER, C. R., KEATING, S. M., GILBERT, S. C., HUYGEN, K., FLETCHER, H. A. & HILL, A. V. 2004. Recombinant modified vaccinia virus Ankara expressing antigen 85A boosts BCG-primed and naturally acquired antimycobacterial immunity in humans. *Nature Medicine*, 10, 1240-4.

MITCHISON, D. A. 1998. The origins of DOT. *International Journal of Tuberculosis Lung Disease*, 2, 863-5.

MITCHISON, D. A. 2005. The Diagnosis and Therapy of Tuberculosis During the Past 100 Years. *American Journal of Respiratory and Critical Care Medicine*, 171, 699-706.

MITCHISON, D. A. 2012. Prevention of drug resistance by combined drug treatment of tuberculosis. *Handbook of Experimental Pharmacology*, 87-98.

MONOD, J. 1949. the growth of bacterial cultures. *Annual Review of Microbiology*, 3, 371-394.

MORRIS, R. P., NGUYEN, L., GATFIELD, J., VISCONTI, K., NGUYEN, K., SCHNAPPINGER, D., EHRT, S., LIU, Y., HEIFETS, L., PIETERS, J., SCHOOLNIK, G. & THOMPSON, C. J. 2005. Ancestral antibiotic resistance in *Mycobacterium tuberculosis*. *Proceedings of the Nationall Academy of Science of the United States of America*, 102, 12200-5.

MOSMANN, T. 1983. Rapid colorimetric assay for cellular growth and survival: Application to proliferation and cytotoxicity assays. *Journal of Immunological Methods*, 65, 55-63.

NAYAK, S. & ACHARJYA, B. 2012. Mantoux test and its interpretation. *Indian Dermatology Online Journal*, 3, 2-6.

NGUYEN, L. & THOMPSON, C. J. 2006. Foundations of antibiotic resistance in bacterial physiology: the mycobacterial paradigm. *Trends in Microbiology*, 14, 304-12.

NIEDERWEIS, M., DANILCHANKA, O., HUFF, J., HOFFMANN, C. & ENGELHARDT, H. 2010. Mycobacterial outer membranes: in search of proteins. *Trends in Microbiology*, 18, 109-16.

NIKAIDO, H. 2009. Multidrug resistance in bacteria. *Annual Review of Biochemistry*, 78, 119-46.

NIKAIDO, H. & PAGÈS, J. M. 2012. Broad-specificity efflux pumps and their role in multidrug resistance of Gram-negative bacteria. *FEMS Microbiology Reviews*, 36, 340-63.

NIKAIDO, H. & TAKATSUKA, Y. 2009. Mechanisms of RND multidrug efflux pumps. *Biochimca et Biophysica Acta*, 1794**,** 769-81.

O'DONNELL, G., BUCAR, F. & GIBBONS, S. 2006. Phytochemistry and antimycobacterial activity of *Chlorophytum inornatum*. *Phytochemistry*, 67, 178-82.

O'DONNELL, G., POESCHL, R., ZIMHONY, O., GUNARATNAM, M., MOREIRA, J. B., NEIDLE, S., EVANGELOPOULOS, D., BHAKTA, S., MALKINSON, J. P., BOSHOFF, H. I., LENAERTS, A. & GIBBONS, S. 2009. Bioactive pyridine-*N*-oxide disulfides from *Allium stipitatum*. *Journal of Natural Products*, 72, 360-5.

O'DONNELL, G. & GIBBONS, S. 2007. Antibacterial activity of two canthin-6-one alkaloids from *Allium neapolitanum*. *Phytotherapy Research*, 21, 653-7.

O'TOOLE, G., KAPLAN, H. B. & KOLTER, R. 2000. Biofilm formation as microbial development. *Annual Reviews in Microbioogyl*, 54, 49-79.

OSMAN, K., EVANGELOPOULOS, D., BASAVANNACHARYA, C., GUPTA, A., MCHUGH, T. D., BHAKTA, S. & GIBBONS, S. 2012. An antibacterial from *Hypericum acmosepalum* inhibits ATP-dependent MurE ligase from *Mycobacterium tuberculosis*. *International Journal of Antimicrobial Agents*, 39, 124-9.

PACE, C. N., VAJDOS, F., FEE, L., GRIMSLEY, G. & GRAY, T. 1995. How to measure and predict the molar absorption coefficient of a protein. *Protein Science*, 4, 2411-23.
PIDDOCK, L. J. 2006. Clinically relevant chromosomally encoded multidrug resistance efflux pumps in bacteria. *Clinical Microbiology Reviews*, 19, 382-402.
PIDDOCK, L. J. 2013. Antibiotic action: helping deliver action plans and strategies. *Lancet Infectious Diseases*, 13, 1009-11.
PIDDOCK, L. J. 2014. Understanding the basis of antibiotic resistance: a platform for drug discovery. *Microbiology*, 160, 2366-73.
POOLE, C. F. 2003. Thin-layer chromatography: challenges and opportunities. *Journal of Chromatography A*, 1000, 963-84.
PURI, A., SAXENA, R., SAXENA, R. P., SAXENA, K. C., SRIVASTAVA, V. & TANDON, J. S. 1993. Immunostimulant agents from *Andrographis paniculata*. *Journal of Natural Products*, 56, 995-9.
QUINN, T., O'MAHONY, R., BAIRD, A. W., DRUDY, D., WHYTE, P. & FANNING, S. 2006. Multi-drug resistance in *Salmonella enterica*: efflux mechanisms and their relationships with the development of chromosomal resistance gene clusters. *Current Drug Targets*, 7, 849-60.
RAMASWAMY, S. & MUSSER, J. M. 1998. Molecular genetic basis of antimicrobial agent resistance in *Mycobacterium tuberculosis*: 1998 update. *Tubercle and Lung Disease*, 79, 3-29.
RAWAT, R., WHITTY, A. & TONGE, P. J. 2003. The isoniazid-NAD adduct is a slow, tight-binding inhibitor of InhA, the *Mycobacterium tuberculosis* enoyl reductase: adduct affinity and drug resistance. *Proceedings of the National Academy of Science of the United States of America*, 100, 13881-6.
REUSCH, W. 2007. "UV-Visible Spectroscopy." *Organic Chemistry Online*.
RICHARDSON, J. F. & REITH, S. 1993. Characterization of a strain of methicillin-resistant *Staphylococcus aureus* (EMRSA-15) by conventional and molecular methods. *Journal of Hospital Infection*, 25, 45-52.
RIZI, K., MURDAN, S., DANQUAH, C. A., FAULL, J. & BHAKTA, S. 2015. Development of a rapid, reliable and quantitative method - "SPOTi" for testing antifungal efficacy. *Journal of Microbiological Methods*, 117, 36-40.
ROCK, D. 1997. Tuberculosis: a global emergency. *Work*, 8, 93-105.
RODRIGUES, L., RAMOS, J., COUTO, I., AMARAL, L. & VIVEIROS, M. 2011. Ethidium bromide transport across My*cobacterium smegmatis* cell-wall: correlation with antibiotic resistance. *BioMed Central Microbiology*, 11, 35.
RODRIGUES, L., WAGNER, D., VIVEIROS, M., SAMPAIO, D., COUTO, I., VAVRA, M., KERN, W. V. & AMARAL, L. 2008. Thioridazine and chlorpromazine inhibition of ethidium bromide efflux in *Mycobacterium avium* and *Mycobacterium smegmatis*. *Journal of Antimicrobial Chemotherapy*, 61, 1076-82.
RODRIGUES, L. C., DIWAN, V. K. & WHEELER, J. G. 1993. Protective effect of BCG against tuberculous meningitis and miliary tuberculosis: a meta-analysis. *International Journal of Epidemiology*, 22, 1154-8.
ROSS, J. I., FARRELL, A. M., EADY, E. A., COVE, J. H. & CUNLIFFE, W. J. 1989. Characterisation and molecular cloning of the novel macrolide-streptogramin B resistance determinant from *Staphylococcus epidermidis*. *Journal of Antimicrobial Chemotherapy*, 24, 851-62.
SACCHETTINI, J. C., RUBIN, E. J. & FREUNDLICH, J. S. 2008. Drugs versus bugs: in pursuit of the persistent predator *Mycobacterium tuberculosis*. *Nature Reviews Microbiology*, 6, 41-52.
SALO, W. L., AUFDERHEIDE, A. C., BUIKSTRA, J. & HOLCOMB, T. A. 1994. Identification of *Mycobacterium tuberculosis* DNA in a pre-Columbian Peruvian mummy. *Proceedings of the National Academy of Sciences of the United States of America*, 91, 2091-4.
SANTHA, T., NAZARETH, O., KRISHNAMURTHY, M. S., BALASUBRAMANIAN, R., VIJAYAN, V. K., JANARDHANAM, B., VENKATARAMAN, P., TRIPATHY, S.

P. & PRABHAKAR, R. 1989. Treatment of pulmonary tuberculosis with short course chemotherapy in south India-5-year follow up. *Tubercle*, 70, 229-34.

SCHAEFER, W. B., MARSHAK, A. & BURKHART, B. 1949. The growth of *Mycobacterium tuberculosis* as a function of its nutrients. *Journal of Bacteriology*, 58, 549-63.

SEPKOWITZ, K. A. 1996. How contagious is tuberculosis? *Clinical Infectious Diseases*, 23, 954-62.

SHAH, N. S., WRIGHT, A., BAI, G. H., BARRERA, L., BOULAHBAL, F., MARTIN-CASABONA, N., DROBNIEWSKI, F., GILPIN, C., HAVELKOVA, M., LEPE, R., LUMB, R., METCHOCK, B., PORTAELS, F., RODRIGUES, M. F., RUSCH-GERDES, S., VAN DEUN, A., VINCENT, V., LASERSON, K., WELLS, C. & CEGIELSKI, J. P. 2007. Worldwide emergence of extensively drug-resistant tuberculosis. *Emerging Infectious Disease*, 13, 380-7.

SHIU, W. K., MALKINSON, J. P., RAHMAN, M. M., CURRY, J., STAPLETON, P., GUNARATNAM, M., NEIDLE, S., MUSHTAQ, S., WARNER, M., LIVERMORE, D. M., EVANGELOPOULOS, D., BASAVANNACHARYA, C., BHAKTA, S., SCHINDLER, B. D., SEO, S. M., COLEMAN, D., KAATZ, G. W. & GIBBONS, S. 2013. A new plant-derived antibacterial is an inhibitor of efflux pumps in *Staphylococcus aureus*. *International Journal of Antimicrobial Agents*, 42, 513-8.

SIMEON, J., FINK, M., ITIL, T. M. & PONCE, D. 1970. D-Cycloserine Therapy of Psychosis by Symptom Provocation. *Comprehensive Psychiatry*, 11, 80-88.

SINGH, G., MAURYA, S., DELAMPASONA, M. P. & CATALAN, C. A. 2007. A comparison of chemical, antioxidant and antimicrobial studies of cinnamon leaf and bark volatile oils, oleoresins and their constituents. *Food and Chemical Toxicology*, 45, 1650-61.

SRIVASTAVA, S., MUSUKA, S., SHERMAN, C., MEEK, C., LEFF, R. & GUMBO, T. 2010. Efflux-pump-derived multiple drug resistance to ethambutol monotherapy in *Mycobacterium tuberculosis* and the pharmacokinetics and pharmacodynamics of ethambutol. *Journal of Infectious Diseases*, 201, 1225-31.

STAPLETON, A. 2003. Novel approaches to prevention of urinary tract infections. *Infectious Disease Clinic of North America*, 17, 457-71.

STAVRI, M., PIDDOCK, L. J. & GIBBONS, S. 2007. Bacterial efflux pump inhibitors from natural sources. *Journal of Antimicrobial Chemotherapy*, 59, 1247-60.

SUNDARAMURTHY, V. & PIETERS, J. 2007. Interactions of pathogenic mycobacteria with host macrophages. *Microbes and Infection* 9, 1671-9.

SUZUKI, Y., KATSUKAWA, C., TAMARU, A., ABE, C., MAKINO, M., MIZUGUCHI, Y. & TANIGUCHI, H. 1998. Detection of kanamycin-resistant *Mycobacterium tuberculosis* by identifying mutations in the 16S rRNA gene. *Journal of Clinical Microbiology*, 36, 1220-5.

TORTOLI, E., CICHERO, P., PIERSIMONI, C., SIMONETTI, M. T., GESU, G. & NISTA, D. 1999. Use of BACTEC MGIT 960 for recovery of mycobacteria from clinical specimens: multicenter study. *Journal of Clinical Microbiology*, 37, 3578-82.

VALDIANI, A., KADIR, M. A., TAN, S. G., TALEI, D., ABDULLAH, M. P. & NIKZAD, S. 2012. Nain-e Havandi *Andrographis paniculata* present yesterday, absent today: a plenary review on underutilized herb of Iran's pharmaceutical plants. *Molecular Biology Reports*, 39, 5409-24.

VENTOLA, C. L. 2015. The antibiotic resistance crisis: part 2: management strategies and new agents. *P T*, 40, 344-52.

VISEN, P. K., SHUKLA, B., PATNAIK, G. K. & DHAWAN, B. N. 1993. Andrographolide protects rat hepatocytes against paracetamol-induced damage. *Journal of Ethnopharmacology* , 40, 131-6.

VIVEIROS, M., LEANDRO, C. & AMARAL, L. 2003. Mycobacterial efflux pumps and chemotherapeutic implications. *International Journal of Antimicrobial Agents*, 22**,** 274-8.

VIVEIROS, M., MARTINS, M., RODRIGUES, L., MACHADO, D., COUTO, I., AINSA, J. & AMARAL, L. 2012. Inhibitors of mycobacterial efflux pumps as potential boosters for anti-tubercular drugs. *Expert Review of Anti-Infective Therapy*, 10, 983-98.

VON REYN, C. F. & VUOLA, J. M. 2002. New vaccines for the prevention of tuberculosis. *Clinical Infectious Diseases*, 35, 465-74.

WALSH, V. & GOODMAN, J. 1999. Cancer chemotherapy, biodiversity, public and private property: the case of the anti-cancer drug taxol. *Social Science and Medicine*, 49, 1215-25.

WANG, J. Y., HSUEH, P. R., WANG, S. K., JAN, I. S., LEE, L. N., LIAW, Y. S., YANG, P. C. & LUH, K. T. 2007. Disseminated tuberculosis: a 10-year experience in a medical center. *Medicine (Baltimore)*, 86, 39-46.

WANG, Y. Q., WU, Z. F., KE, G. & YANG, M. 2015. An effective vacuum assisted extraction method for the optimization of labdane diterpenoids from *Andrographis paniculata* by response surface methodology. *Molecules*, 20, 430-45.

WATNICK, P. & KOLTER, R. 2000. Biofilm, city of microbes. *Journal of Bacteriology*, 182, 2675-9.

WELLINGTON, E. M., BOXALL, A. B., CROSS, P., FEIL, E. J., GAZE, W. H., HAWKEY, P. M., JOHNSON-ROLLINGS, A. S., JONES, D. L., LEE, N. M., OTTEN, W., THOMAS, C. M. & WILLIAMS, A. P. 2013. The role of the natural environment in the emergence of antibiotic resistance in gram-negative bacteria. *Lancet Infectious Diseases*, 13, 155-65.

WEN, L., XIA, N., CHEN, X., LI, Y., HONG, Y., LIU, Y. & WANG, Z. 2014. Activity of antibacterial, antiviral, anti-inflammatory in compounds andrographolide salt. *European Journal of Pharmacology*, 740, 421-7.

WHO 2014. World Health Organization. Antimicrobial Resistance:Global Report on Surveillance.

WILLIAMS, D. H. & FLEMMING, I. 1995. *Spectroscopic methods in organic chemistry*, McGraw-Hill Publishing Company.

WORLD HEALTH ORGANISATION 2015. Global Tuberculosis Control. Geneva, Switzerland.

WRIGHT, G. D. 2011. Molecular mechanisms of antibiotic resistance. *Chemical Communications (Cambridge)*, 47, 4055-61.

WRIGHT, G. D. 2014. Something old, something new: revisiting natural products in antibiotic drug discovery. *Canadian Journal of Microbiology*, 60, 147-54.

WUBE, A., GUZMAN, J. D., HUFNER, A., HOCHFELLNER, C., BLUNDER, M., BAUER, R., GIBBONS, S., BHAKTA, S. & BUCAR, F. 2012. Synthesis and antibacterial evaluation of a new series of N-Alkyl-2-alkynyl/(E)-alkenyl-4-(1H)-quinolones. *Molecules*, 17, 8217-40.

XU, C., CHOU, G. X. & WANG, Z. T. 2010. A new diterpene from the leaves of *Andrographis paniculata* Nees. *Fitoterapia*, 81, 610-3.

ZHANG, C. Y. & TAN, B. K. 1997. Mechanisms of cardiovascular activity of *Andrographis paniculata* in the anaesthetized rat. *Journal of Ethnopharmacology*, 56, 97-101.

ZHANG, L., LIU, Q., YU, J., ZENG, H., JIANG, S. & CHEN, X. 2015. Separation of five compounds from leaves of *Andrographis paniculata* (Burm. f.) Nees by off-line two-dimensional high-speed counter-current chromatography combined with gradient and recycling elution. *Journal of Separation Science*, 38, 1476-83.

ZUMLA, A., CHAKAYA, J., CENTIS, R., D'AMBROSIO, L., MWABA, P., BATES, M., KAPATA, N., NYIRENDA, T., CHANDA, D., MFINANGA, S., HOELSCHER, M., MAEURER, M. & MIGLIORI, G. B. 2015a. Tuberculosis treatment and management--an update on treatment regimens, trials, new drugs, and adjunct therapies. *Lancet Respiratory Med*icine 3, 220-34.

ZUMLA, A., MAEURER, M., MARAIS, B., CHAKAYA, J., WEJSE, C., LIPMAN, M., MCHUGH, T. D. & PETERSEN, E. 2015b. Commemorating World Tuberculosis Day 2015. *Int J Infect Dis,* 32**,** 1-4.

ZUMLA, A. I., GILLESPIE, S. H., HOELSCHER, M., PHILIPS, P. P., COLE, S. T., ABUBAKAR, I., MCHUGH, T. D., SCHITO, M., MAEURER, M. & NUNN, A. J. 2014. New antituberculosis drugs, regimens, and adjunct therapies: needs, advances, and future prospects. *Lancet Infectious Diseases,* 14**,** 327-40.

Appendix

Appendix 1: ^{1}H NMR spectrum (expanded) of **A-1** in $CDCl_3$ (500 MHz)

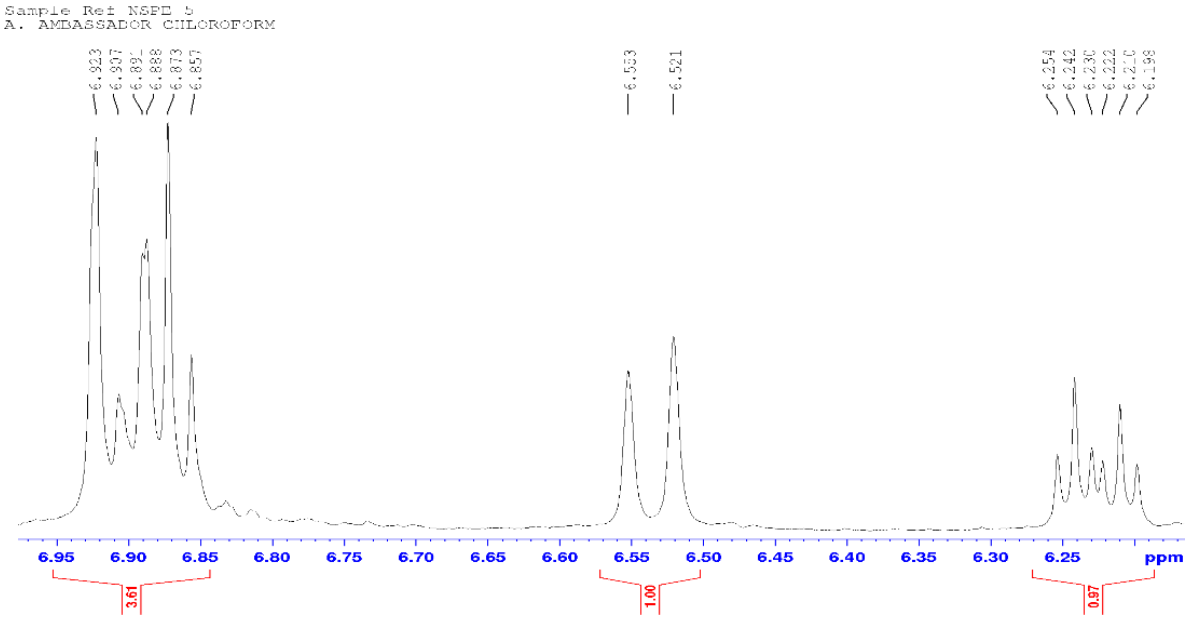

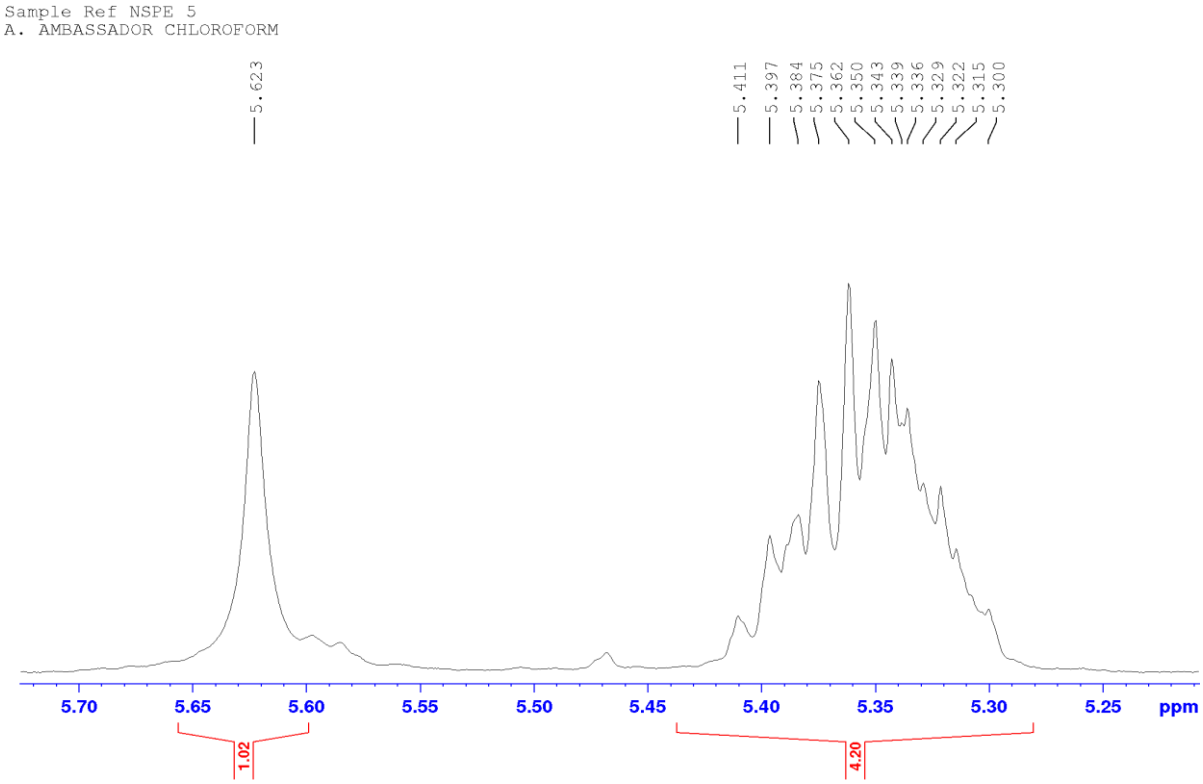

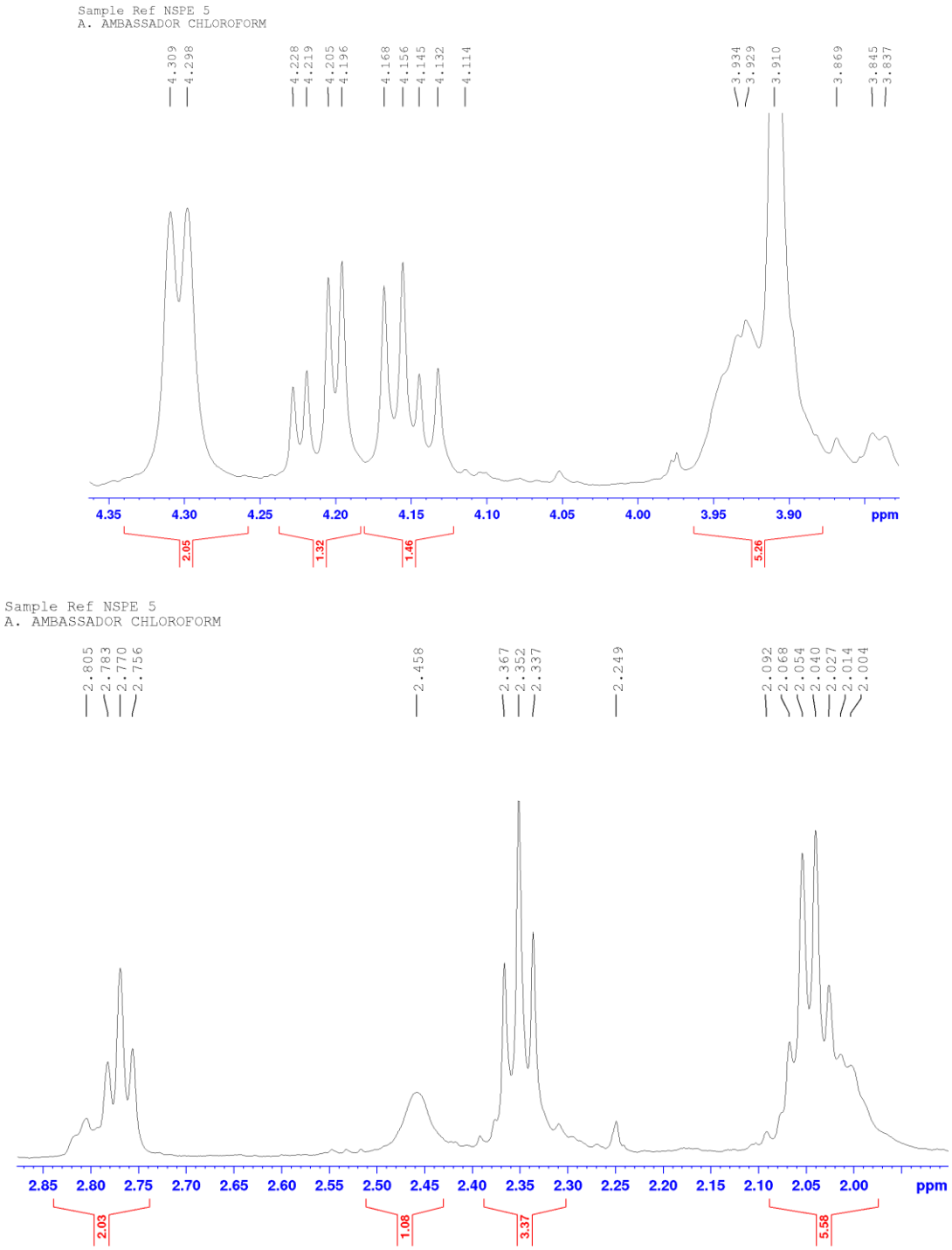

^{1}H NMR spectrum (expanded) of **A-1** in $CDCl_3$ (500 MHz)

Appendix 2: ^{1}H NMR (500 MHz) spectra of synthesized methyldisulfides.

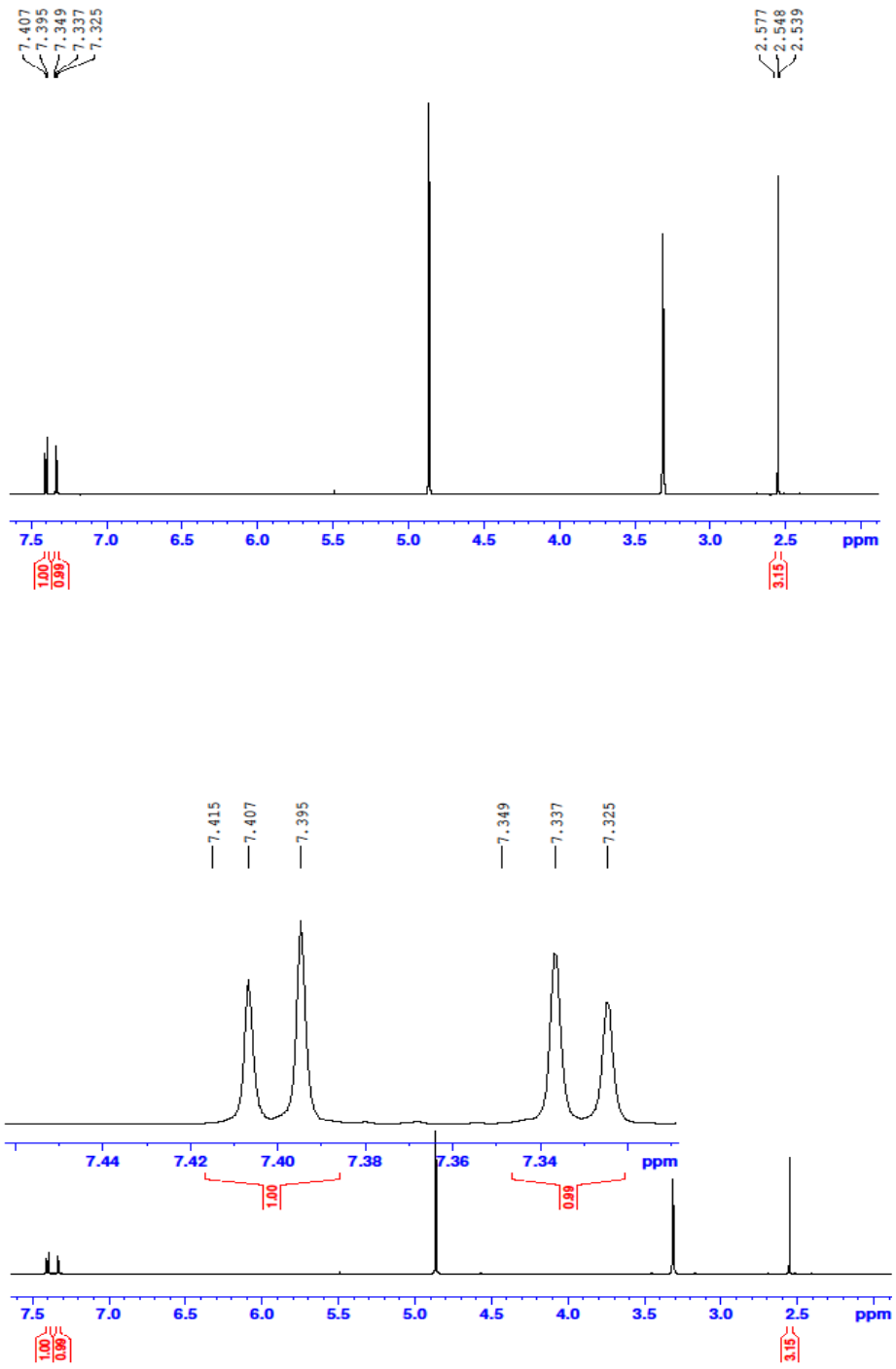

^{1}H NMR spectrum of Compound **2** in CD_3OD (500 MHz)

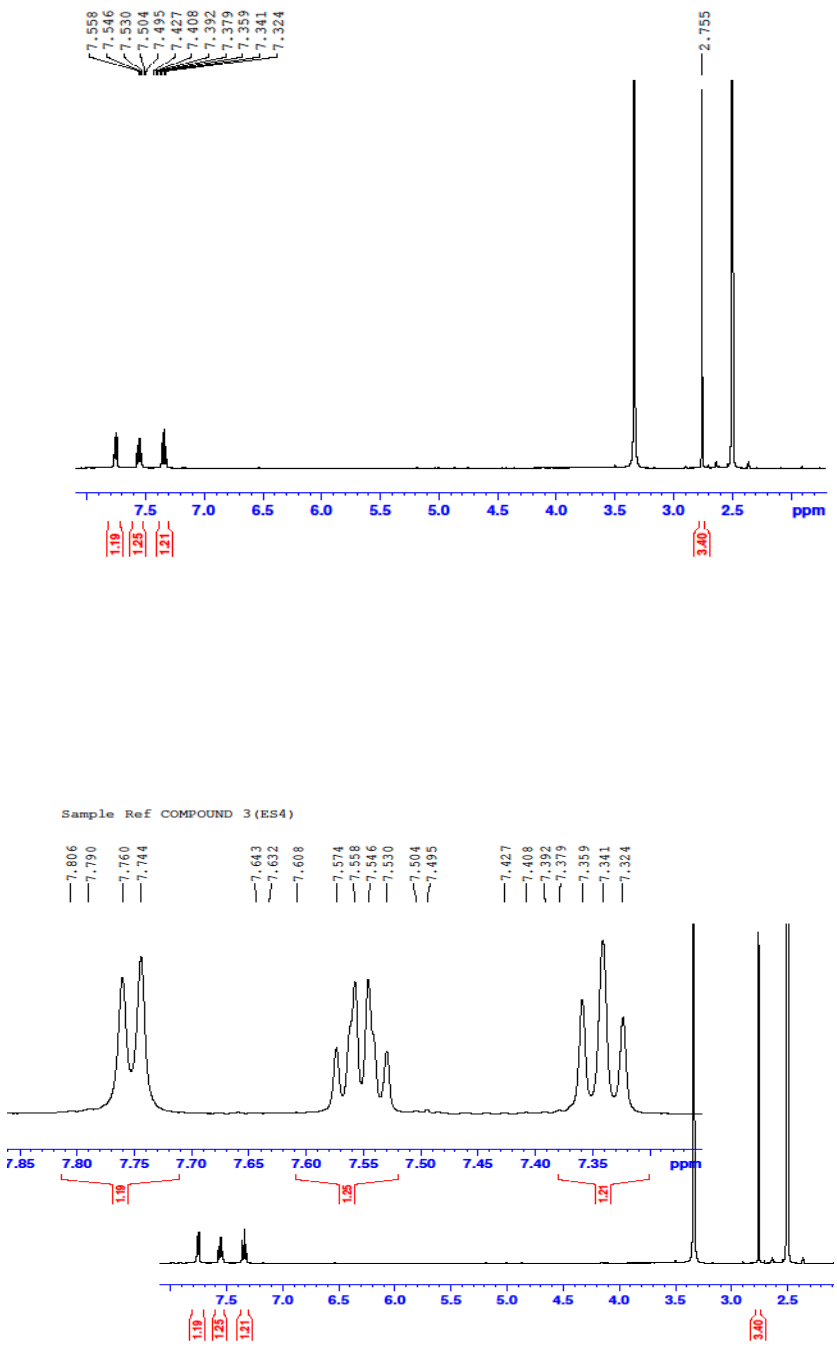

^{1}H NMR spectrum of Compound **3** in $(CD_3)_2SO$ (500 MHz)

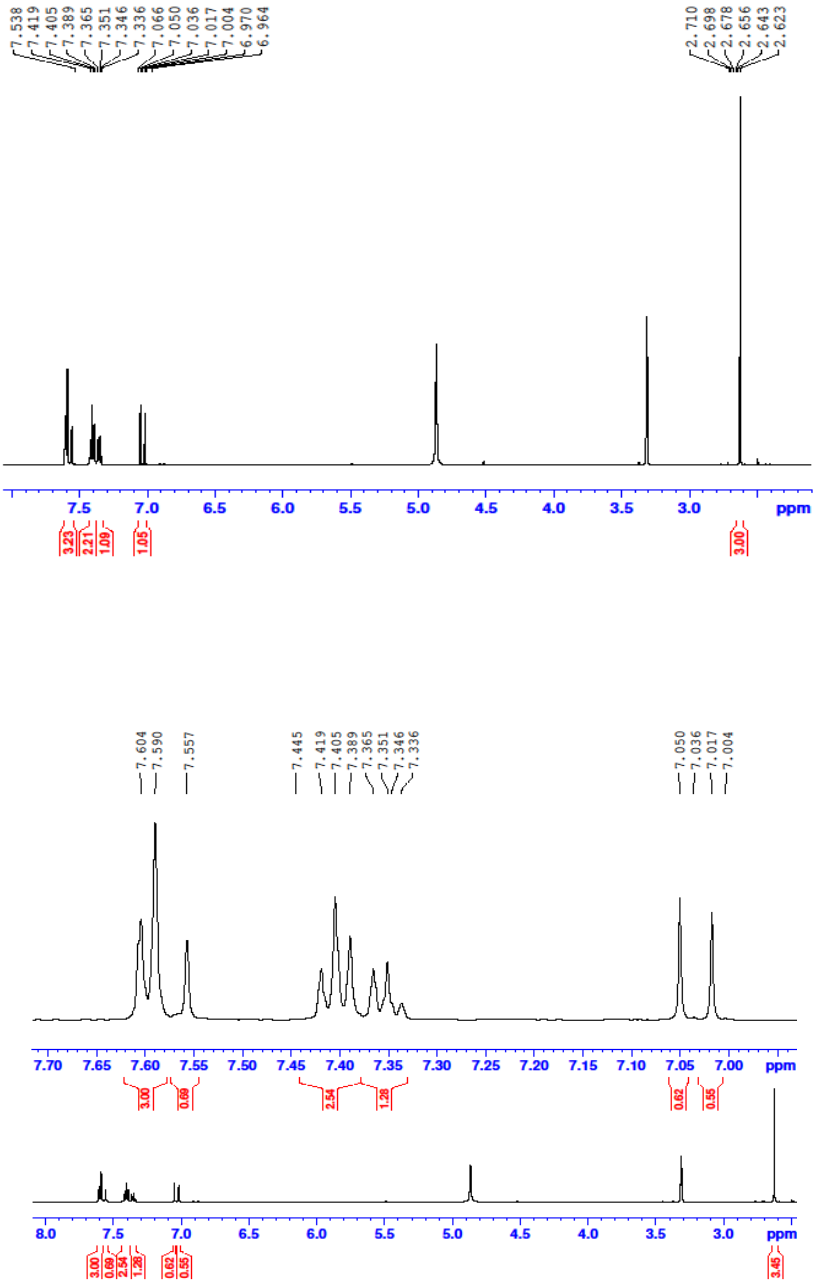

^{1}H NMR spectrum of Compound **4** in CD_3OD (500 MHz)

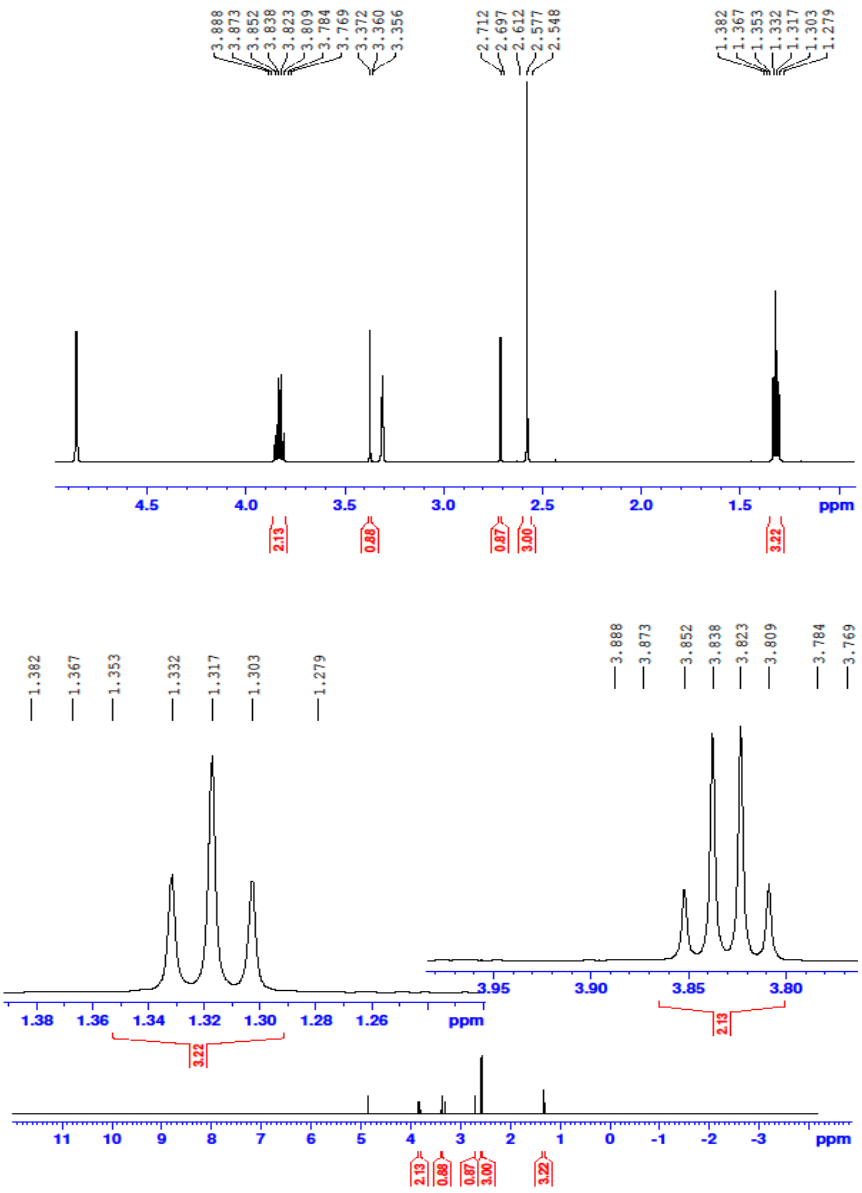

^{1}H NMR spectrum of Compound **5** in CD_3OD (500 MHz)